An investigation into nonstructural proteins NS3 and NS3A of African Horsesickness virus

By

Tracy Leonora Meiring

Submitted in fulfillment of the requirements for the degree

Magister Scientiae

In the Faculty of Natural and Agricultural Sciences (Department of Genetics)
University of Pretoria

Pretoria
November 2001

Dedicated to my parents, Jean and Piet Meiring

ACKNOWLEDGEMENTS

I wish to express my sincere thanks to the following people:

Dr. V. Van Staden (supervisor) for her guidance, motivation and support throughout this study

Prof. H. Huismans (co-supervisor) for his continuous support and criticism

Michelle van Niekerk for advice, assistance and debate

Members of the Genetics Department of the University of Pretoria for their assistance and interest, especially Pamela De Waal and Francois Maree

Dr. Marco Romito at the Onderstepoort Veterinary Institute

Chris van der Merwe and Alan Hall at the EM unit, University of Pretoria

My family and friends for their encouragement

The NRF for financial support

SUMMARY

An investigation into nonstructural proteins NS3 and NS3A of African horsesickness virus

By

Tracy Leonora Meiring

Supervisor: Dr. V van Staden
Department of Genetics
University of Pretoria

Co-supervisor: Prof. H. Huismans
Department of Genetics
University of Pretoria

For the degree MSc

The aims of this investigation were to compare the nonstructural proteins, NS3 and NS3A, of African horsesickness virus (AHSV) and to further characterise the cytotoxic properties of these proteins.

NS3 and NS3A are encoded from two in-phase overlapping reading frames on the smallest double-stranded (ds) RNA genome segment, segment 10 (S10) of AHSV. The proteins differ only with respect to the presence of an additional 10 or 11 amino acids, depending on the serotype, at the N-terminal of NS3. All known orbiviruses have been shown to encode two closely related proteins from S10. Sequence analysis of the N-terminal region of the NS3 proteins of the different serotypes of AHSV and various orbiviruses revealed that this region is not highly conserved.

Both AHSV NS3 and NS3A are membrane-associated and cytotoxic to insect cells causing membrane permeabilisation and eventual cell death when expressed individually (Van Staden *et al.,* 1995; Van Staden *et al.,* 1998; Van Niekerk *et al.,* 2001a). AHSV infection of Vero cells results in the synthesis of both proteins in equimolar amounts (Van Staden, 1993). The effect on the cytotoxic properties of these proteins when expressed together in insect cells was therefore investigated here.

Whether co-expressed or expressed individually NS3 and NS3A caused a dramatic decrease in the viability of insect cells. The NS3 protein is therefore representative of the NS3 and NS3A proteins together in terms of its cytotoxic effect.

The effect of the exogenous addition of NS3 on the membrane permeability of Vero cells was also investigated. The NS3 protein was found to cause a rapid increase in the membrane permeability of Vero cells. The cytotoxic properties of NS3 appear therefore not to be limited to their endogenous effects on insect cells.

The AHSV-3 NS3 and NS3A proteins were expressed as histidine tagged recombinants in the baculovirus expression system, to allow for the purification of large quantities of protein for functional and comparative studies. The resulting NS3 histidine fusion product, however, displayed a decrease in solubility, probably as a result of incorrect folding due to the presence of the histidine tag extension at the N-terminus of the protein.

To produce antibodies that detect NS3, and not NS3A, in AHSV infected cells, the N-terminal region unique to AHSV-3 NS3 was displayed on the surface of the AHSV core protein, VP7. The chimeric protein VP7-NS3 displayed the same structural characteristics as the wildtype VP7 protein, aggregating into highly insoluble crystals. Antiserum was prepared against purified VP7-NS3 and analysed in terms of its ability to recognise denatured and non-denatured AHSV-3 NS3. Although the antiserum was shown to contain antibodies directed against VP7 epitopes no immune reaction with NS3 was observed. The use of alternate sites on the surface region of VP7 for the display of such a small peptide needs to be investigated.

Although no functional differences between NS3 and NS3A were identified in this investigation, the finding that NS3 causes membrane permeability or damage to Vero cells represents the first indication that this AHSV protein causes extracellular membrane damage in mammalian cells. Many viral membrane damaging proteins or viroporins are thought to contribute significantly to the severity of virus-induced pathogenesis. The mechanism of membrane damage and the contribution of the membrane damaging properties of NS3 to AHSV-induced pathogenesis needs to be investigated.

OPSOMMING

'n Studie van nie-strukturele proteïene NS3 en NS3A van Perdesiekte virus

Deur

Tracy Leonora Meiring

Promotor: Dr. V. van Staden
Departement Genetika
Universiteit van Pretoria

Mede-promotor: Prof. H. Huismans
Departement Genetika
Universiteit van Pretoria

vir die graad MSc

Die doel van hierdie studie was om die nie-strukturele proteïene, NS3 en NS3A van perdesiekte virus (PSV), te vergelyk en om die sitotoksiese eienskappe van hierdie proteïene verder te karakteriseer.

NS3 en NS3A word gekodeer vanaf twee oorvleuelende in-fase oop leesrame op die kleinste dubbeldraad (dd) RNA genoomsegment, S10 van PSV. Hierdie twee proteïene verskil slegs van mekaar ten opsigte van 'n addisionele 10 of 11 aminosure, afhangend van die serotipe, aan die N-terminus van die NS3 proteïen. Alle bekende orbivirusse kodeer vir twee byna identiesse proteïene vanaf S10. Aminosuur volgorde analise van die N-terminale gebiede van die NS3 proteïene van die verskillende PSV serotipes en verskeinde orbivirusse, het bewys dat hierdie gebied nie hoogs gekonserveerd is nie.

Beide NS3 en NS3A is sitotoksies vir *Sf9* selle wanneer hulle alleen uitgedruk is in die baculovirus ekspressie sisteem (Van Staden *et al.,* 1995; Van Staden *et al.,* 1998; Van Niekerk *et al.*, 2001a). PSV infeksie van Vero selle lei tot die ekspressie van beide NS3 en NS3A in omtrent dieselfde hoeveelhede (Van Staden,1993). Om die sitotoksiese effek van ko-ekspressie van NS3 en NS3A in insekselle te bestudeer, is

insekselle geïnfekteer met rekombinante baculovirusse wat NS3 en NS3A uitdruk. Dit is bewys dat ko-ekspressie van NS3 en NS3A nie die sitotoksiese effek van hierdie proteïene verander nie.

Die effek van eksogeniese NS3 op die selmembraan permeabiliteit van Vero selle is ook bestudeer. NS3 veroorsaak 'n vinnige toename in die permeabiliteit van Vero selmembrane. Die sitotoksiese eienskappe van NS3 is daarom nie beperk tot hulle endogeniese effek op insekselle nie.

Om groot hoeveelheide van die PSV-3 NS3 en NS3A proteïene te bekom, is die S10 geen en 'n verkorte vorm van die S10 geen uitgedruk as histidien fusieproteïene in die baculovirus ekspressie sisteem. Die NS3 fusieproteïen het 'n sterk afname in solubiliteit getoon in vergelyking met die wildetipe NS3 proteïen en is vir hierdie rede nie gebruik vir die suiwering van NS3 nie.

Om tussen NS3 en NS3A te onderskei in PSV geïnfekteerde selle is antiserum teen die N-terminale gebied van NS3 berei deur gebruik te maak van die PSV strukturele proteïen, VP7. Die eerste 12 aminosure van NS3 is op die oppervlakte van VP7 vertoon. Dit is bewys dat die VP7-NS3 chimera dieselfde strukturele eienskappe as die wildetipe VP7 proteïen vertoon. Antiserum teen die VP7-NS3 proteïen is in hase berei, maar dit is aangetoon dat geen immuun reaksie met NS3 voorkom nie. Altenatiewe posisies op die oppervlakte van VP7 moet ondersoek word.

Die bevinding dat NS3 membraan permeabilisering in Vero selle veroorsaak is die eerste aanduiding dat die PSV proteïen eksogeniese membraan beskadiging veroorsaak. Baie sitotoksiese proteïene of viroporins dra by tot virus geïnduseerde patogenese. Die bydra van NS3 tot PSV geïnduseerde patogenese moet bepaal word.

ABBREVIATIONS

aa	amino acids
AHS	African horsesickness
AHSV	African horsesickness virus
Amp	ampicilin
Amps	amperes
ATCC	American type culture collection
bp	base pairs
BRD	Broadhaven virus
BTV	bluetongue virus
°C	degrees Celcius
cDNA	complementary deoxyribonucleic acid
CHV	Chuzan virus
Ci	Curie
CLP	core-like particle
cm^3	centimeter cubed
CPE	cytopathic effect
cys	cysteine
Da	Dalton
DEPC	diethylpyrocarbonate
DNA	deoxyribonucleic acid
dNTP	deoxyribonucleotide triphosphate
ds	double stranded
EC	endothelial cells
EDTA	ethylenediaminetetra-acetic acid
EHDV	Epizootic hemorrhagic disease virus
EM	electron microscope
ER	endoplasmic reticulum
et al.	and others
EtBr	ethidium bromide
fcs	foetal calf serum
Fig	figure
FMDV	Foot-and-mouth disease virus
g	gravitational force
G	gauge
gent	gentamycin
GTP	guanosine triphosphate
h	hour/s
HBsAgs	HBV surface antigens
HBV	hepatitis B virus
HD	hydrophobic domain
His	histidine
HIV	Human Immunodeficiency virus
h.p.i	hours post infection
Hyg B	hygromycin B
i.e.	that is
IM	intramuscular
IP3	inosytol triphosphate
IPTG	isopropyl-β-D-thiogalactopyranoside
IRES	internal ribosome entry site
ISA50	incomplete seppic adjuvant
k	kilo
kan	kanamycin

L1,L2,L3	large segments 1, 2 or 3
LB	Luria broth
LLP1	lentivirus lytic peptide 1
M	molar
M4,M5,M6, M7	medium segments 4,5,6 or 7
MEM	minimal essential medium
min	minute/s
ml	millilitre
mM	millimolar
MMOH	methyl mercuric hydroxide
MOI	multiplicity of infection
mRNA	messenger ribonucleic acid
ng	nanograms
nm	nanometers
NS1, NS2,NS3	nonstructural proteins 1, 2 or 3 (refers to *orbivirus*)
NSP4	nonstructural protein 4 (refers to *rotavirus*)
NTA	nitrilo-tri-acetic acid
OIE	Office international des Epizooties
ORF	open reading frame
OVI	Onderstepoort Veterinary Institute
P	particulate
PAGE	polyacrylamide gel electrophoresis
pBS	bluescribe plasmid
PBS	phosphate buffered saline
PCR	polymerase chain reaction
pfu	plaque forming units
p.i.	post infection
pmol	picomolar
PSB	protein solvent buffer
PSV	perdesiekte virus
RNA	ribonucleic acid
rNTP	ribonucleic acid triphosphate
rpm	revolutions per minute
RRL	rabbit reticulolysate
RT	reverse transcriptase
S	supernatant
S1 – S10	segments 1 to 10 (refers to *orbiviruses*)
^{35}S	radioactive Sulphur 35
SDS	sodium dodecyl sulphate
sec	second/s
Sf9	*Spodoptera frugiperda* insect cells
SIV	Simian immunodeficiency virus
SSP	single shelled particle
ss	single stranded
TE	Tris EDTA
tet	tetracyclin
TM	transmembrane
U	units
UHQ	ultra high quality water
µg	micrograms
µl	microlitres
µm	micrometers
UP	University of Pretoria
V	volts

VIB	virus inclusion body
VLP	virus-like particle
VMP	viral membrane protein
VP1 – 7	virus protein 1 to 7
v/v	volume per volume
v/w	volume per weight
X-gal	5-bromo-4-chloro-3-indolyl-β-D-galactopyranoside
3-D	three dimensional

LIST OF BUFFERS

Elution buffer:

20 mM Tris-HCl pH 8.5, 100 mM KCl, 100 mM imidazole, 10 mM 2-mercaptoethanol, 10% (v/v) glycerol

Lysis buffer without detergent:

50 mM Tris-HCl pH 7.5, 300 mM NaCl, 1 mM PMSF, 1 mM 2-mercaptoethanol

Na-K-P buffer:

0.075 M KH_2PO_4/NaH_2PO_4, pH7.4

PBS:

137 mM NaCl, 2.7 mM KCl, 4.3 mM $Na_2HPO_4.7H_2O$, 1.4 mM KH_2PO_4; pH7.3

Protein solvent buffer (PSB)(2x):

0.125 M Tris-HCl pH8, 4% SDS, 20% glycerol, 10% 2-mercaptoethanol

STE buffer:

0.01 M NaCl, 0.01 M Tris-HCl pH 7.6, 0.0001 M EDTA

TAE buffer:

0.04 M Tris, 0.002 M EDTA; pH8.5

TBS buffer:

500 mM NaCl, 25 mM Tris, pH7.6

TE buffer:

0.01 M Tris-HCl pH7.6, 0.001 M EDTA

TGS buffer:

0.025 M Tris-HCl pH 8.3, 0.192 M glycine, 0.1% SDS

Wash buffer:

20 mM Tris-HCl pH8.5, 500 mM KCl, 20 mM imidazole, 10 mM 2-mercaptoethanol, 10% (v/v) glycerol

CONTENTS

Acknowledgements ii

Summary iii

Opsomming v

Abbreviations vii

List of buffers x

CHAPTER 1:

LITERATURE REVIEW

1.1 INTRODUCTION 1

1.2 AFRICAN HORSESICKNESS VIRUS 1

1.2.1 Classification 1

1.2.2 Epidemiology 2

1.2.3 Pathogenesis 2

1.2.4 Prevention and control 4

1.2.5 Molecular biology 4

1.2.5.1 Proteins of the outer capsid 5

1.2.5.2 Proteins of the inner capsid 5

1.2.5.3 Non-structural proteins 6

1.3 NS3 RELATED PROTEINS OF VIRUSES IN THE REOVIRIDAE FAMILY 9

1.3.1 BTV NS3 and NS3A 9

1.3.2 Rotavirus NSP4 10

1.4 VIRAL MEMBRANE PROTEINS 12

1.5 MODIFICATION OF MEMBRANE PERMEABILITY BY ANIMAL VIRUSES 14

1.5.1 Viroporins 14

1.6 DUAL IN-FRAME TRANSLATION INITIATION 16
1.6.1 Mechanism for translation initiation at dual initiation sites 16
1.6.2 Examples of dual initiation in viruses 16
1.6.2a Foot-and-Mouth Disease Virus L proteins 17
1.6.2b Hepatitis B Virus Surface Glycoproteins 17
1.6.2c Rabies Virus Phosphoprotein 18
1.6.2d Simian Virus 40 VP2 and VP3 18
1.6.3 Examples of dual initiation in Eukaryotes 19
1.6.4 Functional differences in protein isoforms 19

1.7 AIMS OF THIS STUDY 20

CHAPTER 2:
EXPRESSION OF AHSV NS3 AND NS3A AS HISTIDINE TAG FUSION PROTEINS AND ANALYSIS OF THEIR CYTOTOXIC EFFECT

2.1 INTRODUCTION 22

2.2 MATERIALS AND METHODS 23
2.2.1 Materials obtained 23
2.2.2 Exogenous addition of NS3 to Vero cells 24
2.2.2.1 Cells and viruses 24
2.2.2.2 Preparation of *Sf9* cell extracts containing NS3 24
2.2.2.3 SDS-PAGE 25
2.2.2.4 Western immunoblots 25
2.2.2.5 Preparation of Vero cells 25
2.2.2.6 Hygromycin B membrane permeabilisation assay 26
2.2.3 Co-expression of AHSV-3 NS3 and NS3A 26
2.2.3.1 Determination of cell viability by trypan blue staining 26
2.2.4 Cloning of NS3 and NS3A into pFastBac HTc 26
2.2.4.1 Polymerase chain reaction 26

2.2.4.2 Plasmid DNA isolation 27
2.2.4.3 Phenol-chloroform extraction 28
2.2.4.4 Optical density analytical measurements 28
2.2.4.5 Klenow enzyme fill-in reactions 28
2.2.4.6 Restriction enzyme digestions 28
2.2.4.7 Purification of DNA fragments from agarose 29
2.2.4.8 Ligation of DNA fragments 29
2.2.4.9 Prepaparation of competent cells 29
2.2.4.10 Transformation of recombinant DNA into competent cells 29
2.2.5 DNA sequencing 30
2.2.5.1 Plasmid DNA purification for cycle sequencing 30
2.2.5.2 Automated sequencing 30
2.2.6 Baculovirus expression of histidine tagged NS3 and NS3A 31
2.2.6.1 Preparation of competent DH10Bac cells 31
2.2.6.2 Transposition of recombinant genes into Bacmid DNA 31
2.2.6.3 Isolation of composite Bacmid DNA 31
2.2.6.4 Transfection of *Sf9* insect cells with Bacmid DNA 32
2.2.6.5 Amplification of Baculovirus recombinants 32
2.2.6.6 Titration of viruses 32
2.2.6.7 Analysis of protein expression 33
2.2.7 Protein solubility assays 33
2.2.7.1 Basic solubility assay 33
2.2.7.2 Binding of HTc-NS3 to Ni^{2+}-resin 33
2.2.7.3 Comparison of solubility of HTc-NS3 and NS3 34
2.2.8 Sequence analysis of N-terminal residues of NS3 34

2.3 RESULTS 35
2.3.1 The effect of extracellular addition of NS3 to Vero cells 35
2.3.2 The cytotoxic effect of coexpression of NS3 and NS3A in insect cells 37
2.3.3 Cloning of the NS3A gene into the pFastBac HTc vector 39
2.3.4 Expression of NS3 and NS3A as histidine tag fusion proteins 44

2.3.5 Analysis of solubility of HTc-NS3 and binding to nickel resin 46
2.3.6 Sequence analysis of N-terminal region of NS3 49

2.4 DISCUSSION 55

CHAPTER 3:
IMMUNOLOGICAL DISPLAY OF THE N-TERMINAL AMINO ACIDS OF NS3

3.1 INTRODUCTION 63

3.2 MATERIALS AND METHODS 64
3.2.1 Cloning the 12 N-terminal amino acids of NS3 into VP7mt200 64
3.2.2 Baculovirus expression of VP7-NS3 65
3.2.2.1 Plaque purification 65
3.2.3 Hydrophobicity analysis 66
3.2.4 Solubility analysis and purification of VP7-NS3 66
3.2.5 Scanning electron microscopical analysis 66
3.2.6 Immunisation schedule 66
3.2.7 Evaluation of antiserum raised against VP7-NS3 67
3.2.7.1 Western blot 67
3.2.7.2 Immune precipitation of NS3 67
3.2.7.2.1 In vitro transcription and translation of NS3 serotype 3 67
3.2.7.2.2 Immune precipitation 68
3.2.8 Immunogold labelling of VP7-NS3 68

3.3 RESULTS 69
3.3.1 Cloning of N-terminal region of NS3 into VP7mt200 69
3.3.2 Baculovirus expression of VP7-NS3 71
3.3.3 Hydrophobicity profile of VP7-NS3 73
3.3.4 Solubility analysis and purification of VP7-NS3 73
3.3.5 Electron Microscopy 75

3.3.6 Evaluation of antiserum raised against VP7-NS3 78

3.4 DISCUSSION **83**

CHAPTER 4:
CONCLUDING REMARKS **90**

CONGRESS PARTICIPATION AND PUBLICATIONS **96**

REFERENCES **97**

CHAPTER 1

LITERATURE REVIEW

1.1 INTRODUCTION

African horsesickness (AHS), which is endemic to sub-Saharan Africa, is a non-contagious but infectious disease of equines. The severity of the disease is well illustrated by a recent outbreak in the Western Cape, South Africa, in which only 3 of the 34 affected horses survived (P.G. Howell, personal communication). The aetiological agent of the disease, African horsesickness virus (AHSV), was identified as early as 1901 by Sir Arnold Theiler (Theiler, 1921).

1.2 AFRICAN HORSESICKNESS VIRUS

1.2.1 Classification

AHSV is a member of the *Orbivirus* genus within the *Reoviridae* family (Verwoerd *et al.*, 1979). The *Reoviridae* family is characterised by (i) a segmented double-stranded RNA genome of 10 to 12 segments, and (ii) virus particles (60 – 80nm) with an inner protein coat and one or two icosahedral capsids. On the basis of differences in morphology and physiological properties this family can be sub-divided into nine genera, the *Orbiviruses* being the largest subgroup (reviewed in Urbano & Urbano, 1994).

Orbiviruses are distinguished from other *Reoviridae* by their ability to multiply in insects and vertebrates, and their sensitivity to low pH conditions, lipid solvents and detergents. Bluetongue virus (BTV) is the type species of this genus (Borden *et al.*, 1971) and is comparable both in morphology and molecular constitution to AHSV (Roy *et al.*, 1994). On the basis of cross-neutralisation studies of the major outer capsid protein, VP2, 25 serotypes have been defined for BTV and 9 for AHSV (McIntosh, 1958; Howell, 1962; Gorman & Taylor, 1985).

1.2.2 Epidemiology

AHSV infects equids, the usual hosts being horses, mules, zebras and donkeys. The disease however is more severe in horses than donkeys or mules (Coetzer & Erasmus, 1994). Occasional hosts include elephants, onager, camels and dogs (after eating infected blood or horsemeat). AHS is not directly contagious, but is transmitted by biting midges (*Culicoides imicola*)(Du Toit, 1944; Moore & Lee, 1972). Venter and co-workers (2000) recently identified *Culicoides botilinos* as another potential vector of AHSV. Moist mild conditions and high temperatures favour the presence of these insect vectors.

AHS is endemic in the central and eastern tropical regions of Africa, from where it spreads regularly to southern Africa and occasionally to northern Africa (Coetzer & Erasmus, 1994). Isolated outbreaks have occurred in Spain (1966, 1987-90), in the Near and Middle East (1959-63) and in Portugal (1989) (Mellor, 1993). The disease not only affects the export of horses from southern Africa, but also has a large impact on the export of zebras to international conservation reserves (Lubroth, 1988).

1.2.3 Pathogenesis

African horsesickness has been allocated Office International des Epizooties (OIE) List A status. The disease caused by AHSV ranges from sub-clinical to acute with mortality rates of 0-100% in horses (reviewed in Burrage & Laegreid, 1994). In 1921 Sir Theiler described four clinical forms of AHS on the basis of time of onset, clinical presentation, mortality and the organs affected (Laegreid *et al.*, 1992a; Laegried *et al.*, 1992b). These are the pulmonary, cardiac, mixed and horsesickness fever forms. The form of AHS seen in infected horses may be as a result of several factors, including the route of infection, tropism of sub-populations of viral particles (Erasmus, 1972) and host immune status, genetic susceptibility and permissivity (Laegried *et al.*, 1993). Laegreid and co-workers, (1993) showed that the viral virulence phenotype is the primary determinant of the form of disease expressed by experimentally infected naïve horses.

Pulmonary AHS or 'dunkop' is an acute disease characterised by high fever, severe pulmonary oedema, pleural effusion and mortality approaching 100% of affected horses. This form has an incubation period of only 4 to 5 days and affects the lungs, spleen, hydrothorax, bronchial and mediastinal nodes. Cardiac AHS or 'dikkop' is subacute and results in pronounced oedema of the subcutaneous and intermuscular tissues of the head and neck. Large amounts of fluid are also present in the pericardial sac, while multifocal haemorrhages of the epi-, endo-, and myocardium are observed. Although some animals do recover, the mortality rate is nevertheless high (50-80%). The incubation period is variable, between 7 to 14 days. The mixed form of the disease is the most common and displays features of both the pulmonary and cardiac forms. This form has a greater than 80% mortality rate and an intermediate incubation period of 5 to 7 days. The mildest form of AHS is the fever form, here affected horses develop a transient subacute fever, some scleral infection and mild depression. The incubation period is 5 to 14 days, and all affected horses recover (Coetzer & Erasmus, 1994; Laegreid *et al.,* 1993; Burrage & Laegreid, 1994).

The principal pathological features of African horsesickness are, therefore, oedema, effusion and haemorrhage. Skowneck *et al.,* (1995) suggest that the loss of endothelial cell (EC) barrier function may be the cause of these prominent features. AHSV has been experimentally shown to infect pulmonary microvascular endothelial cells. Severely affected cells display pronounced cell swelling with some discontinuity of the plasma membrane and loss of structural detail (Laegreid *et al.,* 1992a). Multiple mechanisms may be involved in the development of this pulmonary microvascular leakage. Damage to the EC and loss of integrity of intercellular junctions could result in the loss of EC barrier function and the subsequent development of oedema (Laegreid *et al.,* 1992a; Laegried *et al.,* 1992b). Thus the lethal event in acute AHS, pulmonary oedema, may be related to the infection and damage of pulmonary endothelial cells (Laegried *et al.,* 1992a; Laegreid *et al.,* 1992b). In an experiment conducted by Laegreid *et al.* (1992b) the ability of two virulence variants of AHSV serotype 4 (AHSV-4) to infect EC correlated to the pathogenicity of these variants for horses. The difference in ability of virulence variants of AHSV to cause acute disease may therefore be as a result of differences in their ability to infect and damage EC.

1.2.4 Prevention and control

There is currently no efficient treatment for AHS. In an attempt to control outbreaks, horses in southern Africa are vaccinated annually with a polyvalent attenuated vaccine. Immunisation with this vaccine does however have side-effects, in severe cases fatal enchaphilitis has been reported (reviewed in Coetzer & Erasmus, 1994). The horses may, furthermore, not be exerted for at least three weeks following immunisation. Once an outbreak of AHS has occurred a monovalent vaccine may be administered once the serotype has been identified. The first reverse transcription polymerase chain reaction (RT-PCR) amplification method for serotyping of AHSV was recently developed, and will allow for rapid and reliable identification and discrimination between the nine AHSV serotypes using L2. This is vital at the start of an outbreak to enable the early selection of a vaccine to control the spread of the disease (Sailleau *et al.*, 2000). The only other methods of control include quarantine and slaughter of infected animals, destruction of cadavers, and control of insect vectors (insecticides, repellants and screens). Alternative subunit vaccines for AHSV are currently being investigated.

1.2.5 Molecular biology

AHSV possesses a double stranded RNA (dsRNA) genome composed of 10 segments packaged within the core of a double layered capsid (Bremer, 1976; Huismans, 1979; Mecham & Dean, 1988). The genome segments are of different sizes, three large, designated L1-L3, three medium, M4-M6, and four small, S7-S10. The 5' and 3' non-coding regions of the genome segments range in length from 12 to 35 base pairs (bp) and 29 to 100 bp respectively (Roy *et al.*, 1994). Like BTV, the 5' and 3' end sequences of each segment show partial inverted complementarity and may form secondary structures when in the single stranded RNA (ssRNA) form (Roy *et al.*, 1994). Each genome segment encodes at least one protein. Seven structural (VP1-VP7) and four non-structural (NS1-NS3, NS3A) proteins have been identified (Oellerman *et al.*, 1970; Bremer, 1976; Grubman & Lewis, 1992; Laviada *et al.*, 1993).

1.2.5.1 Proteins of the outer capsid:

The outer capsid of the virus is composed of VP2 and VP5. Lewis and Grubman (1991) confirmed VP2 as the major exposed protein on the virus particle. This protein is encoded by the L2 genome segment and is the most variable AHSV protein with up to 64% variation on the amino acid level across serotypes (Vreede & Huismans, 1994). VP2 contains the major serotype specific and neutralising epitopes of AHSV (Burrage *et al.*, 1993).

Bentley and co-workers (2000) have identified a number of antigenic determinants located in the amino terminal half of VP2. The antigenic structure of AHSV-4 VP2 was recently determined by Martínez-Torrecuadrada and co-workers (2001). Fifteen antigenic sites were identified, of which three induced neutralising antibodies for AHSV-4. These characteristics make VP2 an ideal candidate for a subunit vaccine. Still, the relatively low neutralisation titres found by Martinez-Torrecuadrada *et al.* (2001) make the possibility of producing a synthetic vaccine for AHSV unlikely.

VP5 is encoded by segment M6 and is less exposed on the virion surface than VP2. This protein is present in small amounts in infected cells, and is insoluble and possibly cytotoxic when expressed in insect cells (Roy *et al.*, 1994). Other than its structural role little is known about the function of AHSV VP5. Hassan and co-workers (2001) propose a role for BTV VP5 in virus-cell penetration, based on their finding that purified VP5 was able to permeabilise mammalian and *Culicoides* insect cells, inducing cytotoxicity. Both VP2 and VP5 of AHSV may influence the virulence phenotype expressed by a given virus isolate (O'Hara *et al.*, 1998).

1.2.5.2 Proteins of the inner capsid:

The inner core is composed of two major proteins, VP3 and VP7, and three minor proteins VP1, VP4 and VP6 (Bremer, 1976).

VP3, encoded by L3, is the innermost component of the core and forms a scaffold on which clusters of VP7 trimers are arranged (Hewat *et al.*, 1992; Prasad *et al.*, 1992). Both these proteins are highly conserved amongst serotypes and contain the group specific antigenic determinants. When co-expressed these proteins spontaneously aggregate into empty core-like particles (French & Roy, 1990; Maree *et al.*, 1998). In

contrast to the cognate protein in BTV, AHSV VP7, encoded by S7, is highly insoluble and hydrophobic (Roy *et al.*, 1991). When expressed in insect cells VP7 spontaneously assembles into immunogenic disc-shaped crystals (Chuma *et al.*, 1992). The possibility of using these crystals as antigen delivery systems is currently under investigation (Maree, 2000). Tan and co-workers (2001) recently identified an RGD motif between residues 168 and 170 of BTV VP7 as being responsible for the attachment of the core to *Culicoides* cells.

Little is known of the functions of the minor core proteins VP1, VP4 and VP6 of AHSV, presumably they have similar enzymatic functions to their cognate proteins in BTV. VP1, encoded by L1, is postulated to be the virus replicase-transcriptase, capable of elongating ssRNA (Roy *et al.*, 1994). VP4 expressed from the M4 segment may have guanyl transferase activity for the methylation of the mRNAs during transcription (Roy *et al.*, 1994). VP6, encoded by S9, has strong ds- and ssRNA binding ability and may have helicase activity. This is supported by sequence similarities between VP4 and the helicase enzyme of *E. coli* (Turnbull *et al.*, 1996).

1.2.5.3 Non-structural proteins:

The nonstructural proteins NS1, NS2, NS3/A of AHSV are encoded by the M5, S8 and S10 segments respectively. While NS1 and NS2 are highly conserved, the NS3 proteins are the second most variable AHSV gene products (Van Niekerk *et al.*, 2001b).

AHSV NS1 dimers assemble as helically coiled tubules in the cytoplasm of infected cells and are believed to play a role in virus transport (Huismans & Els, 1979; Urakawa & Roy, 1988; Roy, 1996). The protein contains 16 cysteine residues of which 9 are conserved at the same relative positions in BTV NS1. The residues at position 337 and 340 in BTV NS1 have been shown to be necessary for tubule formation and may be as essential in AHSV NS1. The AHSV protein however has a lower sedimentation rate than BTV NS1 and does not display the same ladder-like structure (Maree & Huismans, 1997, Van Staden *et al.*, 1998).

AHSV NS2 is a major component of the virus inclusion bodies routinely observed in AHSV infected cells. This protein is thought to be involved in recruiting mRNA during

virion assembly at these sites, substantiated by its ability to bind ssRNA (Uitenweerde *et al.,* 1995). NS2 is phosphorylated at specific serine residues and is, in fact, the only viral phosphorylated protein present in AHSV infected cells (Devaney *et al.,* 1988). Theron and co-workers (1994) found that the phosphorylated version of EHDV NS2 bound ssRNA less efficiently than the unphosphorylated form. Another important feature of NS2 is the presence of conserved hydrophobic domains and potential β-turns at the N-terminus of the protein. Zhao *et al.,* (1994) found that the amino terminus of BTV NS2 was essential for ssRNA binding.

The smallest genome segment of AHSV encodes two related proteins NS3 and NS3A, where NS3A is a truncated version of NS3 lacking the 10 or 11 N-terminal amino acids (Van Staden & Huismans, 1991; Mertens *et al.,* 1984; Van Dijk & Huismans, 1988). Initiation of synthesis of these two proteins has been shown to occur at two in-phase AUG initiation codons in the same open reading frame (Van Staden & Huismans, 1991). The presence of the second in-frame start codon is conserved in all 9 serotypes of AHSV and in the S10 genes of other *Orbiviruses* including BTV, epizootic hemorrhagic disease virus (EHDV), Palyam virus, Broadhaven virus (BRD) and Chuzan virus (Van Staden & Huismans, 1991; Moss *et al.,* 1992; De Sá *et al.,* 1994; Jensen *et al.,* 1994; Yamakawa *et al.,* 1999). The sequence and length of the N-terminal extension present in NS3 but not NS3A is, however, variable.

Other regions or features of AHSV NS3 and NS3A conserved in BTV NS3/A and the NS3/A proteins of other orbiviruses include:

- A proline rich region between amino acids 22 and 34
- A highly conserved domain between residues 43 and 92, and
- Two hydrophobic domains (HD) at amino acids 116 to 137 and 154 to 176 (Van Staden *et al.,* 1998).

NS3 has been shown to be present in the membrane components of infected cells associated with virus release (Stoltz *et al.,* 1996). The protein is possibly retained on the cell membrane by the conserved hydrophobic domains and may mediate the egress of the virion from infected cells in the final stages of virus morphogenesis as proposed for BTV NS3 (Hyatt *et al.,* 1993). In the computational conformational model proposed by Van Staden and co-workers (1995) both the hydrophobic regions form transmembrane

domains that span the membrane with the terminal regions located in the cytoplasm. Alternatively only one of the putative transmembrane regions could span the membrane with the amino-terminus orientated in the endoplasmic reticulum (ER) lumen as seen in the analogous protein in rotavirus, NSP4 (Chan *et al.,* 1988). This model was also proposed for the NS3 protein of EHDV, a related orbivirus (Jensen & Wilson, 1995).

Only small amounts of NS3 are detected when expressed as a recombinant in the baculovirus system or in Vero cells infected with AHSV, unlike BTV NS3 which is expressed at higher levels. No NS3A was detected in *Spodoptera frugiperda* (*Sf9*) cells infected with recombinant baculoviruses expressing the full length S10 gene (Van Staden *et al.,* 1995). Expression of NS3A was achieved by the truncation of the full length NS3 gene (Van Staden *et al.,* 1998).

AHSV NS3 was found to be cytotoxic when expressed in the baculovirus expression system in insect cells causing disruption of the cellular membrane and increased membrane permeability (Van Staden *et al.,* 1995; Smit, 1999). Substitution mutations in the hydrophobic domains of NS3 abrogated this cytotoxic effect, while mutations in the proline rich and highly conserved regions had little effect (Van Staden *et al.,* 1998; Van Niekerk *et al.,* 2001a). The cytotoxicity of NS3 appears, therefore to be dependant on its membrane association (Van Niekerk *et al.,* 2001a). No significant difference between the cytotoxicity of NS3 and NS3A in insect cells was observed (Van Niekerk *et al.,* 2001a).

Many aspects of the functioning of, role of and reasons for the conservation of NS3 and NS3A in the viral life cycle remain unclear. As these proteins are the subject of this investigation, a comparison to the cognate proteins in other orbiviruses is, therefore, necessary. In addition, a greater understanding of viral membrane proteins, cytotoxic proteins and proteins expressed from overlapping reading frames is essential. Each of these aspects will, therefore, be discussed in the following sections.

1.3 NS3 RELATED PROTEINS OF VIRUSES IN THE REOVIRIDAE FAMILY

1.3.1 BTV NS3 and NS3A:

The S10 genome segment of BTV encodes NS3 and NS3A from the same open reading frame (ORF)(Van Dijk & Huismans, 1988). Expression of the BTV NS3 gene in the baculovirus system results in the production of both proteins. NS3A expression however is more variable than NS3 and usually occurs at a lower level (French *et al.,* 1989; Bansal *et al.,* 1998).

These proteins, unlike the AHSV NS3 proteins, display a high degree of sequence conservation and homology amongst the BTV serotypes (Hwang *et al.,* 1992). Conserved features of BTV NS3 and NS3A include two hydrophobic domains, two N-linked glycosylation sites (63 and 150), a cluster of six proline residues near the N-terminus, two conserved cysteine residues (137 and 181) and a tyrosine residue at position 159 (Hwang *et al.,* 1992). Sera from sheep infected with homologous and heterologous BTV react with NS3 and NS3A expressed in the baculovirus system, suggesting that these proteins are highly conserved group specific antigens (French *et al.,* 1989).

NS3 and NS3A have been detected in regions of the plasma membrane associated with membrane perturbation (Hyatt *et al.,* 1991). Hyatt and co-workers (1993) found that NS3 and NS3A mediate the release of virus-like particles (VLPs), but not core-like particles (CLPs), from infected cells. These proteins are therefore believed to be involved in the final stages of BTV morphogenesis.

Both the hydrophobic domains (HDs) of NS3 and NS3A are proposed to span the membrane and only the site at amino acid 150 between the transmembrane regions is glycosylated (Bansal *et al.,* 1998). Deletion of part of the first HD (H1) abolishes glycosylation. H1 appears therefore to be responsible for the introduction of the protein into the ER for the addition of the carbohydrate group (Bansal *et al.,* 1998). This glycosylation serves to protect the protein from degradation either before or after cell membrane insertion (Bansal *et al.,* 1998).

Neither BTV proteins have been reported to be cytotoxic. The BTV and AHSV NS3 proteins may have some functional similarity to the NSP4 protein of rotavirus, a member of the *Reoviridae* family.

1.3.2 Rotavirus NSP4:

The non-structural glycoprotein NSP4 is an integral membrane protein localised in the endoplasmic reticulum (ER) of rotavirus infected cells. NSP4 is a protein of 175 amino acids with three internal hydrophobic domains. The second hydrophobic domain acts as the only transmembrane domain while the C-terminal domain lies on the cytoplasmic side and the N-terminal domain in the lumen of the ER (Taylor *et al.,* 1992). NSP4 assembles as homotetramers mediated by α-helical coiled coil structures adopted by the cytoplasmic region between residues 95 and 137 (Maass & Atkinson, 1990; Taylor *et al.,* 1996). These NSP4 oligomers act as receptors for the binding of and translocation across the ER membrane of single-shelled rotavirus particles (SSP) (Meyer *et al.,* 1989). The C-terminal amino acids 161 to 175 of NSP4 facilitate binding to SSP (Au *et al.,* 1993). O'Brein *et al.,* (2000) used solid-phase binding assays to show that the binding of NSP4 to SSP requires at least 17 of the C-terminal 20 amino acids (156 to 175), including the final methionine residue. Binding to the SSP involves VP6, the major structural protein on the surface of rotavirus SSP (Au *et al.,* 1989). NSP4 has also been shown to bind VP4, an outer capsid protein (Mattion *et al.,* 1994). After translocation of the rotavirus SSP, removal of the transient envelope requires the glycosylation of NSP4 (Petrie *et al.,* 1983).

Several of the cytopathic effects seen in rotavirus infection are also evident when NSP4 is expressed alone in mammalian or bacterial cells or when added extracelluarly to cells such as gastrointestinal epithelial cells. Expression of NSP4 from a recombinant vaccinia virus in cultured mammalian cells causes a loss in plasma membrane integrity, profound morphological changes and eventually cell death (Newton *et al.,* 1997). In *Sf9* cells the expression of NSP4 results in a potentially toxic increase in the concentration of Ca^{2+} in the cytoplasm (Tian *et al.,* 1994). Purified NSP4 releases calcein incorporated into liposomes, disrupts microsomes and appears, therefore, to have direct membrane-

destabilising activity (Tian *et al.,* 1996b). NSP4 furthermore induces paracellular leakage in polarised MDCK-1 epithelial cells (Tafazoli *et al.*, 2001).

A membrane-proximal domain of NSP4 (residues 54 to 74) was identified as being important in mediating the cytopathic effects of NSP4 in MA104 cells (Newton *et al.,* 1997). This region is rich in basic amino acids and has the potential to form a cationic amphipathic helix structure, a feature common to many membrane-destabilising proteins (Newton *et al.,* 1997). Browne *et al.,* (2000) confirmed these findings by identifying the domain of NSP4 between residues 48 and 91 as the mediator of internal membrane destabilisation when NSP4 is expressed in *E. coli* cells. Localised disruption of the ER membrane may affect the permeability of the ER and cause an increase in the rate of Ca^{2+} leakage. An increase in intracellular calcium concentration causes cell lysis and the release of viral particles during the final stages of rotavirus morphogenesis (Tian *et al.* 1996a; Ruiz *et al.,* 2000). The oligomerisation of several rotavirus proteins as well as the integrity of rotavirus particles, furthermore, also requires the presence of Ca^{2+} (Ruiz *et al.,* 2000).

Free NSP4 has also been identified as a viral enterotoxin due to its ability to promote diarrhoea, similar to that in virus-induced disease, when administered to infant mice (Ball *et al.,* 1996). A peptide (residues 114 to 135) derived from the cytoplasmic domain of NSP4 has been shown to possess enterotoxic activity (Ball *et al.,* 1996). This enterotoxic activity is possibly mediated by a putative plasma membrane receptor that triggers a phospholipase C-mediated increase in intracellular Ca^{2+}, following binding of NSP4 to human intestinal cells (Dong *et al.,* 1997). An increase in intracellular Ca^{2+} results in enhanced Cl^- secretion in intestinal epithelial cells and diarrhoea. Purified NSP4 and the NSP4 114-135 peptide, however, also released calcein from calcein-loaded liposomes and disrupted microsomes and may, therefore, have direct membrane destabilising activity (Tian *et al.,* 1996b). Zhang *et al.,* (2000) have identified a secreted, cleavage product of NSP4 (aa 112-175) in the early media from rotavirus-infected cells and demonstrated that this peptide was a functional enterotoxin. Browne *et al.,* (2000) suggest that the membrane-destabilising and enterotoxic activities of NSP4 are mediated by different regions of the protein. The mechanism by which endogenous NSP4 causes

an increase in intracellular calcium, furthermore, appears to be unrelated to phospholipase C activity (Tian *et al.*, 1995).

One of the key mechanisms in the development of diarrhea during rotavirus infection in infants, increased intestinal secretion, is therefore stimulated by the intracellular or extracellular action of the rotavirus non-structural protein, NSP4 (Estes *et al.,* 2001). NSP4, in conjunction with other rotavirus proteins, VP3, VP4 and VP7, therefore, plays an important role in determining viral pathogenicity (Kirkwood *et al.,* 1996).

1.4 VIRAL MEMBRANE PROTEINS

The majority of viral membrane proteins (VMP) are complex high molecular weight transmembrane oligomers (Doms *et al.,* 1993). Topologically, membrane proteins can be classified into three groups. Type 1 proteins span the lipid bilayer once with their N-termini orientated towards the ER lumen and their C-termini exposed on the cytoplasmic side. These proteins generally possess a cleavable signal peptide. Type 2 proteins span the membrane in the opposite orientation with their N-termini in the cytoplasm, their C-termini in the ER lumen and typically possess a permanent insertion signal. Type 3 membrane proteins span the membrane more than once (Garoff, 1985).

Viral membrane proteins are typically translated on membrane-bound ribosomes and co-translationallly inserted into the ER in an unfolded form. This co-translational translocation begins in the cytosol with the synthesis of the first hydrophobic segment of a nascent polypeptide, either a signal or transmembrane (TM) sequence. Translocation, folding and conformational maturation of these proteins occurs by the same mechanisms used by cellular membrane proteins. These processes are not spontaneous events but require the participation of numerous folding enzymes and molecular chaperones within the ER (Doms *et al.,* 1993). An increasingly complex macromolecule, the translocon (Walter & Lingappa 1986) is responsible for the transport and biogenesis of proteins at the ER membrane. The translocon recognises potential membrane-spanning domains in membrane proteins, orientates these domains with respect to each other and the ER

membrane and facilitates their integration into the lipid bilayer (Hedge & Lingappa, 1997).

Once inserted into the ER membrane, folding of the various topological domains of a membrane protein occurs under different conditions in different environments, namely the ER lumen, the ER membrane or the cytosol. The ectodomain of the protein folds in the ER lumen and typically comprises the bulk of the protein's mass and all of the carbohydrate moieties and disulphide bonds. The transmembrane domain or domains adopt an α-helical configuration within the hydrophobic interior of the ER membrane, each domain containing at least 20 to 22 hydrophobic amino acids flanked by charged residues. The cytoplasmic domain of the protein folds within the cytosol, presumably according to the same rules that apply to cytosolic proteins and often contains sites necessary for interaction with viral components (Doms *et al.,* 1993).

After folding in the ER, membrane proteins are often assembled into oligomers immediately or during transit in the Golgi apparatus. Oligomerisation may be as a result of disulphide bond formation or, more commonly, non-covalent interactions. For example, coiled-coil domains often stabilise the protein and allow for protein dimerisation where the α-helical coils wind around each other (Bassel-Duby *et al.,* 1985).

Post-translational targeting occurs via the default pathway used by cellular membrane proteins, unless the protein contains additional sorting signals. This pathway is from the ER to the Golgi apparatus, across the Golgi from the cis to the medial and finally the trans components and on to the cell surface. In the Golgi apparatus further modifications such as glycosylation may occur (Hedge & Lingappa, 1997). Once correctly folded, modified, assembled and targeted to the cell membrane the VMP can perform its specific function.

The functions of viral membrane proteins are diverse and include binding viral particles to receptors on the host cell plasma membrane, mediating membrane fusion, directing virus morphogenesis at the budding site and acting as receptor-destroying enzymes for virus release (Doms *et al.,* 1993). A further, novel function for VMP was discovered by Pinto and co-workers in 1992, when it was found that the small integral membrane protein, M2, of Influenza A virus had ion channel activity that allowed the protein to modify the permeability of the membrane into which it was inserted.

Subsequent to this, many small viral membrane proteins have been discovered that modify membrane permeability. This membrane permeabilisation may play a critical role not only in the viral life cycle but also in viral pathogenesis.

1.5 MODIFICATION OF MEMBRANE PERMEABILITY BY ANIMAL VIRUSES:

A number of animal viruses induce membrane permeability changes during infection. These modifications are observed either early during the infection of host cells or later in the replicative cycle following viral gene expression (Carrasco, 1994). Early and late membrane permeabilisation occur via different mechanisms. Early membrane permeabilisation may be as a result of co-entry of toxins with virus particles during infection. Late membrane permeabilisation requires the expression of viral genes and, therefore, one or more viral protein is responsible for the permeability changes observed. A greater understanding of the changes that accompany the disruption of the cell membrane by a viral protein is necessary.

Alterations in the permeability of host cell membranes most commonly enhance the permeability of the cell to monovalent cations with a subsequent decrease in membrane potential (Carrasco *et al.,* 1989). Sodium ions accumulate in the cell while potassium ions leak out. Viral mRNAs translated late during infection are, therefore, adapted with special structures for optimum translation under these altered conditions (Carrasco, 1994). Late virus enduced membrane permeabilisation may also affect the concentration of calcium ions, the pH of infected cells and enhance the permeability of the cell to other compounds for example hydrophilic antibiotics such as Hygromycin B (Carrasco, 1994). Viral gene products involved in the modification of membrane permeability may, furthermore, activate phospholipase C and, possibly, phospholipase A2 leading to the release of choline and the formation of high concentrations of inositol-3-phosphate (IP3) and arachidonic acid in the medium. This, in turn, would lead to the formation of prostaglandins or diacylglycerol and lysophosphatidylcholine which destabilise and permeabilise the membrane (Carrasco, 1994).

1.5.1 Viroporins:

Viroporin is the name given to a family of virus proteins that alter membrane permeability (Carrasco, 1989). In many cytolytic viruses a single gene product or viroporin is the primary cause of the cytopathic effect (CPE) observed. General characteristic structures or structural motifs of viroporins have been identified (Carrasco, 1994):

- Viroporins are generally short proteins of between 50 and 120 amino acids
- Viroporins frequently contain a higher than normal content of leucine and isoleucine residues and a lower overall glycine content
- Viroporins are integral membrane proteins with at least one membrane spanning domain, which may form an amphipathic helix
- Viroporins often occur as oligomers, usually tetramers, that form hydrophilic pores allowing non-specific diffusion of low molecular weight compounds and ions
- Viroporins may contain regions of basic amino acids that could destabilise the lipid bilayer.

Viroporins appear, therefore, to possess activities like some ionophores or membrane-active toxins. The primary function of viroporins is to permit the release of mature virions from infected cells, accompanied by modifications in the morphology and metabolism of the cell. The rotavirus protein NSP4 and the influenza virus protein M2 discussed earlier are examples of viroporins. Other examples include: HIV Env and Vpr proteins (Piller *et al.,* 1996), poliovirus 2BC (Barco & Carrasco, 1998), hepatitis virus A 2C (Jecht *et al.,* 1998), vaccinia virus A38L (Sanderson *et al.,* 1996), togavirus 6K protein (Sanz *et al.,* 1994) and Japanese encephalitis virus NS2B-NS3 (Chang *et al.,* 1999). Some of these proteins, for example NSP4 (Ball *et al.,* 1996) and Vpr (Piller *et al.,* 1998), have been shown not only to alter membrane permeability when expressed in cells as recombinants but also when added extracellularly to cells in purified form. All these proteins play an integral role in the viral replication cycle and possibly in the pathogenesis of the related disease.

1.6 DUAL IN-FRAME TRANSLATION INITIATION

1.6.1 Mechanisms for translation initiation at dual initiation site:

Three mechanism for generating more than one protein from a single mRNA in eukaryotes have been described. These are context-dependant leaky scanning, reinitiation and possibly direct internal initiation (Kozak, 1999). All three mechanisms represent an escape from the constraints imposed by the first-AUG rule in eukaryotes.

Reinitiation involves the production of two proteins from separate ORFs on the same mRNA (Kozak, 1987) and will not be discussed here. Direct internal initiation was first proposed for the translation of the picornavirus polyprotein. In this model the ribosome and other protein factors recognise a nucleotide sequence with significant secondary structure, termed the internal ribosome entry site (IRES), on the substrate mRNA. This internal ribosome entry is believed to facilitate translation initiation at internal start codons on the mRNA independent of the m^7cap structure (Gale *et al.*, 2000). Although interesting, further experimental evidence is necessary to substantiate this hypothesis (Kozak, 1999). Little consensus exists between the IRES sites identified.

Leaky scanning is the most frequently observed mechanism and occurs when the 40S ribosomal subunit bypasses the first AUG and instead initiates at a downstream AUG codon. The absence of a good context around the first AUG is the most probable cause of leaky scanning (Kozak, 1995, Kozak, 1999). Initiation sites in eukaryotic mRNAs usually conform to all or part of the sequence GCCRCCaugG (Kozak, 1987). The most highly conserved positions within this consensus sequence are the purine, usually A, at –3 and the G at +4 (where the AUG codon is numbered +1 to +3). Mutations affecting these two positions strongly impair initiation (Kozak, 1999) while the rest of the sequence contributes only marginally. An AUG codon can, therefore, be classified broadly as weak or strong based on positions –3 and +4.

1.6.2 Examples of dual initiation in viruses:

The use of in-frame AUG codons for the production of long and short protein isoforms appears to be more common in viruses than in cellular mRNAs (Kozak, 1987, refer to Table 1.1). This allows the virus to maximise its genome coding capacity and potentially encode functionally distinct proteins from a common mRNA. Some examples are discussed here to illustrate this.

a. Foot-and Mouth Disease Virus L proteins:

Initiation of translation can occur at more than one start codon in some picornaviruses, probably the best example being the Leader protein in foot-and-mouth disease virus (FMDV). This protein is produced in two distinct forms, Lab and Lb. Lab has an additional 28 amino acids at its amino-terminus compared to Lb and both are encoded from dual initiation sites *in vivo* and *in vitro* (Belsham, 1992). The in-frame AUG is conserved in all 7 serotypes of FMDV. Studies indicate that leaky scanning is the mechanism for translation initiation (López de Quinto & Martinez-Salas, 1999). Expression of the two proteins separately was achieved through mutation of the start codons, however both Lab and Lb appear to function with the same activity and specificity (Medina *et al.,* 1993). Although the additional sequences in Lab are quite variable between different strains of FMDV (Sangar *et al.,* 1987), they therefore appear not to adversely affect the activity of the protein. It is unclear why FMDV has conserved this feature of dual initiation sites. Interestingly, the presence of the AUG corresponding to the second initiation codon, but not the first, is essential for viral replication (Cao *et al.,* 1995, Piccone *et al.,* 1995).

b. Hepatitis B Virus Surface Glycoproteins:

Hepatitis B virus (HBV) is an enveloped DNA virus. The nucleocapsid of this virus is surrounded by a host-derived lipid envelope containing three viral surface proteins, termed S, M and L. These three HBV surface antigens (HBsAgs) are translated from a single ORF from three in-phase start codons. The S protein is the smallest of these polypeptides and the most abundant. The next largest protein, M, contains the S domain

Table 1.1 Examples of genes that produce two proteins from the same open reading frame.

GENE	PROTEIN PRODUCT
Simian virus 40 late 19S mRNA	VP2 and VP3 (Sedman & Mertz, 1988)
Rotavirus SA11 segment 9	37K and 35K (VP7) (Kozak, 1991)
West Nile flavivirus	V2 core proteins (Kozak, 1991)
Dengue (type 3) flavivirus	C and C' (Kozak, 1991)
Foot-and-mouth disease virus	Lab and Lb (Belsham, 1992)
Hepatitis B virus	Human, S,M and L; Duck, S and L (Heermann *et al.*, 1984)
Feline leukemia virus	$gPr80^{gag}$, $gPr65^{gag}$ (Koza, 1991)
Rift Valley fever (bunya)virus	M proteins (Kozak, 1991)
Cucumber necrosis virus	p20 and p21 (Johnston & Rochon, 1996)
Cowpea mosaic virus RNA-M	95K and 105K (Kozak, 1991)
Barley stripe mosaic virus	βb and βb' (Petty & Jackson, 1990)
African horsesickness virus segment 10	NS3 and NS3A (Van Staden & Huismans, 1991)
Bluetongue virus segment 10	NS3 and NS3A (Mertens *et al.*, 1984; Van Dijk & Huismans, 1988)
Herpes simplex virus, thymidine kinase gene	43K, 39K and 38K (Haarr *et al.*, 1985)
Epstein-barr virus, BBXLF1	Deoxythymidine kinase (Holton & Gentry, 1996)
Rabies virus, P gene	P1 – P5 (Chenik *et al.*, 1995)
Rice Dwarf phytoreovirus, segment S11	P11a and P11b (Suzuki *et al.*, 1991)
Chicken brain cells	Creatine kinase (Kozak, 1991)
Human tumor cell lines	N-myc (Kozak, 1991)
Yeast	CCAse: Small (Kozak, 1991)
Yeast	MOD5p: Small (Kozak, 1991)
Plants	AlaRS: Small (Kozak, 1991)
Epithelial cells, annexin XIII	Annexin XIIIa and XIIIb (Lecat *et al.*, 2000)
Rat liver, fumarase	Cytosolic and mitochondrial fumarases (Suzuki *et al.*, 1992)
Aradopsis thaliana, valyl- and threonyl-tRNA synthetases	Mitochondrial and cytosolic forms (Soiciet *et al.*, 1999)
p55PIK, regulatory subunit of phosphoinositide 3-kinase	54kDa and 50kDa (Xia & Serrero, 1999)

and a hydrophilic extension of 55 amino acids arising from the translation of the PreS2 domain. The L protein is the largest of the HBsAgs and contains a domain of 119 residues encoded from the PreS1 region in addition to the 55 PreS2 amino acids and the N-terminal S domain (Heermann *et al.,* 1984). The S protein is the major constituent of infectious virions. The L protein is necessary for virion maturation, while S also plays a role in this but alone is not sufficient (Ueda *et al.,* 1991). The M protein appears to be dispensable and is not found in all HBV subtypes (Santantonio *et al.,* 1992; Summers *et al.,* 1991). Virions contain differential amounts of the three surface proteins. Initiation codon context and leaky scanning are the prominent factors involved in the differential synthesis of the HBsAgs and represent a type of translational control (Sheu & Lo, 1992; Gallina *et al.,* 1992). Poisson and co-workers (1997) demonstrated that both PreS1 and S domains interact with core particles and propose that this double interaction may be necessary for virion morphogenesis. PreS1 peptide binds specifically to plasma membranes derived from human liver cells and may be responsible for receptor binding during infection (Lin *et al.,* 1991). The PreS2 domain found in the L and M proteins contains a cell permeable motif that may play a crucial role in the internalisation of the viral particle (Oess & Hildt, 2000). The S and L proteins are, therefore, both essential and functionally distinct in HBV.

c. Rabies Virus Phosphoprotein:

The P gene of Rabies virus encodes five related proteins (P1-P5) from alternative in-frame AUG codons *in vivo* (Chenik *et al.,* 1995). Mutational analysis identified leaky scanning as the mechanism for translation initiation. Immunofluorescence studies indicated that these P products were found in the cytoplasm of transfected cells, however, the proteins initiated from the third, fourth and fifth AUG codons were found mostly in the nucleus. The N-terminal deletions could remove a cytoplasmic retention signal or expose a nuclear localisation signal. However, no such domains were found by sequence searches of the P gene. The migration of these small proteins may simply be due to passive diffusion, although deletion of the 120 C-terminal amino acids of the P protein did not result in migration to the nucleus. This nuclear localisation may have biologic effects on virus multiplication (Chenik *et al.,* 1995).

d. Simian Virus 40 VP2 and VP3:

Structural proteins VP2 and VP3 of Simian Virus 40 (SV40) are encoded within the same open reading frame by dual in-frame initiation so that the amino acid sequence of VP3 corresponds to the C-terminal two-thirds of VP2 (Sedman & Mertz, 1988). VP2 and VP3 are found in infected cells at a steady-state ratio (Dabrowski & Alwine, 1988). Leaky scanning and not proteolytic processing was found to be the mechanism for VP2 and VP3 synthesis. Good and co-workers (1988) propose that the ratio of synthesis of VP2 relative to VP3 is largely determined by the efficiency with which ribosomes initiate translation at the two start codons, and so may represent a means of translational regulation. SV40 appears, therefore, to co-ordinate the expression of pairs of genes so that each structural protein is present at the correct molar ratio for virion production (Sedman & Mertz, 1988).

1.6.3 Examples of dual initiation in eukaryotes:

The use of alternative translation initiation at two in-phase AUG codons is a less common occurrence in cellular mRNAs, probably due to less stringent genome size restrictions. Some examples where this has been found to occur are: rat liver fumarases (Suzuki *et al.,* 1992), valyl- and threonyl-tRNA synthetases (Souciet *et al.,* 1999), and annexin XIII (Lecat, 2000) (Table 1.1). An interesting similarity between some of the examples mentioned here is that the two protein isoforms are differentially localised, due to the presence of either retention, secretion or signal sequences at the N-terminus of the longer isoform. This dual targeting seems to be one of the mechanisms used by eukaryotic cells to localise proteins to different cellular compartments where the same function is required (Small *et al.,* 1998).

1.6.4 Functional differences in protein isoforms:

From the examples discussed above, it is clear that the use of alternate in-frame start codons represents a general mechanism used in viruses for producing related polypeptides with similar but distinctly different biological properties. This would increase

the potential complexity of protein function with minimal redundancy of genetic information (Haarr *et al.,* 1985). Increased complexity and functional differentiation could, for example, be achieved in the following ways:

- Through oligomerisation where the presence of different polypeptide monomers could extend the range of potential complexes formed.
- Through a functional domain in the N-terminal region that could for example control basal protein turnover, the localisation of the full-length protein or even change the activity or specificity of the protein.
- Through alterations in the ratio of full-length to shorter proteins, thus offering an additional level of regulation.
- Through the usage of the second AUG in a cell-type dependant manner.

The simplicity of this mechanism allows viruses to sample new versions of a polypeptide as they evolve.

1.7 AIMS OF THIS STUDY

The wide conservation of the second start codon in the NS3 gene of orbiviruses particularly in AHSV, indicates a possible distinct role for NS3 and NS3A in the viral life cycle. When expressed in insect cells as baculovirus recombinants, both proteins have been shown to be cytotoxic, causing membrane permeabilisation and cell death. This appears to be unique to the NS3 proteins of AHSV when compared to the cognate proteins of other orbiviruses. NS3 and NS3A of AHSV may be more closely related, on a functional level, to the NSP4 protein of rotavirus. In fact, NS3 and NS3A appear to share many of the characteristics of the lytic viroporin proteins discussed and may play an important role in the virulence and pathogenicity of AHSV. The effect of the AHSV NS3 proteins on mammalian cells has, as yet, not been studied.

The aims of this study were to characterise and compare the NS3 and NS3A proteins of AHSV, in terms of their cytotoxicity and localisation in infected cells. This implies elucidating an approach for distinguishing between these almost identical proteins in AHSV infected cells. In order to achieve these aims the following aspects were investigated:

1. The effect, if any, of extracellular NS3 on the membrane permeability of mammalian cells (Chapter 2).

2. A comparison of the cytotoxic effect of individual and co-expression of NS3 and NS3A in insect cells (Chapter 2).

3. The individual expression of NS3 and NS3A and large scale purification of these proteins (Chapter 2).

4. The production of polyclonal antibodies directed against the N-terminal amino acids of NS3, for use in the investigation of the localisation of NS3 in AHSV infected cells (Chapter 3).

CHAPTER 2:

EXPRESSION OF AHSV-3 NS3 AND NS3A AS HISTIDINE TAG FUSION PROTEINS AND ANALYSIS OF THEIR CYTOTOXIC EFFECT

2.1 INTRODUCTION:

The AHSV nonstructural proteins, NS3 and NS3A, are encoded from two in-frame overlapping reading frames on segment 10 (Van Staden and Huismans 1991). The cognate genes in related orbiviruses also encode two almost identical proteins, which differ only with respect to an additional short N-terminal extension in the longer isoform. The reason for this conserved feature is not yet clear and was addressed in this study.

The segment 10 products may be related to other cytolytic proteins or viroporins, based on the finding that NS3 and NS3A are cytotoxic to insect cells, together with the presence of characteristic viroporin structural features in these proteins (Van Niekerk *et al.*, 2001a). The effect of NS3 and NS3A on mammalian cell membranes has not yet been investigated, and the proteins have not been expressed in a mammalian expression system. Several cytolytic proteins such as NSP4 of rotavirus (Tian *et al.,* 1996; Tafazoli *et al.,* 2001) and HIV-1 virus protein R (Vpr) (Macreadie *et al.,* 1996) have been shown to exert their membrane destabilising activity on prokaryotic and eukaryotic cells when expressed endogenously and when added, in purified form, exogenously to cell cultures. The effect of the exogenous addition of NS3 on the membrane permeability of mammalian cells was therefore investigated here.

Expression of the segment 10 gene from a recombinant baculovirus in insect cells results in the synthesis of NS3 only, at low levels (Van Staden *et al.,* 1995). Expression of NS3A was achieved by the removal of the nucleotides preceding the second initiation codon (Van Niekerk *et al.,* 2001a). Both proteins were found to be cytotoxic to insect cells when expressed individually, causing cell membrane permeability and eventual cell death (Van Staden *et al.,* 1995;

Van Niekerk *et al.,* 2001a). In this study the cytotoxic effect on insect cells of co-expression of NS3 and NS3A was investigated, as AHSV infected cells show expression of both proteins in equimolar amounts. This was achieved by co-infection of insect cells with recombinant baculoviruses expressing NS3 and NS3A, and monitoring cell death.

The availability of purified NS3 and NS3A would allow for further comparative and functional studies. The NS3 and NS3A proteins were, therefore, expressed as histidine fusion proteins in the baculovirus expression system.

The Bac-to-Bac™ baculovirus expression system provides a way of producing high levels of protein expression in an eukaryotic expression system. This has the advantage over prokaryotic systems in that the recombinant proteins are processed more correctly with respect to post-translational modifications such as disulphide bonds, glycosylation and phosphorylation and are therefore also likely to fold properly. It has been reported that many recombinant proteins expressed by means of the baculovirus expression system are functionally similar to their authentic counterparts (O'Reilly *et al.,* 1992; Luckow *et al.,* 1993). The production of recombinant baculoviruses expressing NS3 and NS3A as histidine tag fusion products would allow for the purification of the proteins and subsequent functional studies.

2.2 MATERIALS AND METHODS

2.2.1 Materials obtained:

Plasmids:
pAM25 (Dr V van Staden, Department of Genetics, University of Pretoria) AHSV-3 NS3 gene cloned into the *Bam*HI site of pUC13.
pBS-NS3H (AE Mercier, Department of Genetics, University of Pretoria) AHSV-3 NS3 gene cloned into *Bam*HI site of pBS, sequence not confirmed.
pBacHTc-NS3 (AE Mercier) AHSV-3 NS3 gene, subcloned from pBS-NS3H, into *Nar*I and *Bam*HI sites of baculovirus transfer vector pFastBacHTc, sequence not confirmed.

Recombinant baculoviruses:
Bac-NS3 (CC Smit, Department of Genetics, University of Pretoria) recombinant baculovirus expressing AHSV-3 NS3 from polyhedrin promoter.
Bac-NS3A (CC Smit) recombinant baculovirus expressing AHSV-3 NS3A (truncated S10 gene lacking first 30 nucleotides) from polyhedrin promoter.

Antisera:
α-β-gal-NS3: (Dr V van Staden) polyclonal antiserum raised in rabbits to a denatured form of a bacterially expressed β-galactosidase-NS3 fusion protein.
α-NS3: (Dr V van Staden) polyclonal antiserum raised in rabbits to a denatured form of AHSV-3 NS3 expressed in insect cells as a recombinant baculovirus protein.

Primer:
NS3PEco: (M van Niekerk, Department of Genetics, University of Pretoria) primer complementary to the 3' end of AHSV-2/3 S10 gene, for the amplification of NS3/A gene, that includes an *Eco*RI site for cloning purposes.

2.2.2 Exogenous addition of NS3 to Vero cells

2.2.2.1 Cells and viruses:

The GIBCO BRL BAC-to-BAC^{TM} baculovirus expression system was used for all protein expressions (Life Technologies, Luckow *et al.*,1993). *Spodoptera frugiperda* (*Sf9*) cells were used for baculovirus infections (American Type Culture Collection (ATCC), CRL1711, supplied by Sterilab). *Sf9* cells were maintained in confluent monolayers or as suspension cultures in spinner flasks at 27°C in Grace's insect medium containing 10% foetal calf serum (FCS), as well as antibiotics and fungizone (Highveld Biologicals). Cell culture techniques are essentially as described in the BAC-to-BAC^{TM} baculovirus expression system manual (GIBCO BRL, Life Technologies).

Cell density and viability were determined by the addition of the vital exclusion dye, Trypan Blue (0.4%), in a 1:1 ratio and inspection under a haemocytometer. Cells that were able to exclude the dye were considered viable. Typically spinner or shaker cultures were seeded at $0.2x10^6$ cells/ml and allowed to grow to a density of $2x10^6$ cells/ml in a final volume of 50-100 ml.

2.2.2.2 Preparation of *Sf9*-cell lysates containing NS3

Sf9 cell monolayers seeded at 1×10^7 cells in 75 cm^3 flasks were infected with wildtype baculovirus, or infected with a recombinant baculovirus expressing NS3 (Bac-NS3) at a Multiplicity of Infection (MOI) of 4 plaque forming units per cell (pfu/cell). The cells were harvested 30 hours post infection (h.p.i), resuspended in lysis buffer without detergent (50 mM Tris-HCl, pH 7.5; 300 mM NaCl; 1 mM PMSF, 1 mM 2-mercaptoethanol) at 2×10^7 cells/ml and mechanically lysed with a dounce homogeniser. Protein expression was

confirmed by SDS-polyacrylamide gel electrophoresis (SDS-PAGE) and Western blot. Cell lysates were placed on ice and used immediately.

2.2.2.3 SDS-PAGE:

Protein expression from recombinant baculoviruses was analysed by electrophoresis under denaturing conditions in SDS-PAGE gels. As described by Sambrook *et al.* (1989) this method allows for the separation of proteins based on their molecular size. 12% or 15% separating (12% or 15% polyacrylamide; 0.375 M Tris-HCl, pH 8.8; 0.1% SDS; 0.008% TEMED; 0.08% ammonium persulphate) and 5% stacking (5% polyacrylamide; 0.125 M Tris-HCl, pH6.8; 0.1% SDS; 0.008% TEMED; 0.08% ammonium persulphate) polyacrylamide gels were prepared and cast between 7x10 cm glass plates. Protein samples were denatured in an equal volume of Protein Solvent Buffer (0.125 M Tris, pH 8; 4% SDS; 20% glycerol; 10% 2-mercaptoethanol) by heating at 96°C for 5 min. DNA was degraded by sonication for 10 min to decrease the viscosity of the sample. The denatured samples were then electrophoresed at 120-130 V in 1xTGS (0.3% Tris; 1.44% Glycine; 0.1% SDS) using the Hoefer Mighty Small^{TM} II SE 250 unit for 2 hours.

2.2.2.4 Western immunoblots:

Protein samples for immunoblotting were first separated by SDS-PAGE (2.2.2.3). Proteins were then transferred to Hybond-C membranes (AEC Amersham) in a submerged blotting apparatus (EC 140 miniblot module). After transfer was completed the gel was removed and stained in 0.125% Coomassie Blue, 50% methanol, 10% acetic acid and destained in 5% acetic acid, 5% methanol to verify transfer. The membrane was washed for 5 min in 1x PBS and non-specific binding sites blocked by incubation at room temperature for 30 min in 1% blocking solution (1% milk powder in 1x PBS). The membrane was then incubated overnight in a 1/100 dilution of the primary antibody, in this case a rabbit monospecific serum directed against a β-gal-NS3 fusion protein, in 1% blocking solution. The antiserum was then removed and the membrane washed three times for 5 min each in wash buffer (0.05% Tween in 1x PBS). A secondary antibody solution, a 1/1000 dilution of protein A conjugated to horseradish peroxidase (Cappel) in blocking solution, was then incubated with the membrane for 1 h. Unbound antibody was removed by washing three times in wash buffer and once in 1x PBS for 5 min each. Antibody binding was visualised by the addition of enzyme substrate (a mixture of 60mg 4-chloro-1-naphthol in 20ml methanol and 60µl hydrogen peroxide in 100ml 1xPBS). The reaction was allowed to proceed until bands became visible. Blots were rinsed with dH_2O and air-dried.

2.2.2.5 Preparation of Vero cells

Vero cells were maintained as confluent monolayers in 75cm^3 flasks at 37°C with 5% CO_2 in MEM (minimal essential medium) supplemented with 5% FCS and antibiotics (Highveld Biologicals).

For membrane permeabilisation assays, Vero cells were seeded on 24-well plates at 50% confluency and incubated overnight at 37°C with 5% CO_2 in MEM growth medium supplemented with 5% FCS and antibiotics (Highveld Biologicals). Twelve wells were seeded for each time interval to be assayed.

2.2.2.6 Hygromycin B membrane permeabilisation assay

Membrane permeabilisation assays were modified from the method described by Chang *et al.*,(1999). Growth medium was removed from Vero cells and replaced with equimolar amounts of crude cell extracts from *Sf9* cells infected with wild type baculovirus or Bac-NS3 prepared under 2.2.2.2 and supplemented with MEM growth medium. Six wells of Vero cells were treated in this way for each time interval for each *Sf9* cell lysate preparation. After 45, 90, 135 and 180 min the lysates were removed and MEM medium without methionine added with or without Hygromycin B (Hyg B;500µg/ml, Roche Diagnostics), each in triplicate for each of the wildtype baculovirus or Bac-NS3 infected *Sf9* cell lysate preparations. Cells were starved of methionine in the presence or absence of Hyg B for 30 min. The medium was replaced with MEM without methionine and 100 µCi ^{35}S-methionine (Separations) and labelling allowed to occur for 30 min. Vero cells were kept at 37°C with 5% CO_2 throughout the assay. The medium was removed and the cells rinsed twice in PBS to remove any remaining traces of ^{35}S-methionine. The cells were lysed in 50 µl lysis buffer (1% Nonidet P-40; 150 mM Tris-HCl pH 7.5; 1 mM EDTA with 20 µg/ml PMSF). A 50 µL TCA solution (5% trichloroacetic acid; 20 mM sodium pyrophosphate) was then added to this to precipitate proteins. A 50 µL sample of the precipitated proteins was blotted onto fibreglass discs (GF/C Whatman). The discs were washed with 70% ethanol, air-dried and placed in scintillation fluid (Beckman) and counted in a Beckman 3801 β counter. The percentage ^{35}S-methionine incorporated into permeabilised cells was calculated as follows:

$$\text{Percentage permeabilised VERO cells} = \frac{\text{Incorporation of } S^{35} \text{ in presence of Hyg B}}{\text{Total protein (Incorporation in absence of Hyg B)}} \times 100$$

Calculated values were used to plot ^{35}S-methionine incorporation graphs.

2.2.3 Co-expression of AHSV-3 NS3 and NS3A in insect cells:

2.2.3.1 Determination of cell viability by trypan blue staining

50 ml spinner cultures of *Sf9* cells at 1 x 10^6 cells/ml were infected with baculoviruses at a MOI of 5-10 pfu/cell. 100 µl aliquots of infected cells were removed every 3 hours from 0-48 h.p.i and stained in an equal volume of 0.4% trypan blue in 1x PBS. The number of stained cells were counted using a haemocytometer and expressed as a percentage of the total cell population. Protein expression was confirmed by SDS-PAGE analysis and Western blot.

2.2.4 Cloning of the AHSV-3 NS3A gene into pFastBacHTc:

2.2.4.1 Polymerase chain reaction:

Two primers were designed to specifically amplify the region of the AHSV-3 S10 gene encoding NS3A. The primer sequences were 5'-CGTTCGAA ATGATGCATAATGAATC-3' (NS3Ahfor) and 5'-CG***GAATTC***GTAAGTCGTTA TCCCGG-3'(NS3pEco). The sequences incorporated a *Sfu* I site (underlined) at the 5' end and an *Eco*RI site (bold italic) at the 3' end of the gene for insertion of the NS3A gene into the pBS and pFASTBAC HTc vectors. PCR reactions were set up as follows: 50 ng pAM25, 50 μmol of each dNTP, 1.5 mM $MgCl_2$, 10 μl 10 x reaction buffer (Promega) and 100 pmol of each primer were mixed and made up to 99.5 μl with UHQ. The DNA template was denatured at 95°C for 5 min in a thermocycler ("hot start" PCR) and 0.5 μl *Taq* DNA polymerase (5U/μL, Promega) added. A Hybaid (Omnigene) programmable thermocycler was used to perform 30 cycles of PCR. The primary denaturation was followed by an annealing cycle of 45 sec at 53°C as determined by the primer sequence. Primer extension occurred at 72°C for 45 sec. This primary cycle was followed by 28 cycles where denaturation took place at 95°C, primer annealing at 55°C for 45 sec and extension at 72°C for 3 min. The final cycle allowed for elongation for 5 min. PCR products were then analysed by 2% agarose gel electrophoresis in 1XTAE (0.04 M Tris-acetate, 1 mM EDTA, pH 8.5) using a Biorad Mini Sub™ electrophoresis unit. The addition of 1% Ethidium Bromide to the agarose gels allowed for the visualisation of the DNA under UV light. The size of the DNA fragments was estimated by comparison of their migration during electrophoresis with standard molecular weight size markers (*Hae*III digested ϕX174, Promega and Lambda *Hin*dIII digested DNA (SMII), Roche).

2.2.4.2 Plasmid DNA isolation:

Single bacterial colonies were selected from LB-agar plates. These colonies were used to inoculate 3ml liquid cultures in Luria-Bertani (LB) medium (1% bacto-tryptone (m/v), 0.5% bacto-Yeast extract (m/v), 1% NaCl (m/v), pH 7.4) in the presence of ampicillin (100 μg/ml) and/or tetracyclin (12.5 μg/ml). Cultures were amplified at 37°C overnight.

Plasmid isolations were done according to the alkaline-lysis method of Birnboim and Doly (1979) as described by Sambrook *et al.* (1989). Briefly, the overnight cultures were harvested by bench-top centrifugation for 1 min, and the pellet suspended in 100 μL of ice-cold lysis buffer containing 25 mM Tris-HCl, pH 8.0, 50 mM glucose and 10 mM EDTA. This mixture was incubated at room temperature for 5 min and on ice for 1 min. 200 μl 0.2 N NaOH, 1% SDS (alkaline-SDS buffer) was added to lyse the resultant spheroplasts, and incubated on ice for a further 5 min. Precipitation of protein, high molecular weight RNA and bacterial genomic DNA with 150μl ice-cold 3 M NaAc pH 4.8 for 5 min on ice, allowed for the removal of these contaminants. Plasmid DNA was then separated from the SDS-precipitated contaminants by centrifugation for 10 min. Plasmid DNA in the recovered supernatant was precipitated by the addition of 2 volumes of 96% ethanol at –20°C for 30 min. The precipitate was collected

by desktop centrifugation, washed with 80% ethanol, dried under vacuum, and resuspended in 30 µl 1XTE buffer (10 mM Tris, pH7.4, 1 mM EDTA, pH 8). Isolated plasmid preparations were analysed by 1% agarose gel electrophoresis (2.2.4.1).

2.2.4.3 Phenol-chloroform extraction:

Deproteination of DNA was achieved by phenol-chloroform extractions. An equal volume of a 1:1 phenol and chloroform mixture was added to the DNA samples to denature any proteins present. The denatured proteins in the phenol were separated from the DNA by desktop centrifugation, and the upper aqueous layer containing the DNA removed. 1 volume of chloroform was added to the DNA to remove any residual phenol. Precipitation of the DNA was carried out in 2 volumes 96% ethanol in the presence of 1/10 volume 3M NaAc. After centrifugation for 30 min the DNA was washed with 80% ethanol, vacuum-dried and resuspended in TE buffer (Ausubel *et al.*,1988).

2.2.4.4 Optical density analytical measurements of plasmid DNA concentration:

The concentration of DNA in purified samples was determined by measurement of the optical density at 260 nm (OD_{260}). The DNA sample was diluted 100x in Ultra High Quality H_2O (UHQ) and the OD_{260} determined using pure UHQ H_2O as the calibration medium. The concentration of the DNA was calculated using the extinction coefficient for double stranded DNA, $1A_{260} \equiv 50$ µg/ml and multiplication with the dilution factor. The purity of the sample was estimated by measuring the OD_{280} and determining the ratio of OD_{260} to OD_{280}. A ratio above 1.6 was taken as indicative of protein contamination and the DNA purified further using the phenol-chloroform extraction method (2.2.4.3). The presence of residual salt was evaluated by determining the OD_{320}. Samples with a reading higher than 0.001 were re-precipitated and washed in 70% ethanol to ensure the removal of the salt.

2.2.4.5 Klenow enzyme fill-in reactions:

Klenow enzyme was used to fill in overhangs to create blunt ends. Approximately 1 µg of DNA from PCR reactions was mixed with 2 µl Klenow enzyme(2 U/µl), 3 µl 10x buffer B (10 mM Tris HCl, 5 mM MgCl, 1 mM 2-mercaptoethanol)(Boehringer Mannheim), 2 µl dNTPs (5 mM of each dNTP) and made up to 30 µl with ddH_2O. The reaction was performed at 37°C for 30 min after which the enzyme was heat inactivated at 60°C for 10 min and the DNA allowed to reanneal at room temperature for 10 min.

2.2.4.6 Restriction enzyme digestions:

All restriction enzyme reactions were carried out in the restriction enzyme's recommended salt buffer, at its optimal pH and temperature (Promega or Boehringer Mannheim). In general reactions were performed in a final volume of 20µl for 1-2 hours. Digested DNA products were analysed on 1% agarose

gels. The size of the DNA fragments was estimated by comparison of their migration during electrophoresis with standard molecular weight size markers (*Hae*III-digested ϕX174, Promega and *Hin*dIII-digested Lambda DNA (SMII), Roche).

2.2.4.7 Purification of DNA fragments from agarose:

Restriction fragments to be isolated were excised from 1% agarose gels with a razor and purified using the Geneclean™ II reaction Kit (Bio101). In this procedure a silica matrix (glassmilk) is used, that binds selectively and specifically to ds- and ssDNA. The excised gel was melted at 55°C in 2.5 volumes 6M NaI. The DNA was then allowed to bind to 5 µl glassmilk at room temperature for 30 min, followed by 5 min on ice. DNA bound to the glassmilk was then collected by desktop centrifugation and washed 3x with 500 µl NEW Wash solution (NaCl, EDTA, EtOH and H_2O). The washed DNA was then eluted in TE buffer or UHQ H_2O at 45-55°C.

2.2.4.8 Ligation of DNA fragments:

Purified restriction fragments were ligated to the linearised vector using 1µL of a 10x ligation buffer (66 mM Tris-HCl, pH 7.5; 5 mM $MgCl_2$; 1 mM ATP) and 1 unit of T4 DNA Ligase in a reaction volume of 10 µL (Boehringer Mannheim). Generally a ratio of 3:1 of insert DNA to vector was used. The reaction was carried out at 16°C for 16 hours.

2.2.4.9 Preparation of competent cells:

The $CaCl_2$ method described by Sambrook *et al* (1989) was used to prepare competent XL1-Blue (*E. coli*) cells. 1 ml of an overnight culture was used to inoculate 100 ml LB-broth, and the cells allowed to grow to log phase (OD_{550} of 0.5) by shaking at 37°C. Cells were then collected by centrifugation at 5000 rpm for 5 min, and resuspended in half the original volume of ice-cold 50 mM $CaCl_2$. After incubation on ice for 30 min, the cells were again collected by centrifugation and resuspended in 1/20 of the original volume in $CaCl_2$. Competent cells were snap-frozen in liquid Nitrogen and stored at -70°C in glycerol or placed on ice for 1 h prior to use.

2.2.4.10 Transformation of recombinant DNA into competent cells:

100 µl of competent cells were mixed with 5 µl of ligation mixture and placed on ice for 30 min to allow for the binding of the DNA to the cell membranes. Transformation of the DNA into the cells was made possibly by a brief heat shock for 90 seconds at 42°C, followed by 2 min on ice. 1 ml pre-warmed LB-broth was then added and the culture incubated for 1 h at 37°C, to allow for the expression of the antibiotic resistance genes. 150 µl samples of the cultures were plated onto LB-agar plates (1.2% agar in LB medium) containing 100 µg/ml ampicillin and 12.5 µg/ml tetracyclin. 50 µl 2% X-gal (5-bromo-4-chloro-3-indolyl-β-D-galactoside) and 10 µl 100mM/2% IPTG (isopropyl-β-D-thiogalactopyranoside) was added to plates streaked with XL1-Blue cells

transformed with pBS recombinants for blue-white selection. Plates were incubated at 37°C overnight. Recombinants that were successfully transformed with pBS with the insert were identified as white colonies that grew in the presence of the appropriate antibiotics. For XL1-Blues transformed with pFastBac recombinants selection was performed by restriction digestion of plasmid DNA.

2.2.5 DNA sequencing:

2.2.5.1 Plasmid purification for cycle sequencing

Plasmid DNA used for sequencing was purified using one of the two commercially available kits for the isolation of high quality DNA (Quigen plasmid mini purification protocol; Boehringer Mannheim High Pure Plasmid Isolation Kit Protocol). The kits were used according to the instructions supplied by the manufacturer, the principle being essentially the same as the alkaline-lysis method described above. In short, the cells were grown as before but lysed in an RNase-containing lysis buffer (50 mM Tris-HCl, pH 8.0; 1.0 mM EDTA; 100 µg/ml RNase A). Purification columns containing either anion exchange resin under the appropriate pH and low salt conditions (750 mM NaCl; 50 mM MOPS, pH 7; 15% isopropanol; 0.15% Triton X-100, Qiagen) or a "high pure filter-tube" where nucleic acids are specifically bound to the surface of glass fibres or silica materials in the presence of a chaotropic salt (Boehringer Mannheim) were used to bind the plasmid DNA. Unbound traces of proteins, RNA, dyes and low molecular weight impurities were removed by washing the column with a medium salt buffer (1.0 M NaCl; 50 mM Tris-HCl, pH 8.5; 15% isopropanol). Elution of the plasmid DNA was then achieved either by direct elution in UHQ H_2O (Boehringer Mannheim) or by a high salt buffer treatment (1.25 M NaCl; 50 mM Tris-HCl, pH 8.5; 15% isopropanol) followed by precipitation to remove salt in 0.7 volumes isopropanol at room temperature, washing in 70% ethanol, freeze-drying and resuspension in UHQ H_2O (Quigen).

2.2.5.2 Automated sequencing

DNA sequencing was performed by cyclic enzymatic extension reactions using dye-labelled terminators. The sequence reactions were analysed using the ABI Prism™ 310 Genetic Analyser (Perkin-Elmer). The automated cycle sequencing method was adapted from the Sanger method of sequencing (Sanger *et al.,* 1977; Prober *et al.,* 1987).

Briefly, 300 ng purified plasmid DNA was mixed with 8.0 µL Terminator ready reaction mix (A/C/G/T-dye terminators, dITP, dATP, dCTP, dTTP, Tris-HCl (pH 9.0), $MgCl_2$, thermal stable pyrophosphatase, and AmpliTaq DNA polymerase FS). 3.2-5 pmol M13 specific forward or reverse primers were used to sequence recombinant pBS subclones, as pBS contains the same MCS as M13 vectors (Stratagene). The final volume was made up with ddH_20 to 20 µl. The MJ-PTC-200 Thermal cycler was used for the cycle sequencing reactions (Peltier thermal cycler) using thin wall 500 µl eppendorf tubes. Thermal cycling

was performed according to the protocol specified by the Perkin Elmer thermal cycler.

Thermal cycling was started with a rapid thermal ramp to 96°C followed by 30 seconds at 96°C to denature the template. This was followed by a rapid ramp to 50°C. Elongation was accomplished by a rapid ramp to 60°C followed by 4 min at this temperature. This cycle was repeated for 25 cycles. After which a ramp to 4°C followed where the reaction was stopped and held until removed from the Thermal cycler.

The cycle sequencing reaction was precipitated by either NaAc or ammonium acetate (NH_4Ac) in 100% EtOH and vacuum dried. The dried sequencing extension products were resuspended in template suppression reagent (Perkin Elmer), heated to 95°C for two min to denature the DNA and placed on ice until ready for use. Sequencing reactions were then run on the ABI PrismTM 310 for analysis. The Sequencing Analysis and Sequence Navigator (Perkin Elmer) were used to analyse raw data produced and compare multiple sequences of different sequencing reactions of the same sequence as described in the ABI Prism Comparative PCR sequencing guide, Perkin Elmer (1995).

2.2.6 Baculovirus expression of histidine tagged NS3 and NS3A:

2.2.6.1 Preparation of competent DH-10Bac cells:

Competent DH10Bac™ cells were prepared according to the DMSO method of Chung and Miller (1988). A 3 ml overnight culture of DH-10Bac cells was used to inoculate 100 ml LB medium and allowed to grow to early log phase at 37°C. Cells were then collected by centrifugation at 5000 rpm for 5 min at 4°C. The pelleted cells were resuspended in 1/10 of the original volume of ice-cold TSB (1.6% Peptone; 1% yeast extract; 0.5% NaCl; 10% polyethyleneglycol; 1 M $MgCl_2$; 1 M $MgSO_4$) and incubated for 20 min on ice before transformation.

2.2.6.2 Transposition of recombinant genes into the bacmid DNA:

100 ng of each of the donor plasmids, pFastBac-HTc containing the NS3 and NS3A genes, was mixed with 100 µl competent DH10Bac™ cells and incubated on ice for 20 min. A heat shock for 45 sec at 42°C allowed for the transformation of the DNA into the cells. 900 µl TSBG growth medium (TSB with 20 mM glucose) was added to each transformation mixture and the cells incubated at 37°C for 4 hours. 100 µl of each culture was plated onto LB-agar plates containing 50 µg/ml kanamycin sulphate, 12.5 µg/ml gentamycin, 40 µg/ml IPTG and 50 µL of 2% X-gal per agar plate. The plates were incubated at 37°C for 24 hours. White colonies were selected and plated onto the same medium to ensure that they were recombinant composite Bacmid containing cells.

2.2.6.3 Isolation of composite bacmid DNA:

Recombinant colonies identified in 2.2.6.2 were used to inoculate 2 ml LB-broth containing 50 µg/ml kanamycin and 7 µg/ml gentamycin and incubated at 37°C for 16 h with shaking. The cells from 1 ml of these cultures were harvested

by desktop centrifugation for 1 min. The protocol adapted from Amemiya *et al.* (1994) for the isolation of high molecular weight Bacmid DNA was used (BAC-to-BAC™ Baculovirus expression system manual). In short, the DH10BAC cell pellet was resuspended in 300 µl of solution 1 (25 mM Tris-HCl, pH 8; 50 mM glucose and 10 mM EDTA) for disruption of the cell membranes. The addition of 300 µl of an alkaline-SDS buffer (0.2 N NaOH; 1% SDS) for 5 min at room temperature allowed for the denaturation of proteins and DNA. The pH of the solution was decreased through the addition of 300 µl solution 3 (3 M Potassium acetate, pH 5.5), so allowing for the precipitation of proteins and genomic DNA and the reannealing of the plasmid DNA. After incubation on ice for 10 min, the insoluble material was removed from the solution by centrifugation at maximum speed for 10 min. The plasmid DNA in the supernatant was precipitated in 800 µl isopropanol on ice for 10 min. The DNA was collected by desktop centrifugation for 15 min at maximum speed. The recombinant Bacmid DNA was then washed with 70% ethanol, air-dried briefly and resuspended in 40 µl TE buffer.

2.2.6.4 Transfection of *Sf9* cells with bacmid DNA:

Six well (35mm) tissue culture plates were seeded with $1x10^6$ cells/well in 2 ml Grace's medium with antibiotics (Highveld Biologicals) and allowed to attach for 1 h. Recombinant Bacmid DNA isolated in 2.2.6.3 was transfected into insect cells by lipofection (Felgner *et al.*,1987). For each transfection reaction 6 µl of Bacmid DNA was diluted in 100 µl Grace's medium without antibiotics. 6 µl CELLFECTIN™(BRL) reagent was mixed with 100 µl Grace's medium without antibiotics in a separate eppendorf. The diluted Bacmid DNA and CELLFECTIN™ were then mixed and incubated at room temperature for 30 min. 0.8 ml Grace's medium without antibiotics or serum was then added to the lipid DNA complexes. The attached cells were washed twice with Grace's medium without serum or antibiotics and overlayed with the lipid DNA complexes. The cells and DNA were incubated together at 27°C for 5 h after which the DNA was removed and replaced with 2 ml Grace's medium containing antibiotics and serum. The transfected cells were incubated for a further 96 h at 27°C. Recombinant Baculoviruses in the medium were removed and stored at 4°C for later use.

2.2.6.5 Amplification of baculovirus recombinants:

Virus stocks were produced by infecting monolayers of $1x10^7$ cells seeded in 75 cm^3 flasks at a low MOI of 0.1 pfu/cell. Amplification was carried out for 72 h at 27°C after which the medium containing the virus was clarified by centrifugation at 2000 rpm for 5 min and filter sterilisation. Virus stocks were stored at 4°C or at -70°C for long term storage.

2.2.6.6 Titration of viruses:

Sf9 cells were seeded in 35mm 6-well plates at a density of 1.5×10^6 cells/well and allowed to attach for 1 h. Dilution series of the viruses to be titrated were prepared, from 10^{-1} to 10^{-9} in 1 ml Grace's medium. The medium from each

well was removed and replaced with the virus dilutions. The plates were incubated at room temperature for 2 h, after which the inoculum was replaced with sterile 3% low melting agarose (Gibco BRL) at 37°C diluted in an equal volume Grace's medium. The infected cells were incubated at 27°C for 4 days and then stained overnight or for 3-5 hours with 1 ml Neutral Red (100 µg/ml in Grace's medium). Viral plaques appeared as light red patches in a darker red background.

2.2.6.7 Analysis of protein expression:

Sf9 cells were infected with recombinant baculoviruses in 6 well plates seeded at $1x10^6$ cells/well at a MOI of 5-10 pfu/cell. The cells were harvested after 72 h incubation at 27°C for the analysis of protein expression. Cells were collected by centrifugation at 3000 rpm for 5 min and resuspended in 1x PBS. The infected cells were then washed again in PBS and analysed immediately by SDS-PAGE (2.2.2.3) and Western blot (2.2.2.4) or stored at -20°C.

2.2.7 Protein solubility analyses:

2.2.7.1 Basic solubility assays:

Sf9 cells were seeded at a density of 1×10^7 cells in 75 cm^3 flasks and infected with recombinant baculoviruses at a MOI of 2-5 pfu/cell. Cells were harvested 48 – 72 h.p.i by centrifugation at 3000 rpm for 5 min. Cells were then resuspended in lysis buffer A [50 mM Tris-HCl (pH 7.5), 1 mM 2-mercaptoethanol and 1 mM PMSF (phenylmethylsulfonyl fluoride)] at 5 volumes lysis buffer/g cells and incubated on ice for 30 min. In order to investigate the solubility of the histidine tagged protein, in different detergents at different concentrations, this standard lysis buffer was adjusted to contain 0.1%, 0.25%, 0.5%, 1.0% or 2.0% Nonidet P-40 or Triton X-100 respectively. The cells were then mechanically lysed using a needle with a gauge of 22 (Promex) or disrupted with a dounce homogeniser. Insoluble proteins were collected by centrifugation at 2000g for 10 min and resuspended in an equal volume to the soluble proteins in the supernatant. Proteins were analysed by 12% SDS-PAGE (2.2.3.3) and Western blot (2.2.3.4). To determine the solubility of the HTc-NS3 protein in the presence of various salt concentrations (0.15 M, 0.3 M and 0.5 M NaCl) the solubility assay was repeated as above with lysis buffer A containing 1.0% Triton X-100 and the indicated salt concentrations.

2.2.7.2 Binding of HTc-NS3 to Ni^{2+}- resin

1×10^7 *Sf9* cells in 75 cm^3 flasks were infected with BacHTc-NS3, harvested 48 h.p.i. and resuspended in lysis buffer (lysis buffer A + 1.0% Triton X-100, 0.3 M NaCl). Cells were lysed as described in 2.2.7.1 and separated into soluble and insoluble fractions by centrifugation. Charged nickel resin (50, 100 or 200 µl, Gibco BRL, Life Technologies) was added to soluble proteins in the supernatant and allowed to bind for 30 min at 4°C. Samples were centrifuged at a low speed of 1000 rpm for 5 min to collect the resin and bound proteins. The unbound proteins in the supernatant were removed and retained. The resin was

then resuspended in and washed with wash buffer (20 mM Tris-HCl (pH 8.5); 500 mM KCl, 20 mM or 10 mM imidazole, 10 mM 2-mercaptoethanol, 10% (v/v) glycerol). The resin was collected by low speed centrifugation and the supernatant retained for later analysis. Bound proteins were then eluted through the addition of elution buffer (20 mM Tris-HCl (pH 8.5), 100 mM KCl, 100 mM imidazole, 10 mM 2-mercaptoethanol, 10% (v/v) glycerol) to the resin. Eluted proteins were separated from the resin by centrifugation at 1000 rpm for 5 min and retained for analysis. The elution was repeated to ensure that all bound proteins were removed. Samples collected at each stage during the assay were analysed by 12% SDS-PAGE and Western blot.

2.2.7.3 Comparison of solubility of HTc-NS3 and NS3:

In order to compare the solubility of the NS3 fusion protein (HTc-NS3) to the wild type NS3 protein, recombinant baculovirus infected cells were resuspended and lysed in lysis buffer A without detergent and separated into soluble and insoluble fractions as described above (2.2.7.1). Pellet fractions were then resuspended in lysis buffer A with 1.0% Triton X-100, 0.3 M NaCl and incubated on ice for 15 min. Samples were then fractionated again, to determine if the addition of detergent solubilised the protein. Alternatively infected cells were resuspended directly in lysis buffer A with 1.0% Triton X-100, 0.3 M NaCl, lysed and separated into soluble and insoluble fractions as before.

2.2.8 Sequence analysis of N-terminal residues of NS3 and NS3A

The N-terminal residues of NS3 and NS3A were analysed using the subcellular localisation site predictor programs, PSORT (http://psort.nibb.ac.jp/) and iPSORT (http://hypothesiscreator.net/iPSORT/).

PSORT is a computer program used to predict the subcellular localisation sites of proteins from their amino acid sequences using the *k*-nearest neighbours classifier (Horton and Nakai, 1996; Horton and Nakai, 1997). A subprogram within PSORT allows for the recognition or prediction of a signal sequence or leader peptide using McGeoch's method (McGeoch, 1985) with modifications. It considers the N-terminal positively-charged region (N-region) and the central hydrophobic region (H-region) of signal sequences. A discriminant score (termed the PSG score) is calculated from the three values: length of H-region, peak value of H-region and net charge of N-region. A large positive discriminant score means a high possibility to possess a signal sequence but is unrelated to the possibility of its cleavage. Next, PSORT applies von Heijne's method of signal sequence recognition (Horton & Nakai 1997). This is a weight-matrix method and incorporates the information of consensus pattern around the cleavage sites as well as the features of the H-region. Thus it can be used to detect signal-anchor sequences. A large positive output score (GvH score) means a high possibility that it has a cleavable signal sequence. The position of a possible cleavage site is also reported. Other PSORT subprograms allow for the prediction of

transmembrane segments and membrane topology amongst various other applications.

iPSORT is a subcellular localisation site predictor for N-terminal sorting signals. Given a protein sequence (maximum of 30 amino acids), it will predict whether it contains a signal peptide, using an alternative method to the ones described above.

The NS3 N-terminal residues were also scanned against protein profile databases (including Prosite) (http://isrec.isb-sib.ch/). The sequence was furthermore analysed using PattinProt (http://npsa-pbil.ibcp.fr), which scans a protein sequence or a protein database for one or several patterns. The consensus secondary structure of this region was also determined (http://npsa-pbil.ibcp.fr).

2.3 RESULTS

This part of the study aimed to further analyse the cytotoxic properties of AHSV NS3 and NS3A, and to compare these almost identical proteins. The effect of the exogenous addition of the NS3 protein to mammalian cells was investigated. The cytotoxicity of the endogenous proteins to insect cells when expressed either individually or together was also investigated and compared. To prepare large quantities of purified NS3 and NS3A, the NS3 and NS3A genes were cloned into the baculovirus histidine tag transfer vector pFASTBAC HTc. Expression of NS3 and NS3A as histidine fusion proteins would allow for their large scale purification on colomns, in a biologically active form for further functional analyses. The N-terminal region of the NS3 protein was also analysed computationally for the presence of a possible functional domain.

2.3.1 The effect of extracellular addition of NS3 on Vero cells

AHSV NS3 and NS3A have been shown to be cytotoxic to *Sf9* cells, causing membrane permeabilisation and eventual cell death (Van Staden *et al.*, 1995; Van Niekerk *et al.*, 2001a). BTV NS3, however, has not been reported to be cytotoxic when expressed in insect cells. The AHSV NS3 protein may be functionally related to the NSP4 protein of rotavirus (a member of the reoviridae family) discussed in section 1.3.2. The cytotoxic properties of NS3, however, require further investigation. One aspect of NS3 functioning that has not been addressed in the literature is whether the extracellular addition of AHSV NS3 to

cells has an effect on membrane permeability. The aim here was to investigate the effect, if any, of NS3 on the membranes of mammalian cells following extracellular addition of the protein.

As the NS3 protein has not yet been purified in a non-denatured form, it was decided to use crude cell extracts from *Sf9* cells infected with a recombinant baculovirus expressing NS3, for initial membrane permeabilisation assays. As a negative control, *Sf9* cell extracts from wild-type baculovirus infected cells were also prepared as described under Materials and Methods. Expression of the NS3 protein was confirmed by immunoblot with α-β-gal NS3 serum (Figure 2.1(A)). Extracts from Bac-NS3 infected *Sf9* cells contain a protein or band of approximately 24 kDa, that reacts positively with the α-β-gal-NS3 serum, this represents AHSV-3 NS3 (Figure 2.1(A), lane a). Wild type baculovirus infected cells do not have the 24 kDa band (Figure 2.1(A), lane b). Both lanes show a non-specific band at a position just below the 66 kDa size marker.

Approximately equimolar amounts of cell extracts were added to cultured Vero cells and the permeabilisation of the membrane monitored with Hyg B, at 45 min intervals over a 3h period. Hyg B is an aminoglycosidase that is effective in preventing the translocation step in cell-free translation systems. However Hyg B is a very ineffective inhibitor of protein synthesis in intact cells, as it does not cross the plasma membrane (Benedetto *et al.,* 1980). Only permeabilised cells therefore allow the entry of Hyg B, which then subsequently halts protein synthesis. S^{35} metabolic labelling of cellular proteins was used here to monitor protein synthesis in Vero cells, and thereby the uptake of Hyg B and membrane permeabilisation.

Figure 2.1(B) summarises the results from 9 repetitions of the experiment. Wildtype baculovirus-infected *Sf9* cell lysate caused only a slight increase in membrane permeabilisation of Vero cells, with 15% (± 2.6) permeabilised after 3 hours. The addition of *Sf9* cell lysates containing NS3 to Vero cells caused a much larger increase in membrane permeability, with 62% (± 3.8) permeabilisation after 3 h. There was therefore on average a 47% increase in the permeabilisation affected between the wild-type baculovirus- and NS3-

containing lysates. As the only difference between these lysates is the presence of the NS3 protein it is safe to assume that this difference is due to the presence of this protein. The NS3 protein, from this initial study, appears therefore to cause membrane permeabilisation in mammalian cells when added exogenously. Further investigations into this property of NS3 would be greatly aided by the availability of purified NS3, for this purpose the NS3 and NS3A proteins were expressed as histidine fusion products in the Baculovirus system (2.3.3)

2.3.2 Analysis of the cytotoxic effect of co-expression of NS3 and NS3A in insect cells

Both NS3 and NS3A are expressed together in AHSV infected cells (Van Staden *et al.,* 1995). Expression of the AHSV-3 S10 gene in insect cells, however, results in the synthesis of NS3 alone (Van Staden *et al.,* 1995). Expression of AHSV-3 NS3A in insect cells was achieved by the removal of the first initiation codon and bases preceding the second initiation codon. The NS3A protein was found, like NS3, to be cytotoxic to insect cells (Van Niekerk *et al.,* 2001a). It has, however, never been investigated if the combined expression of NS3 and NS3A has an enhanced cytotoxic effect over and above individually expressed NS3 and NS3A. Co-expression of the proteins could conceivably lead to interactions between the proteins that may affect their cytotoxicity. It was, therefore, decided here to investigate the effect on insect cells of the co-expression of these two proteins.

Sf9 cells were co-infected with Bac-NS3 and Bac-NS3A or infected with these baculoviruses separately. As a control, cells were infected with a recombinant baculovirus expressing AHSV NS2 (Bac-NS2) as this protein has been shown not to be cytotoxic to *Sf9* cells (Van Staden *et al.,* 1995). The expression of NS3 and NS3A was analysed at 18, 24, 36 and 42 h.p.i by immunoblot with the α-β-gal-NS3 serum, the results at 24 h.p.i are shown in Figure 2.2(A). Cells infected with Bac-NS3 or Bac-NS3A showed expression of NS3 (24K) or NS3A (23K) at 24 h.p.i (figure 2.2(A), lanes b and c respectively).

(A)

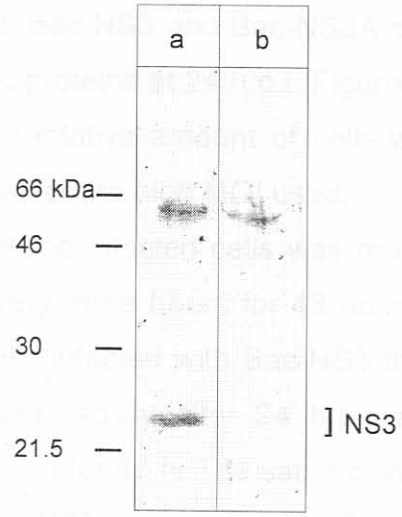

(B)

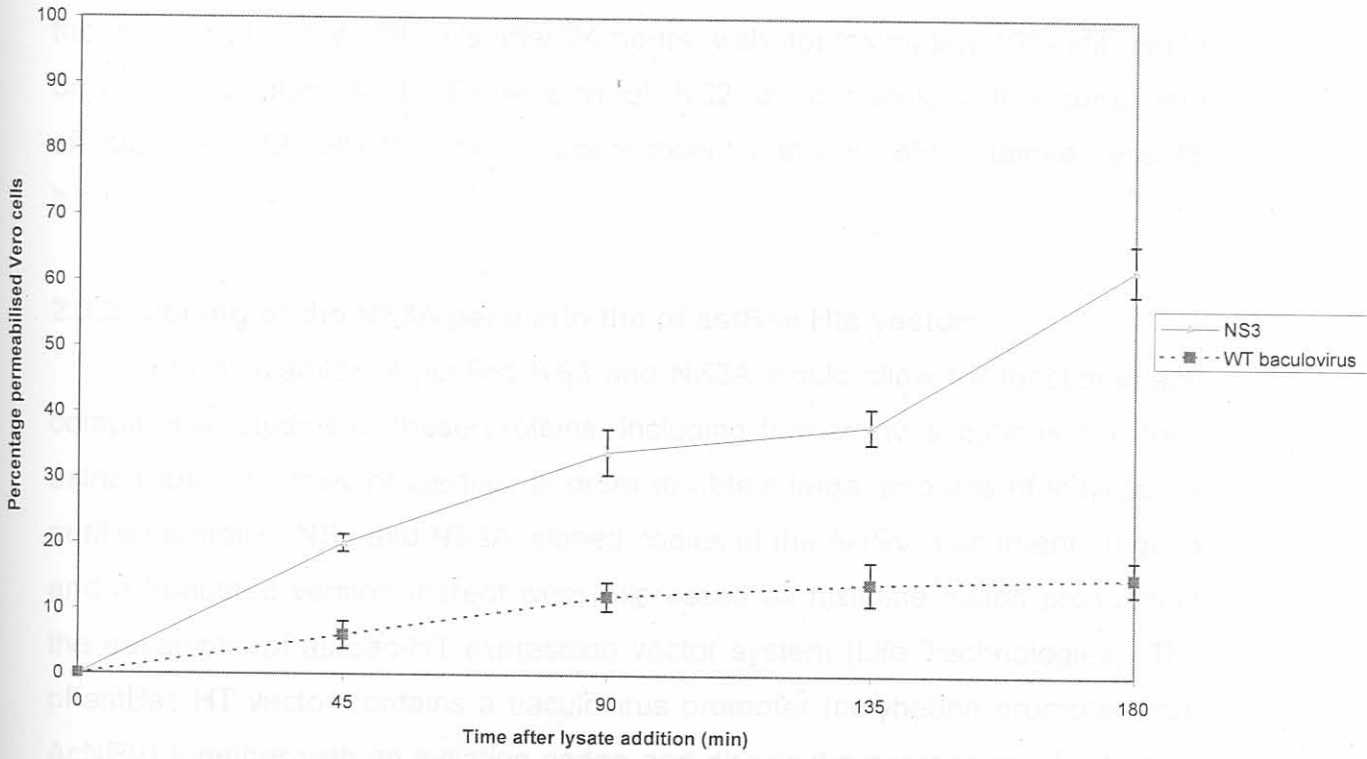

Figure 2.1(A) Western immunoblot analysis of expression of AHSV-3 NS3. *Sf*9 cells were infected with Bac-NS3 (a) or wild type baculovirus (b) and cell lysates prepared 30 h.p.i. Proteins were separated by 12% SDS-PAGE, blotted onto a nitrocellulose membrane and reacted with α-β-gal-NS3 serum. The molecular weights of the rainbow markers and the position of NS3 are indicated. **(B)** Hygromycin B assay of changes in Vero cell membrane permeability following exogenous addition of *Sf*9 cell lysates with or without NS3.

Cells co-infected with Bac-NS3 and Bac-NS3A showed approximately equimolar expression of the two proteins at 24 h.p.i (Figure 2.2(A), lane d). It was assumed that at least a representative amount of cells were co-infected and expressed both proteins, because of the high MOI used.

The viability of the infected cells was monitored using the vital exclusion dye, Trypan blue, every three hours for 48 hours. The results are illustrated in Figure 2.2. In *Sf9* cells infected with Bac-NS3 the number of cells unstained by trypan blue decreased rapidly after 24 h.p.i and only 7% of the cells were unstained or still viable after 48 h. The same cytotoxic effect was observed in *Sf9* cells infected with Bac-NS3A, with less than 20% of the cell population still viable after 48 h. These observations confirm the results from previous studies done by Van Staden *et al.* (1995) and Van Niekerk and co-workers (2001a). Cells co-infected with Bac-NS3 and Bac-NS3A displayed the same dramatic decrease in the number of viable *Sf9* cells after 24 hours, with approximately 10% still viable or unstained after 48 h. Expression of NS2 as a baculovirus recombinant affected the *Sf9* cells to a much lesser extent with only 35% stained cells 48 h.p.i.

2.3.3 Cloning of the NS3A gene into the pFastBac Htc vector:

The availability of purified NS3 and NS3A would allow for functional and comparative studies of these proteins, including further investigations into their extracellular cytotoxic properties. In order to obtain large amounts of individually purified proteins, NS3 and NS3A, cloned copies of the AHSV-3 segment 10 gene and a truncated version thereof were expressed as histidine fusion products in the eukaryotic pFastBac-HT expression vector system (Life Technologies). The pFastBac-HT vector contains a baculovirus promoter (polyhedrin promoter from AcNPV) together with an initiation codon and directs the expression of a foreign protein as a fusion protein with six histidine residues at its amino terminus. Three pFastBac-HT vectors are available (a, b and c) with unique restriction enzyme sites in different reading frames through the cloning linker. These histidine fusion proteins can be easily purified because of the strong affinity of the His-tag

(A)

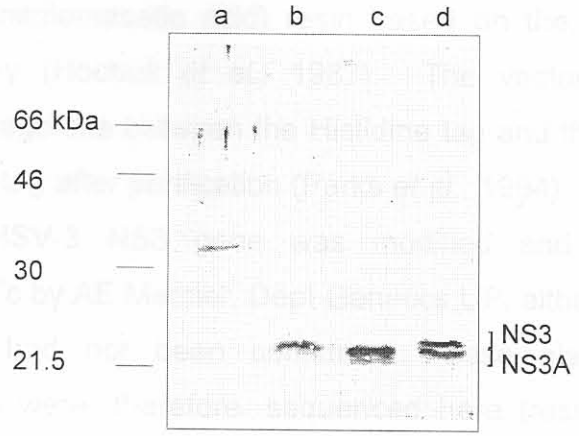

(B)

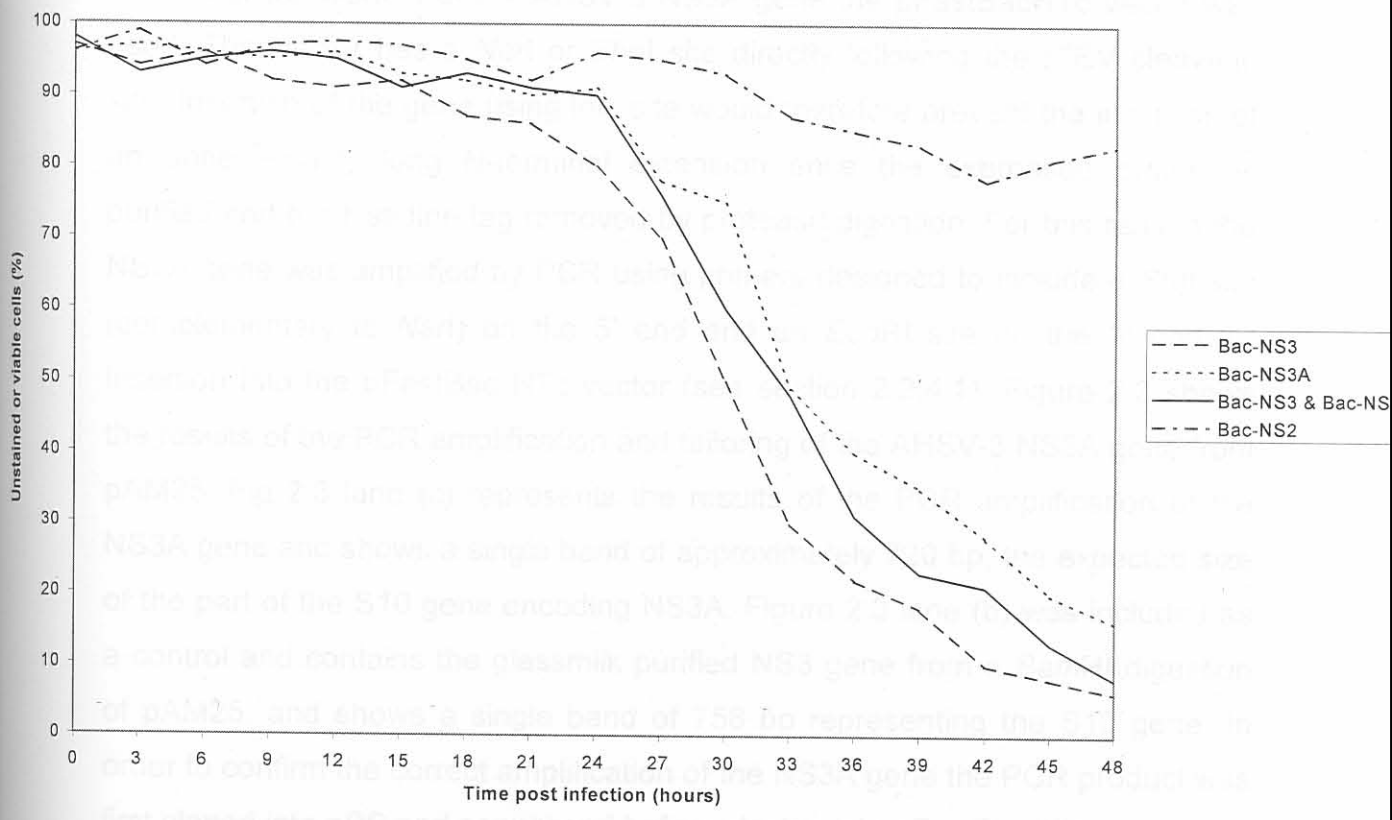

Figure 2.2 (A) Western immunoblot analysis of baculovirus expression of AHSV-3 NS3 and NS3A at 24 h.p.i. *Sf*9 cells were infected with Bac-NS2 (a), Bac-NS3 (b), Bac-NS3A or co-infected with Bac-NS3 and Bac-NS3A (d). Proteins from infected cells were separated by 15% SDS-PAGE and transferred to nitrocellulose membranes for reaction with the α-β-gal-NS3 serum. The molecular weights of the rainbow markers are indicated. **(B)** Trypan blue uptake of *Sf*9 cells infected with recombinant baculoviruses.

for Ni^{2+}-NTA (nitrilotriacetic acid) resin based on the principles of Ni^{2+}-affinity chromatography (Hochuli *et al.*, 1987). The vector also includes a rTEV protease cleavage site between the Histidine tag and the foreign protein, for the removal of the tag after purification (Parks *et al.*, 1994).

The AHSV-3 NS3 gene was modified and cloned into pBS and pFASTBAC HTc by AE Mercier, Dept Genetics UP, although the sequence of the recombinants had not been confirmed. These plasmids, pBS-NS3H and pBACHTc-NS3 were, therefore, sequenced here (results not shown) and the presence, correct reading frame for expression and integrity of the NS3 gene confirmed.

For the cloning of the AHSV-3 NS3A gene the pFastBacHTc vector was used. This vector has a *Nar*I or *Ehe*I site directly following the rTEV cleavage site. Insertion of the gene using this site would therefore prevent the inclusion of an unnecessarily long N-terminal extension once the expressed protein is purified and the histidine tag removed by protease digestion. For this reason the NS3A gene was amplified by PCR using primers designed to include a *Sfu*I site (complementary to *Nar*I) on the 5' end and an *Eco*RI site on the 3' end for insertion into the pFastBac HTc vector (see section 2.2.4.1). Figure 2.3 shows the results of the PCR amplification and tailoring of the AHSV-3 NS3A gene from pAM25. Fig 2.3 lane (c) represents the results of the PCR amplification of the NS3A gene and shows a single band of approximately 720 bp, the expected size of the part of the S10 gene encoding NS3A. Figure 2.3 lane (b) was included as a control and contains the glassmilk purified NS3 gene from a *Bam*HI digestion of pAM25, and shows a single band of 758 bp representing the S10 gene. In order to confirm the correct amplification of the NS3A gene the PCR product was first cloned into pBS and sequenced before cloning into pFastBac-HTc.

Cloning into pBS was achieved by firstly end-filling the PCR product using Klenow polymerase and then digesting the NS3A gene with *Eco*RI. The pBS vector was digested with *Sma*I, a blunt end cutter, and *Eco*RI before the vector and insert were ligated. Following ligation the possible recombinant plasmids were transformed into *E. coli* cells. Plasmid DNA was isolated from possible

recombinants and analysed by *Sful* and *Eco*RI digestion, which should result in the excision of the NS3A gene, if present. The results of the restriction enzyme digestions are given in Figure 2.4. Lane b shows the digestion of the pBS vector, which as expected resulted in the linearisation of the 3.2 kb plasmid. Note that incomplete digestion occurred and that the bright lower band in lane b represents super-coiled plasmid pBS DNA. Digestion of the possible recombinant in lane c (Fig. 2.4) resulted in two bands of 3.2 kb and approximately 700 bp. This is therefore a recombinant with the NS3A gene excised (700bp) and the pBS plasmid linearised (3.2 kb). Lanes (d-h) represents non-recombinant pBS plasmids.

The recombinant plasmid represented in lane c (Fig. 2.4) was digested with *Bgl*II to verify that only a single copy of the NS3A gene was inserted into the pBS vector, as this enzyme does not cleave the pBS plasmid but only the NS3A gene. The recombinant plasmid was cleaved once by this enzyme and linearised indicating the presence of one insert only (results not shown). The recombinant was termed pBS-NS3AH. The plasmid was sequenced (results not shown) and found to contain the NS3A gene and the correct restriction enzyme sites, without any modifications.

The NS3A gene was then sub-cloned into the pFastbac HTc vector. This was acheived by excision of the gene from pBS-NS3AH by *Sful* and *Eco*RI and digestion of the pFastbac HTc plasmid with *Nar*I and *Eco*RI, followed by ligation of vector and insert. Cleavage with the *Sful* and *Nar*I restriction enzymes results in complementary overhangs. Ligated plasmids were transformed into *E. coli* cells and possible recombinant plasmids purified and analysed by *Eco*RV and *Eco*RI digestion. Digestion of the pFastbac HTc plasmid with these enzymes would result in three bands of 3559 bp, 1263 bp and 33 bp. Digestion of a recombinant containing the NS3A gene would result in three bands of 3559 bp, 1263 bp and 733bp, approximately. Figure 2.5 illustrates the results obtained with 5 possible recombinant plasmids. Lane b (Fig 2.5) contains *Eco*RV and *Eco*RI digested pFASTBAC HTc DNA, only two bands (approximately 3559 and 1263 bp) are visible as the 33bp segment is too small for visualisation. Lanes c-e

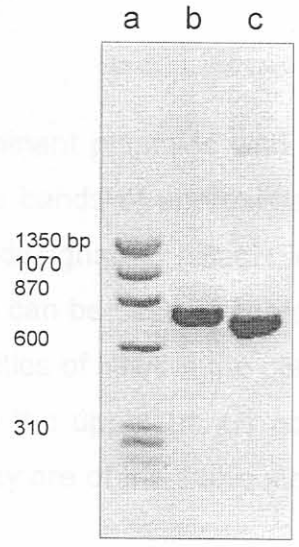

Figure 2.3 Gel electrophoretic analysis of AHSV-3 NS3A gene. The NS3A gene was PCR amplified and tailored from pAM25 (c) and compared to glassmilk purified NS3 (b) obtained from a *Bam*HI digestion of pAM25. *Hae*III-digested ΦX174 was included as molecular weight marker (a).

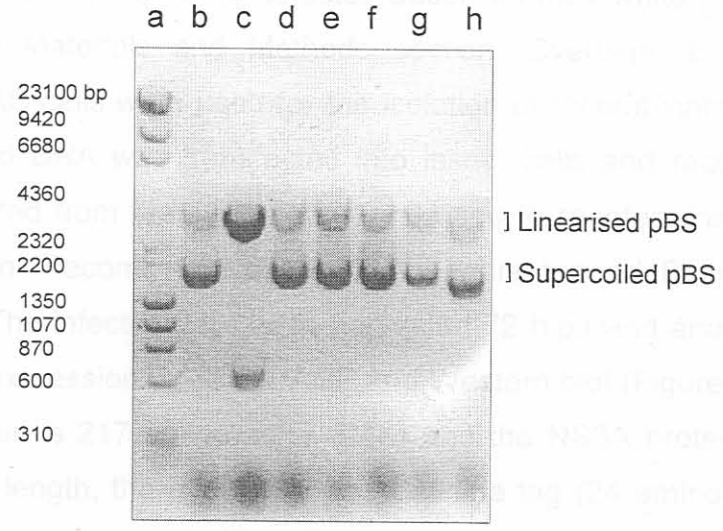

Figure 2.4 Agarose gel electrophoretic analysis of the excision of the AHSV-3 NS3A gene from possible recombinant pBS plasmids, by *Sfu*I and *Eco*RI digestion (c-h). The pBS plasmid was digested with *Sfu*I and *Eco*RI as a negative control (b). *Hin*dIII-digested λ DNA and *Hae*III-digested ΦX174 were included as molecular weight markers (a).

and g (Fig. 2.5) contain recombinant plasmids with the NS3A gene as can be seen from the presence of three bands of approximately 3559 bp, 1263 bp and 733 bp. Recombinants were designated pBacHTc-NS3A. Lane f (Fig 2.5) contained a non-recombinant as can be seen by the presence of only two bands. The presence of the large quantities of RNA in the plasmid extractions in lanes c-g (Fig 2.5) probably resulted in the upper bands occurring at a lower position than those in lane b although they are of the same size.

2.3.4 Expression of NS3 and NS3A as histidine tag fusion proteins

The pBacHTc-NS3 and pBacHTc-NS3A recombinants identified in 2.3.3 were transformed into competent DH10BAC cells for transposition into the BACMID plasmid. Recombinants were selected based on their white phenotype as described in the Materials and Methods section. Overnight cultures of recombinant DH10BAC cells were used for the isolation of recombinant Bacmid DNA. Purified Bacmid DNA was transfected into insect cells and recombinant baculoviruses harvested from the supernatant and used to re-infect insect cells for protein expression. Recombinant baculoviruses were termed BacHTc-NS3 and BacHTc-NS3A. The infected cells were harvested 72 h.p.i and analysed for recombinant protein expression by SDS-PAGE and Western blot (Figure 2.6).

The NS3 protein is 217 amino acids (24K) and the NS3A protein is 205 amino acids (23K) in length, the addition of the histidine tag (24 amino acids in total) should result in an increase in size of approximately 2K. Proteins from *Sf9* cells infected with BacHTc-NS3 have a single definite band of the expected size for HTc-NS3 (26K) (Fig 2.6, lanes d and e). Extracts from *Sf9* cells infected with BacHTc-NS3A have a single band of the expected size for HTc-NS3A (25K) (Fig 2.6, lanes f and g). The presence of the smaller bands above the NS3 and NS3A histidine tag fusion proteins could not be explained. All lanes, including mock-infected (Fig 2.6, lane b) and wild-type baculovirus infected (Fig 2.6, lane c), show a non-specific band at a position just below the 66 kDa size marker.

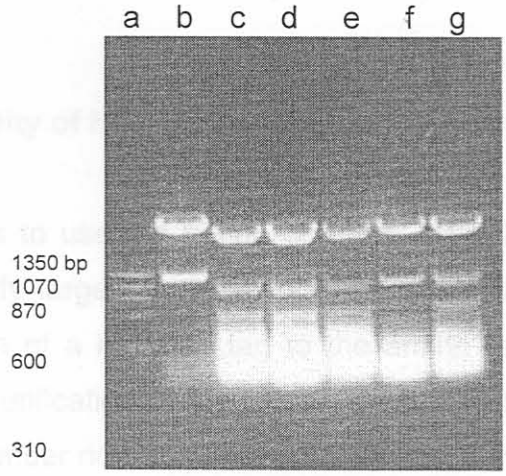

Figure 2.5 Agarose gel electrophoretic analysis of *Eco*RI and *Eco*RV digestion of possible pFastBac HTc NS3A recombinants (c-g). pFastBac HTc was digested with *Eco*RI and *Eco*RV as negative control (b). *Hae*III-digested ΦX174 included as a molecular weight marker (a).

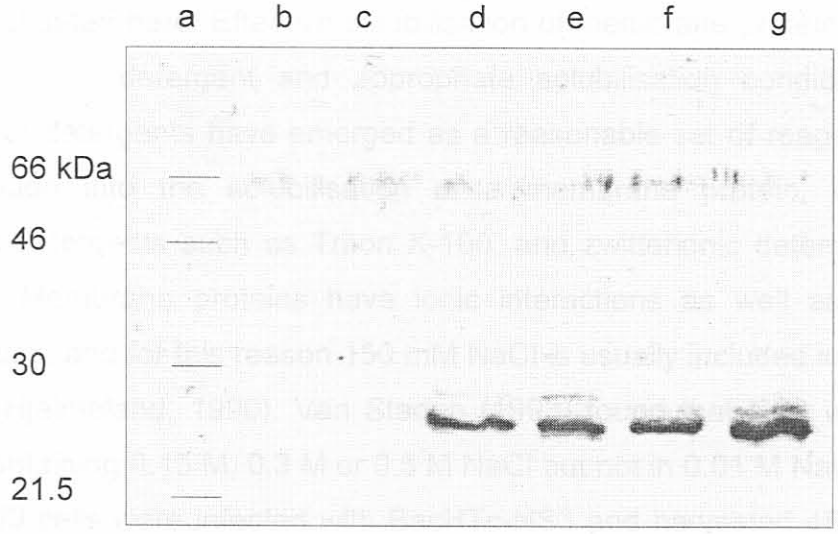

Figure 2.6 Western immunoblot of recombinant baculovirus expression of NS3 and NS3A as histidine tag fusion proteins. *Sf*9 cells were mock-infected (b) or infected with wild-type (c), BacHTc-NS3 recombinant (d,e) or BacHTc-NS3A recombinant (f,g) baculoviruses. Proteins from infected cells were separated by 12% SDS-PAGE and transferred to nitrocellulose membranes for reaction with the α-β-gal-NS3 serum. The molecular weights of the rainbow markers are indicated (a).

2.3.5 Analysis of solubility of HTc-NS3 and binding to nickel resin

The aim here was to use the fusion proteins, HTc-NS3 and HTc-NS3A, produced above, to purify large quantities of NS3 and NS3A in a biologically active form. The addition of a histidine tag to the amino terminus of a protein allows for the one-step purification of the protein on Ni-nitrilo-tri-acetic acid resin columns (Ni-NTA-resin) under non-denaturing conditions, if the protein is soluble. Highly insoluble proteins can only be purified following treatment with denaturing agents such as SDS, which lead to the disruption of the structure or native conformation of the protein with the result that the protein is no longer in a biologically active form. For this reason the solubility of the HTc-NS3 protein was first investigated here. Effective solubilisation of membrane proteins requires the selection of a detergent and appropriate solubilisation conditions. A small number of detergents have emerged as a reasonable set of reagents for a first investigation into the solubilisation of a membrane protein, these include nonionic detergents such as Triton X-100, and zwitterionic detergents such as CHAPS. Membrane proteins have ionic interactions as well as hydrophobic interactions, and for this reason 150 mM NaCl is usually included in solubilisation buffers (Hjelmeland, 1990). Van Staden (1993) found that NS3 was soluble in buffer containing 0.15 M, 0.3 M or 0.5 M NaCl but not in 0.01 M NaCl.

Sf9 cells were infected with BacHTc-NS3 and harvested 48-72 h.p.i., the cells were then disrupted in lysis buffer A (2.2.6.1) adjusted to contain 0.1, 0.25, 0.5, 1.0 or 2.0% Nonidet P-40, a nonionic detergent. Following lysis the cell extracts were separated into soluble (S) and insoluble or pellet (P) fractions by centrifugation. Proteins in each fraction were analysed by SDS-PAGE and Western immunoblot with α-β-gal-NS3 serum, the results are shown in Figure 2.7. As can be seen from Fig 2.7 the most effective Nonidet P-40 concentration was 1.0%, with approximately 50% of the protein solubilised. At 0.1%, 0.25% and 0.5% Nonidet P-40 less than 50% of the HTc-NS3 protein was solubilised, while the protein was completely insoluble in buffer containing 2.0% Nonidet P-40. A non-specific protein band, migrating just below the 66 kDa size marker,

was observed in each lane, this band is commonly seen throughout and represents a non-specific protein recognised by the α-β-gal-NS3 serum.

In order to improve these results another nonionic detergent was investigated, Triton X-100. The solubilisation assay was performed as before with lysis buffer A adjusted to contain 0.1, 0.25, 0.5, 1.0 or 2.0% Triton X-100. Figure 2.8 shows the results obtained with 0.5, 1.0 and 2.0% Triton X-100. As a control the pellet and soluble fractions after treatment with buffer A with 1.0% Nonidet P-40 were included. Treatment with 1.0% Triton X-100 appeared to improve the solubility of the histidine tagged protein, with approximately 60%, repeatably occuring in the soluble fraction. The HTc-NS3 protein was insoluble at 2.0% Triton X-100 and only partly soluble in 0.5% Triton X-100.

Next the optimal salt concentration for solubilisation was determined. BacHTc-NS3 infected *Sf9* cells were lysed as before in lysis buffer A with 1.0% Triton X-100 and 0.15 M, 0.3 M or 0.5 M NaCl. Soluble and pellet fractions after centrifugation were analysed as before (Figure 2.9). The HTc-NS3 protein was 60-80% solubilised in the presence of 0.3 M NaCl and 1.0% Triton X-100. At 0.15 M and 0.5 M NaCl the solubility of HTc-NS3 was significantly lower.

The ability of the solubilised HTc-NS3 to bind to the Ni-NTA-resin was then investigated. Binding of the histidine tag to the Nickel resin may be influenced by the concentration of the imidazole in the wash buffers (GIBCO BRL BAC-to-BAC^{TM} Baculovirus expression manual). The recommended concentration is 20 mM, but decreasing the concentration to between 0-15 mM may significantly improve binding. Two imidazole concentrations in the wash buffer were investigated here, namely 10 mM and 20 mM. The results are shown in Fig 2.10. Briefly, solubilised HTc-NS3 (Fig 2.10, S) was mixed with the charged nickel resin and binding allowed to occur for 30 min. The resin and bound proteins were collected by centrifugation and unbound proteins (Fig 2.10, c,g) retained. The resin was then washed in wash buffer (containing 10 or 20mM imidazole) and collected, while proteins in the supernatant were retained (Fig 2.10, d,h). Bound proteins were then eluted in the presence of elution buffer (containing a high concentration of imidazole)(Figure 2.10, lanes a,e), this step

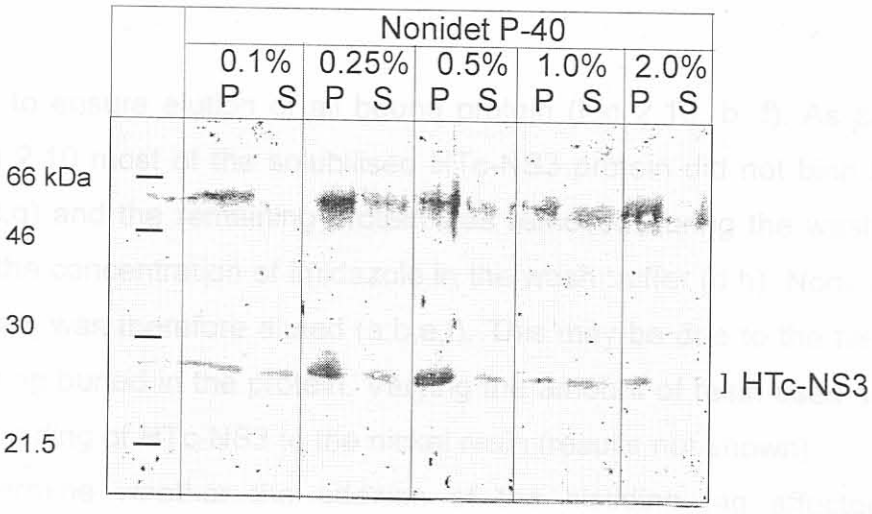

Figure 2.7 Western immunoblot analysis of solubility of HTc-NS3 in lysis buffer A adjusted to contain the indicated concentrations of the nonionic detergent Nonidet P-40. P – pellet fraction containing insoluble proteins, S – supernatant fraction containing solubilised proteins. The molecular weights of the Rainbow markers are indicated

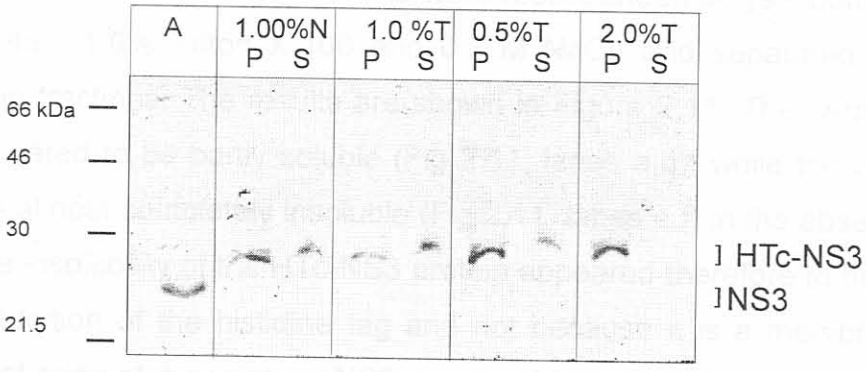

Figure 2.8 Western immunoblot analysis of solubility of HTc-NS3 in lysis buffer A adjusted to contain the indicated concentrations of the detergent Triton X-100. The molecular weight of the rainbow markers are indicated. Proteins from *Sf*9 cells infected with Bac-NS3 were included as a control (A). N-Nonidet P-40, T-Triton X-100.

was repeated to ensure elution of all bound protein (Fig 2.10, b, f). As can be seen from Fig 2.10 most of the solubilised HTc-NS3 protein did not bind to the nickel resin (c,g) and the remaining protein was removed during the wash step regardless of the concentration of imidazole in the wash buffer (d,h). None of the HTc-NS3 protein was therefore eluted (a,b,e,f). This may be due to the histidine residue tag being buried in the protein. Varying the amount of resin used did not influence the binding of HTc-NS3 to the nickel resin (results not shown).

To determine whether the addition of the histidine tag affected the solubility of NS3, the solubility of the HTc-NS3 fusion protein was compared to that of wildtype NS3. *Sf9* cells were infected with Bac-NS3 or BacHTc-NS3 and harvested 48 h.p.i. The cells were then resuspended and lysed in lysis buffer A (without detergent) and separated into soluble and insoluble fractions by centrifugation. Proteins in the pellet fractions were resuspended in lysis buffer A (adjusted to contain 1.0% Triton X-100 and 0.3 M NaCl) and separated into pellet and soluble fractions. The results are shown in Figure 2.11. The wildtype NS3 protein appeared to be partly soluble (Fig 2.11, lanes a,b), while the HTc-NS3 protein was almost completely insoluble (Fig 2.11, lanes e,f) in the absence of detergent. The insolubility of the HTc-NS3 protein appeared therefore to be as a result of the addition of the histidine tag and not because it is a membrane protein. As almost none of the wildtype NS3 remained in the pellet no bands are visible in lanes c and d (Fig 2.11). The pellet fraction in lane e (Fig 2.11), i.e insoluble HTc-NS3, was resuspended in lysis buffer with detergent and, as was found previously, approximately 60-80% of the protein was now solubilised. The insolubility of the protein may therefore be more a function of incorrect folding due to the presence of the histidine tag. It was therefore decided that the HTc-NS3 protein would not be suitable for large scale purification of NS3.

2.3.6 Sequence analysis of the N-terminal region of NS3

As yet no functional differences between AHSV NS3 and NS3A have been reported. The presence of a functional domain in the N-terminal region of NS3, that is absent in NS3A, could potentially result in a functional difference

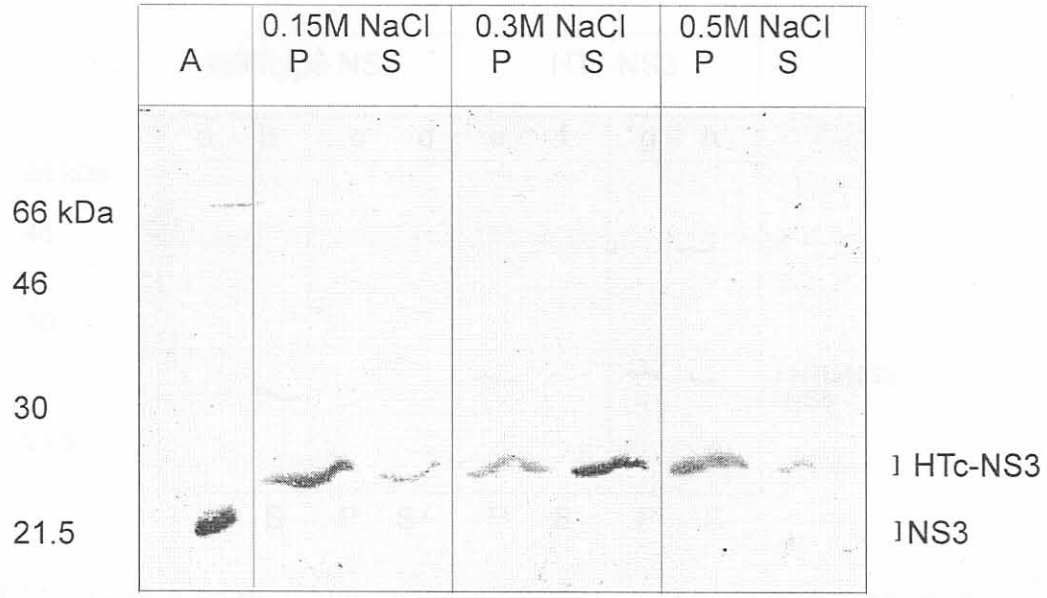

Figure 2.9 Western immnuoblot analysis of solubility of HTc-NS3 in lysis buffer A adjusted to contain 1.0% Triton X-100 and the indicated concentrations of NaCl. Proteins from *Sf*9 cells infected with Bac-NS3 were included as a control (A). The molecular weights of the rainbow size markers are indicated.

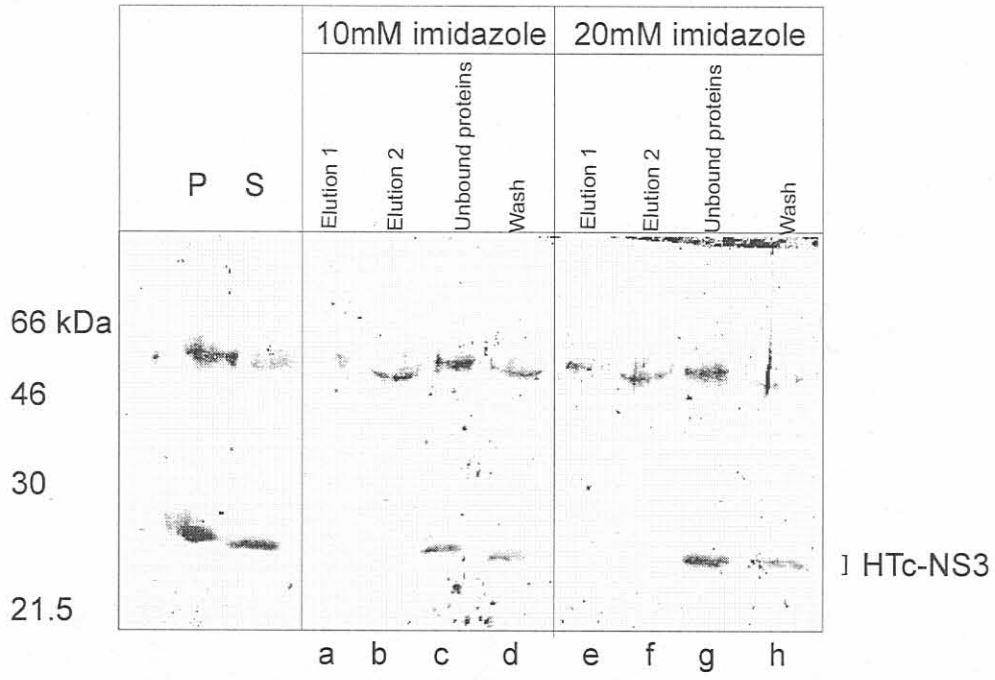

Figure 2.10 Western immunoblot analysis of the binding of the HTc-NS3 protein to Ni-NTA resin. The molecular weights of the size markers are indicated.

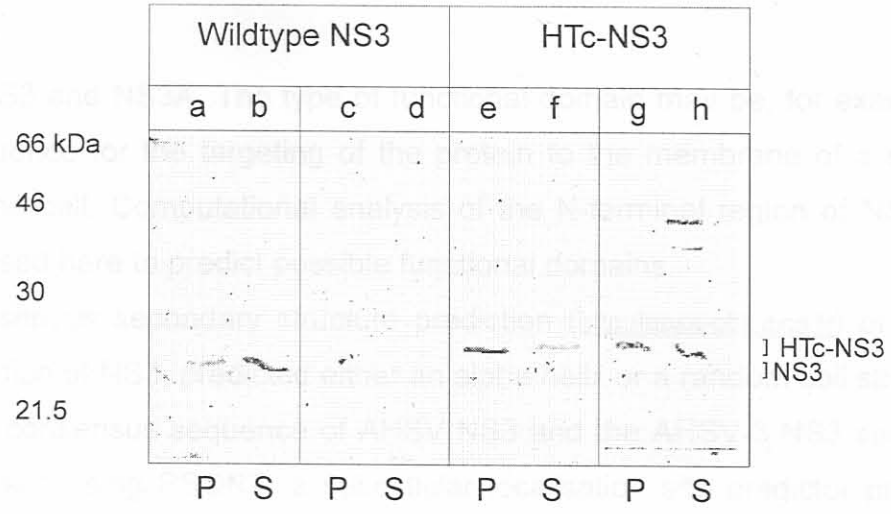

Figure 2.11 Western immunoblot analysis of the comparison of the solubility of HTc-NS3 and wildtype NS3. *Sf*9 cells infected with Bac-NS3 or BacHTc-NS3 were lysed in lysis buffer A and separated into pellet (P)(a and e) and supernatant fractions (S)(b and f). Proteins in pellet fractions were then collected and resuspended in lysis buffer A (adjusted to contain 1.0% Triton X-100 and 0.3M NaCl) and separated into pellet (c and g) and supernatant fractions (d and h). Size markers are indicated.

between NS3 and NS3A. The type of functional domain may be, for example, a signal sequence for the targeting of the protein to the membrane of a specific region in the cell. Computational analysis of the N-terminal region of NS3 was therefore used here to predict possible functional domains.

Consensus secondary structure prediction (http://npsa-pbil.ibcp.fr) of the N-terminal region of NS3, predicted either an alpha helix or a random coil structure.

The consensus sequence of AHSV NS3 and the AHSV-3 NS3 sequence were analysed using PSORT, a subcellular localisation site predictor program. The AHSV-3 NS3 PSG score was –1.74 and the GvH score –5.11 and the protein predicted as not having a signal peptide. iPSORT analysis of the first 10amino acids of NS3 and the first 30 amino acids of NS3A predicted the absence of a signal targeting peptide. The NS3 proteins of some of the Orbiviruses (Table2.1, discussed later), furthermore, contain one or more acidic amino acids, a common feature of signal sequences being the absence of acidic amino acids.

As the N-terminal region may contain a functional domain for another purpose than a signal peptide, the NS3 N-terminal residues were also scanned against protein profile databases (including Prosite) (http://isrec.isb-sib.ch/). The sequence was also analysed using PattinProt (http://npsa-pbil.ibcp.fr) which scans a protein sequence or a protein database for one or several patterns. Neither pattern nor sequence searches revealed significant patterns or profiles (results not shown).

If a functional domain were present in this region the domain would be expected to be relatively conserved. The amino acid sequence of the N-terminal region of NS3 of various orbiviruses and the different AHSV serotypes were compared (Table 2.1). The amino acid sequence of this region in the different serotypes of AHSV NS3 were found not to be highly conserved either in amino acid sequence or in length. The two in-phase methionines were separated by either 9 or 10 amino acids, and only four of these were conserved in all serotypes. When compared to the NS3 proteins of other orbiviruses, such as BTV, EHDV, Broadhaven (BRD) and Palyam (Table 2.1) it can be seen that this

Table 2.1 Amino acid sequences of the N-terminal regions of the NS3 proteins of AHSV, Palyam virus, Broadhaven (BRD) virus, BTV and Epizootic haemorrhagic disease virus (EHDV)

Virus	Sequence
AHSV-1[1], AHSV-2[2],AHSV-8[2]	*MNLASISQSYMS
AHSV-3[3], AHSV-7[2]	MSLATIAENYMM
AHSV-4[2], AHSV-5[2], AHSV-6[4], AHSV-9[3]	MNLAAIAKNYSM
AHSV consensus	M‡ZLA†XIXXZY(X)M
Palyam virus[5]	MLARSLNEYKAM
BRD[6]	MLAALEM
BTV-1,2,10,11,13,17[7]	MLSGLIQRFEEEKM
EHDV[8]	MLSRLVPGVETRIEM

[1] De Sa *et al.*, 1994, [2] Martin *et al.*, 1998, [3] Van Staden & Huismans 1991, [4] Van Niekerk *et al.*, 2001b, [5] De Sa *et al.*, 1994, [6] Moss *et al.*, 1992, [7] Hwang *et al.*, 1992

[8] Jensen *et al.*, 994

*Deduced translation initiation sites for NS3 and NS3A are underlined.

†X indicates any amino acid, ‡Z indicates similar amino acids in the AHSV consensus sequence.

region varies greatly in length and sequence between the different viruses. The number of amino acids between the two methionines ranged from 5 to 13. It should be noted however that the presence of the second methionine or initiation site is conserved between these orbiviruses.

2.4 DISCUSSION

The central aims of this part of the study were to compare the NS3 and NS3A proteins of AHSV and to further characterise the cytotoxic properties of these proteins.

AHSV NS3 is postulated to be related to a family of viral proteins, viroporins, due to the presence of characteristic structural features within the protein and its cytotoxic effect on insect cells when expressed endogenously (Van Staden *et al.*, 1995, Van Staden *et al.*, 1998, Van Niekerk *et al.*, 2001a). The cytotoxic effect of the protein to mammalian cells has not yet been investigated and the protein has not been expressed as a recombinant in mammalian cells.

An alternative to the endogenous expression of the protein in mammalian cells would be the exogenous addition of the purified protein to cultured cells and analysis of the cytotoxic effect. A large number of viroporins have been shown to cause cell membrane permeabilisation when added extracellularly to cell cultures. This toxic effect may occur in much the same manner as natural cytolytic proteins or peptides, such as magainins, cecroporins and melittin, by forming hydrophilic pores through cellular membranes, leading to osmotic disintegrity (Miller *et al.*, 1991, Miller & Montelaro 1992) or via a receptor-mediated mechanism. A number of examples of proteins which display this characteristic include rotavirus NSP4 (Tian *et al.*, 1996b), HIV-1 Vpr (Macreadie *et al.*, 1996; Piller *et al.*, 1998), HIV-1 transmembrane protein (Miller *et al.*, 1993), HIV-1 gp120 (Annunziata *et al.*, 1998), SIV SU envelope glycoprotein (Swaggerty *et al.*, 2000) and vesicular stomatitus (VSV) glycoprotein (Schlegel & Wade 1985). The effect of AHSV NS3 on Vero cell membranes following extracellular addition was, therefore, investigated here.

Sf9 cell extracts from Bac-NS3 and wild-type baculovirus infected cells were prepared as outlined in section 2.3.1. These NS3-containing and wild-type baculovirus extracts were added to Vero cells and the effect on the membrane monitored via the uptake of the membrane impermeable translation inhibitor,

Hyg B. The NS3 protein was found to cause an increase in the uptake of Hyg B from the environment, indicative of an increase in the permeability of the plasma membranes of the Vero cells. The AHSV NS3 protein, therefore, appears to not only be cytotoxic to insect cells, but also causes membrane permeabilisation of Vero (mammalian) cells. This extends the idea that NS3 is a viroporin and can form the basis of future experiments as will be detailed in chapter 4.

The mechanism of NS3 membrane permeabilisation needs to be investigated further. To facilitate this the purification of biologically active NS3 and NS3A was attempted, as will be described later.

AHSV-3 infection of Vero cells results in the expression of both NS3 and NS3A, 13 to 24 hpi, in approximately equimolar amounts (Van Staden *et al.,* 1995). When the full length AHSV-3 segment 10 gene was, however, expressed in the baculovirus system in insect cells, only the NS3 protein (24K) was detected, while the NS3A (23K) protein appeared to be absent (Van Staden *et al.,* 1995). The AHSV S10 gene, therefore, displays different expression patterns in the different cell types. Recombinant baculovirus expression of segment 10 of BTV, in contrast, results in the synthesis of both NS3 and NS3A (French *et al.,* 1989). These results may be explained in the light of recent experimental findings of Chang *et al.,* (1999) who examined the roles of nucleotides flanking a baculovirus AUG initiator codon in modulating translation initiation in lepidopteran insect cells. Based on their findings, substitutions at position –3 (relative to the A of the initiator AUG codon, which was designated +1) did not appear to affect translational initiation efficiency, even though this is a highly conserved position in eukaryotic systems. The +4 and +5 positions were identified as most critical in modulating translation initiation efficiency, with the optimal initiator context being, 5'-NNNAUG**A(A/C/G)**N-3'.

Translation initiation of two proteins from the same mRNA occurs via a context-dependant leaky scanning mechanism (Kozak 1991). When the first AUG is in a sub-optimal context, some ribosomes are allowed to continue scanning along the mRNA and initiate translation at the following AUG, which is in a more favourable context.

The initiation contexts of the NS3 and NS3A genes of AHSV and BTV are given in Table 2.2. In the AHSV-3 S10 gene the first AUG is in a more favourable context for expression in insect cells, according to Chang *et al.,* (1999), than that for the initiation of NS3A. In the BTV S10 gene, however, the NS3A initiation codon is in an optimal context, while that for the NS3 is weaker. This may explain why both proteins are synthesised in insect cells when the S10 gene of BTV is expressed as a baculovirus recombinant, but only NS3 of AHSV-3 is expressed when the same strategy is followed. Expression of AHSV-2 S10 in insect cells, furthermore, also results in the synthesis of NS3 alone (M van Niekerk personal communication) this can also be explained in terms of the initiation context of the two translation start codons.

Both NS3 and NS3A are cytotoxic to insect cells when expressed individually (Van Staden *et al.,* 1995; Van Niekerk *et al.,* 2001a). Expression of the two proteins together in insect cells, as observed in AHSV-infected cells, may potentially lead to interactions between the proteins that affect their cytotoxicity. This has not previously been studied and was, therefore, investigated here.

In this study the co-expression of AHSV-3 NS3 and NS3A was achieved in insect cells by co-infection of cells with recombinant baculoviruses expressing NS3 and NS3A. Another approach for the co-expression of two proteins would be the use of a vector (such as pFastBac Dual) that allows for the cloning and expression of two genes. The baculovirus system depends on site-specific transposition of foreign genes in transfer vectors to the Bacmid DNA. The presence of two almost identical genes, such as NS3 and NS3A, may however interfere with this transposition process. This was therefore not investigated here. Alternatively the initiation codon context surrounding the NS3 and NS3A start codons could be modified in the full length S10 gene.

The cytotoxic effect on insect cells of endogenous expression of both NS3 and NS3A, together, was then investigated. The viability of *Sf9* cells was monitored via the uptake of the vital exclusion dye, Trypan blue. Whether expressed together or individually, the NS3 and NS3A proteins cause a rapid increase in cell death from 24 to 48 h.p.i., at which time only 6-20% of the cell

Table 2.2 Translation initiation codon context for the expression of NS3 and NS3A from S10 genes of various AHSV serotypes and BTV.

Virus	Initiation codon context	
	NS3	**NS3A**
AHSV-3[1]	5'-AUG**AG**U.....	.....AUG**AU**G-3'
AHSV-2[2]	5'-AUG**AA**U.....	.....AUG**UC**A-3'
AHSV-9[1]	5'-AUG**AA**U.....	.....AUG**CA**U-3'
BTV[3]	5'-AUG**CU**A.....	.....AUG**AA**A-3'

[1]Van Staden & Huismans 1991
[2]Van Niekerk *et al.*, 2001b
[3]Hwang *et al.*, 1992

Initiation codons are underlined
+4 and +5 positions are in bold

population remain viable. The cytotoxic effect of either protein individually was therefore similar to the effect when expressed together. There appears to be no interaction between the two proteins that influences this aspect of their functioning. The NS3 protein is therefore representative of NS3 and NS3A in terms of its cytotoxic effect on cells.

The availability of large amounts of purified NS3 and NS3A would facilitate further investigations into the function and role of these proteins in AHSV infection. This part of the study dealt with the expression of the segment 10 genes as histidine tag fusion products in the baculovirus system.

The baculovirus expression system allows for the production of high levels of a foreign protein, in a native form in an eukaryotic system. Expression of the foreign proteins as histidine tag fusion proteins allows for their purification through the strong affinity of the histidine tag for charged Nickel resin (Hochuli *et al.,* 1987; Crowe *et al.,* 1995). Following purification the histidine residues can be removed by rTEV protease cleavage (Parks *et al.,* 1994) with the release of the protein in a biologically active form. The PsaD (peripheral stromal-facing subunit of photosystem I) protein (Minai *et al.,* 2001), the chloroplast triose phosphate-phosphotase translocator protein (Loddenkotter *et al.,* 1993), the Hepatitis B virus preS domains (Nunez *et al.,* 2001), the Rubella virus capsid protein (Schmidt *et al.,* 1998) and the Japanese encephalitis virus NS3 protein (Kuo *et al.,* 1996) were all successfully purifed using this single-step affinity chromatography method. Westra and co-workers (2001) furthermore report the successful purification of four different histidine-tagged recombinant proteins expressed in insect cells.

For the cloning of the AHSV-3 NS3A gene into the pFastBac HT vector, the gene was PCR tailored from a cloned copy of the S10 gene. Primers were designed to amplify only the NS3A gene (i.e. from the second start codon) and to install a *Sful* site at the 5' and an *Eco*RI site at the 3' ends of the gene. The tailored NS3A gene was cloned into pBS and the presence and sequence of the gene confirmed. Next, the NS3A gene was subcloned into pFastBacHTc and the insertion verified by restriction enzyme digestion. The AHSV-3 NS3 gene was

cloned, using a similar strategy, into pBS and pFastBacHTc by AE Mercier. The sequence of the PCR amplified NS3 gene was confirmed here by automated sequencing analysis.

The pBacHTc-NS3 and pBacHTc-NS3A plasmids were used to produce recombinant baculoviruses that express NS3 and NS3A, respectively, as histidine fusion proteins. Western blot analysis of proteins from insect cells infected with these baculoviruses revealed the presence of the fusion proteins (26 kDa HTc-NS3 and 25 kDa HTc-NS3A). Purification of the recombinant fusion proteins, in a nondenatured form, on Ni-NTA resin columns necessitates their solubilisation. The solubility of the HTc-NS3 protein was therefore investigated and optimised here. Maximal solubilisation (60 - 80%) was achieved under conditions of 1.0% Triton X-100, a nonionic detergent, and 0.3 M NaCl. The soluble protein was shown, however, not to bind to the charged nickel resin. Variation of the conditions under which binding occurred did not appear to improve or effect binding, so it was postulated that the histidine tag may be buried within the protein. The wildtype NS3 and HTc-NS3 proteins were compared in terms of their solubility. The addition of the histidine tag to the protein was found to significantly decrease the solubility of NS3. The insolubility of the protein was not due to the membrane associating properties of NS3 as was initially thought. It was decided that the HTc-NS3 protein would not allow for the purification of NS3 in a native form.

Similar findings are reported by Rumlova *et al.,* (2001), who compared classical and histidine-tagged affinity purification techniques, in terms of their applicability in the purification of the Mason-Pfizer monkey virus capsid protein. They showed that the widely used histidine anchor may significantly alter the properties of the protein of interest, in particular the structure or morphology of the protein was dramatically influenced. Lasnik and co-workers (2001), furthermore report that the only efficient way to obtain biologically active protein (human granulocyte colony stimulating factor) was through complete denaturation with guanidine-HCl or urea and subsequent renaturation.

No functional difference between AHSV NS3 and NS3A has been described. As the presence of a functional domain in the N-terminal region of NS3, that is absent in NS3A, may result in a functional difference between these proteins, the amino acid sequence of this region was analysed. Computer predictions and searches where performed to identify any putative functional domains, such as signal sequences, or patterns and motifs.

The N-terminal region of NS3 was first computationally analysed for the presence of a signal sequence that may lead to the differential localisation of the NS3 and NS3A proteins. Signal or leader sequences are usually found at the N-terminus of a protein, and are generally 15-30 amino acids in length. At or close to the N-terminus of signal sequences there are 2-3 polar residues, and within the leader is a hydrophobic core consisting exclusively or very largely of hydrophobic amino acids. There is no other conservation of sequence. There are no acidic groups in the leader, and usually its net charge is approximately +1.7. The leader sequence of proteins targeted to organelles such as the mitochondrion also have little homology. The leaders are usually between 12 and 30 amino acids in length, hydrophilic, consisting of stretches of uncharged amino acids interrupted by basic amino acids and they lack acidic amino acids (Lewin 1994). Membrane proteins may or may not contain a leader sequence and are retained in the membrane by transmembrane regions within the protein.

Sequence analysis of the N-terminal region of NS3 revealed the absence of potential signal sequences. Scanning of this region against protein databases and profiles did not identify any significant patterns or motifs. The N-terminal region of the NS3 protein was furthermore found not to be highly conserved between the different serotypes of AHSV (see Table 2.1). The N-terminal region of the NS3 proteins of related orbiviruses were also found to differ significantly in length and sequence (Table 2.1). The presence of the second methionine (or start codon) was however conserved in all the orbiviruses analysed.

The availability of antibodies directed against the N-terminal residues of NS3 would allow for the specific detection of NS3 and facilitate experimental

analyses of possible functional and localisation differences between NS3 and NS3A. This was investigated and will be discussed in the following chapter.

CHAPTER 3:

IMMUNOLOGICAL DISPLAY OF THE N-TERMINAL AMINO ACIDS OF NS3

3.1 INTRODUCTION

AHSV NS3 and NS3A are encoded from the same open reading frame and are identical except for an additional 10 or 11 amino acids (aa), depending on the serotype, at the N-terminus of NS3 (Van Staden *et al.,* 1995). Polyclonal antibodies (anti-β-gal-NS3 and anti-NS3) directed against either prokaryotic or eukaryotic expressed NS3, therefore, detect both NS3 and NS3A in AHSV infected cells. Localisation studies using these antiserums indicated that NS3 and/or NS3A are associated with the membranes at sites of viral release (Stoltz *et al.,* 1994). The NS3 and NS3A proteins may therefore interact with the viral particle and facilitate release from infected cells. As the NS3 and NS3A proteins could not be distinguished it was unclear whether both proteins display a similar localisation pattern and if both are involved with and necessary for virus release.

The availability of antibodies that are specifically directed against the N-terminal extension of NS3 may potentially be of great benefit in distinguishing between NS3 and NS3A. Antiserum directed against this region of NS3, that is absent in NS3A, would specifically detect NS3 and could be used in localisation studies to identify the regions of the cell specifically associated with NS3 during AHSV infection. This could be compared to localisation studies using the α-β-gal-NS3 serum, and the localisation of NS3 and NS3A determined, should they differ. In this way NS3 and NS3A could be distinguished.

In order to address the problem of preparing antibodies against such small peptide region we explored the possibility of using AHSV VP7 as a delivery system for presenting small peptides to the immune system. AHSV VP7 is a highly hydrophobic protein of 349 amino acids (Roy *et al.,* 1991) and a group-specific immunogenic antigen (Wade-Evans *et al.,* 1997). In AHSV infected cells (Burroughs *et al.,* 1994) or recombinant baculovirus infected cells (Chuma *et al.,* 1992) VP7 aggregates as large, flat hexagonal crystals that appear to be unique to AHSV. These disc-shaped crystals are visible under the light microscope and vary both in number per cell (usually between 1 and 3) and size. The

crystals consist of VP7 trimer subunits that aggregate via interactions between hydrophobic residues to form flat hexagonal sheets (Basak *et al.*, 1996). Each VP7 monomer is composed of two distinct domains. The top (aa 121-249) domain is folded into an anti-parallel β-sandwich while the lower domain (aa 1-120 and 250-348) is composed of α-helices with extended loops between them (Grimes *et al.*, 1995).

The crystallographic structure of VP7 was used to identify hydrophilic regions on the surface of the protein that may be accessible to the environment. Unique restriction enzyme sites for cloning purposes have been inserted into these exposed regions at residues 144-145, 177-178 and 200-201 of AHSV-9 VP7 (Maree, 2000). The resulting insertion mutants were designated VP7mt144, VP7mt177 and VP7mt200 respectively. VP7mt200 has *Hin*dIII, *Xba*I and *Sal*I sites at position 200. This mutated VP7 gene has been cloned into the transfer vector pFASTBAC1 and the protein expressed as a baculovirus recombinant. The insertion was found not to alter the ability of VP7 to form highly ordered crystals (Maree, 2000). This VP7 insertion mutant therefore displays a highly ordered predictable structure, is immunogenic and has a unique cloning site and should therefore fulfil the requirements for an antigen display vector.

It was decided to use the VP7mt200 vector for the display of the N-terminal amino acids of NS3. In this chapter the cloning of the DNA sequence encoding the first 12 amino acids of AHSV-3 NS3 into the cloning site at position 200 of VP7mt200 is described. The resulting chimera, VP7-NS3, was expressed as a baculovirus recombinant and compared to the native VP7 and VP7mt200 proteins in terms of its physical and morphological properties. The VP7-NS3 chimera was subsequently purified and used for the production of polyclonal antiserum directed against NS3.

3.2 MATERIALS AND METHODS:

3.2.1 Cloning 12 N-terminal amino acids of NS3 into VP7mt200

For the cloning of the N-terminal amino acids of NS3 into the vector VP7mt200, two complementary synthetic 53-mer oligonucleotides, with sequences: 5'GCTCTAGAATGAGTCTAGCTACGATCGCCGAAAATTATATGATG***GTCGAC***GAC3' and 5'GTC***GTCGAC***CATCATATAATTTTCGGCGATCGTAGCTAGACTCATTCTAGAGC3' were synthesized. The primers were identical to nucleotides 20 - 55 of the coding strand of the NS3 gene of AHSV-3 (Van Staden, 1993) or its complementary region on the noncoding

strand. This represents the region encoding the first 12 amino acids of NS3. The NS3 sequences were flanked by *Xba*I (underlined) and *Sal*I (bold italics) sites and two or three additional nucleotides to stabilise their 5' ends. A 60 µl mixture was prepared containing 100 pmol of each oligonucleotide in TE buffer. The mixture of the two primers was heated to 95°C for 5 min and placed at 65°C for 1 h. The primer mixture was gradually cooled to room temperature and placed on ice before use. The annealed double stranded oligonucleotide was then digested with *Xba*I and *Sal*I in the appropriate buffer at 37°C for 4 h. The digested product was precipitated in 96% ethanol for 1 h on ice and collected by desktop centrifugation for 15-30 min. Residual salt was removed by washing the pellet with 70% ethanol and recentrifuging. The insert was then dried, resuspended in UHQ and analysed electrophoretically on a 2% agarose gel.

The plasmid pFB-7mt200 was obtained from FF Maree (University of Pretoria) and represents the VP7 insertion mutant, VP7mt200, containing *Hin*dIII, *Xba*I and *Sal*I sites inserted between residues 200 and 201, cloned into the baculovirus transfer vector pFastBac1. The plasmid was digested first with *Sal*I for 1 h and then with *Xba*I for 3 h in the same reaction mixture. The linearised pFB-7mt200 and the NS3-specific insert were ligated and transformed into *E. coli* cells. Plasmid DNA was extracted from a number of possible recombinant colonies and analysed by restriction enzyme digestion and nucleotide sequencing (protocols as described in 2.2.4.6 and 2.2.5). Recombinants were designated pFB-VP7-NS3.

3.2.2 Baculovirus expression of VP7-NS3

Recombinant baculoviruses expressing the VP7-NS3 chimera, AHSV-9 VP7 and VP7mt200 were prepared as described in section 2.2.6. Expression of VP7-NS3 was analysed on 12% SDS-PAGE gels. Gels were stained in 0.125% Coomassie Blue, 50% methanol, 10% acetic acid and destained in 5% acetic acid, 5% methanol. Baculovirus expressed VP7, VP7mt200 and VP7-NS3 were analysed by Western blot (2.2.2.4) with anti-AHSV9, anti-NS3 and anti-β-gal-NS3 sera as primary antisera.

3.2.2.1 Plaque purification

Pure recombinant viral stocks were prepared from single plaques using standard virological methods (O'Reilly *et al.*,1992). Briefly, *Sf9* cells were seeded in 6-well plates as described under 2.2.6.4. Dilution series of the VP7, VP7mt200 and VP7-NS3 recombinant baculovirus were prepared, from 1 x 10^{-1} to1 x 10^{-6}, in 1 ml medium. The medium from each well was removed and replaced with the virus dilution. The plates were incubated at room temperature for 2 h, after which the inoculum was replaced with sterile 3% low melting agarose at 37°C diluted in an equal volume Grace's medium. The infected cells were incubated at 27°C for 4 days and then stained overnight with 1 ml Neutral Red (100 µg/ml in Grace's medium). Baculovirus plaques were plucked as agarose plugs with a sterile Pasteur pipette, placed in 1 ml Grace's medium and resuspended by vortexing. Virus plaques were amplified as described in 2.2.6.5.

3.2.3 Hydrophobicity analysis

Hydropathy plots of AHSV-9 VP7, VP7mt200 and VP7-NS3 were prepared using the Hopp and Woods predictive model (Hopp & Woods, 1981) in the ANTHEPROT package (Geourjon *et al.*, 1991).

3.2.4 Solubility analysis and purification of VP7-NS3

Monolayers of *Sf9* cells were infected with recombinant baculoviruses expressing VP7, VP7mt200 and VP7-NS3 at a MOI of 5-10 pfu/cell and incubated at 27°C. Protein expression was verified under the light microscope after 2 days, and the infected cells harvested by centrifugation at 3000 rpm for 5 min 72 h.p.i. The resulting cell pellet was washed once in 1xPBS, resuspended in 500 µl Lysis buffer (10 mM Tris-HCl, pH 8.0; 150 mM NaCl; 0.25% Nonidet P-40) and incubated on ice for 30 min. 10 strokes of a dounce homogeniser was used to further disrupt the cells, and the nuclei and cell debris removed by centrifugation at 2000 rpm for 5 min. This was repeated three times in order to obtain the maximum amount of crude protein. The cytoplasmic extracts were pooled and separated into soluble and particulate fractions by centrifugation at 5000 rpm for 30 min at 4°C. The fractions were analysed by 12% SDS-PAGE. For purification of the chimeric protein the fraction containing VP7-NS3 was sedimented on a 40 - 75% (w/v) discontinuous sucrose gradient in 0.2M Tris-HCl, pH7.5. The gradient was centrifuged at 12000 rpm for 1 hour at 4°C in a SW41.1 Beckman rotor. Ten 500 µl fractions were collected and a 1/100 sample of each fraction analysed by SDS-PAGE. Fractions containing VP7-NS3 were pooled, diluted 3x in 1xPBS and collected by centrifugation at 22000 rpm for 40 min. Purified VP7-NS3 was analysed by 12% SDS-PAGE and the concentration and purity of the sample determined.

3.2.5 Scanning electron microscopical analysis

Purified VP7-NS3 was fixed in 2.5% Glutaraldehyde in 0.075M KH_2PO_4/Na_2HPO_4 (Na-K-P buffer), pH 7.4 for 30 min. The protein was then filtered onto a 0.2 µm nylon filter, washed three times in Na-K-P buffer and dehydrated by successive treatment in 50%, 70%, 90% and 3x 100% ethanol for 15 min each. The filter was then air dried overnight and mounted onto a stub, spatter coated with gold-beladium and overlayed with a thin layer of carbon. The protein was viewed in a JEOL scanning electron microscope at 5.0 kV.

3.2.6 Immunisation schedule

VP7-NS3 purified as described under 3.2.4 was used to immunise a New Zealand White rabbit. Amounts of antigen were estimated by serial dilution and comparison to protein of known concentration. The immunisation schedule is outlined in Table 3.1, half the antigen was emulsified in ISA 50 (incomplete seppic adjuvant) and half in Quillaja saponin. Both emulsions were then injected intramuscularly into the same rabbit. The rabbit was bled from the ear prior to inoculation and 7 days after the final boost injection. The blood was allowed to clot at 37°C for 1 h and at 4°C overnight. Blood samples were

then centrifuged at 10 000 rpm for 10 min at 4°C and the serum stored at -20°C. Serum was designated anti-SfVP7-NS3.

Table 3.1: Immunisation schedule:

Antigen	Day of immunisation	Amount of antigen (µg)	Adjuvant	Serum obtained
Baculovirus expressed VP7-NS3	1	100	ISA 50 and Quillaja saponin	pre-innoculation serum
	41	70		----------
	70	50		anti-SfVP7-NS3

3.2.7 Evaluation of antiserum raised against VP7-NS3

The antiserum was analysed using two different strategies. The ability of the anti-SfVP7-NS3 to bind NS3 but not NS3A in their denatured forms was tested in a Western blot. The ability to bind NS3 under less denaturing conditions was investigated by immune-precipitation.

3.2.7.1 Western Blot

Sf9 cells seeded at 1x 10^6 cells/well in 6-well plates were infected with wild type baculovirus and recombinant baculoviruses expressing NS3, NS3A and VP7-NS3 at MOI of 5-10 pfu/cell. Cells were harvested as described in 2.2.6.7. Crude protein samples were prepared, separated by SDS-PAGE and immobilised on membranes. A 1/100 dilution of the pre-inoculation serum or the anti-SfVP7-NS3 serum were prepared in 1% blocking solution and used as the primary antibody. Western blots were performed as described in 2.2.2.4.

3.2.7.2 Immune precipitation of NS3:

3.2.7.2.1 *In vitro* transcription and translation of NS3 serotype 3

The plasmid pBS-NS3 containing the NS3 gene from AHSV serotype 3 in the T7 orientation was obtained from C. Smit (Dept. Genetics, University of Pretoria). The plasmid was linearised with *Hind*III, which cleaves in the multiple cloning site (MCS) on the 3' side of the NS3 gene. The digested product was cleaned using the phenol/chloroform-ethanol precipitation protocol described under 2.2.4.3. Digestion was verified by agarose gel electrophoresis.

A 20 µl transcription reaction was prepared containing 15 µl linearised template, 1 µl RNase inhibitor, 100 mM DTT, 2.5 mM of each rNTP, 1 µl T7 RNA polymerase and 2 µl 10 X transcription buffer (PROMEGA). The mixture was incubated for 60 min at 37°C. Transcription efficiency was evaluated on a 0.8% RNA agarose gel.

The translation reactions were carried out using a commercial rabbit reticulocyte lysate kit (Amersham Life Sciences) according to the manufacturer's instructions. The translation mixture contained 2 µl 12.5 x translation mix (without methionine), 1 µl 2.5 M potassium acetate, 0.5 µl 25 mM magnesium acetate, 1.5 µCi/µl [^{35}S] methionine, 10 µl rabbit reticulocyte lysate, approximately 0.5 – 0.8 µg RNA and RNase-free UHQ to a final volume of 25 µl. The reaction was incubated at 30°C for 60-90 min. Protein expression was analysed by SDS_PAGE and autoradiography.

3.2.7.2.2 Immune precipitation

The ^{35}S labeled translation products were incubated in the presence of 5 µl anti-SfVP7-NS3 serum or anti-β-gal-NS3 (positive control) with 0.01M STE for 60 min with shaking at room temperature. Samples were also incubated in the absence of serum as a negative control. Protein A slurry (10% w/v Protein A in 0.01M STE) was added and the mixture incubated as before for 60 min. Bound proteins were collected by desktop centrifugation for 30 sec and the supernatant retained. The pellet was then washed three times in 0.01M STE and resuspended in PBS. Precipitated and unprecipitated proteins were analysed by SDS-PAGE and autoradiography.

3.2.8 Immunogold labeling of purified VP7-NS3

Immunogold labeling experiments were based on the methods of Portner & Murti (1986) and Murti *et al.*(1988). VP7mt200 and VP7-NS3 crystals were purified as described under section 3.2.4. The crystals were adsorbed onto copper 400-mesh Formvar carbon-coated grids and the grids rinsed with TBS (500 mM NaCl and 25 mM Tris, pH 7.6). The grids were then floated on a solution of primary antibody (anti-β-gal-NS3 serum or no serum diluted 25-fold in TBS containing 1% gelatin) for 1 h. Alternatively the purified crystals were incubated overnight at 4°C in the presence of the primary antiserum solution and then adsorbed to the grids. Following thorough rinsing with TBS, the grids were floated on a solution of protein A conjugated with 10 nm coloidal gold particles (Sigma, diluted 20-fold with TBS) for 1 h at room temperature. The samples were then rinsed and viewed directly or stained with 1% aqueous uranyl acetate and viewed in a JEOL transmission electron microscope.

3.3 RESULTS

To produce antibodies that specifically detect NS3, but not NS3A, in AHSV-3-infected cells, the N-terminal region unique to AHSV-3 NS3 was cloned into an antigen display vector, AHSV VP7mt200. The resulting VP7-NS3 chimera was expressed as a baculovirus recombinant and the hydrophobicity profile, solubility and crystal structure of the protein compared to the VP7mt200 vector and the wild-type AHSV-9 VP7 protein from which the vector was derived. Purified VP7-NS3 was used for the production of polyclonal antiserum and the resulting serum analysed in terms of its ability to bind AHSV-3 NS3.

3.3.1 Cloning of N-terminal region of NS3 into VP7mt200

The aim here was to make a recombinant construct, VP7-NS3, that would allow for the expression of the 12 N-terminal amino acids of NS3 on the surface of VP7 crystals (Fig 3.1). The insertion mutant VP7mt200 was chosen as a vector for immunological display as position 200 is believed to be exposed on the surface of the VP7 protein and the insertion of restriction enzyme sites at this site has been shown not to alter the ability of the protein to assemble into hexagonal crystals (Maree 2000). Cloning of a 36 bp region of the AHSV-3 NS3 gene into the *Xba*I/*Sal*I sites of VP7mt200 should therefore result in the expression of the first 12 amino acids of NS3 as an insert at position 200 on the surface of VP7.

Briefly, this entailed the directional cloning of nucleotides 20 – 55 of the AHSV-3 NS3 gene, encoding amino acids 1-12, between the *Xba*I and *Sal*I sites of the vector VP7mt200 cloned into the pFastBac plasmid (Fig 3.1). Plasmid DNA was extracted from possible recombinant *E. coli* colonies and insertion verified by *Pvu*I digestion (Fig. 3.2). The pFB-7mt200 vector has a single *Pvu*I site, digestion with this enzyme therefore results in the linearisation of the 5942 bp plasmid (Fig 3.2, lane b). The NS3-specific sequence contains a further *Pvu*I recognition site so that the insertion of this region into pFBmt200 and subsequent *Pvu*I digestion would result in two bands of approximately 2328bp and 3650bp (Fig 3.2, lanes c and d). Plasmids in which the NS3 sequence was not inserted would therefore be linearised by *Pvu*I digestion (Fig 3.2, lanes e and f). Note that incomplete digestion was achieved in lanes b and c. Automated sequence analysis of

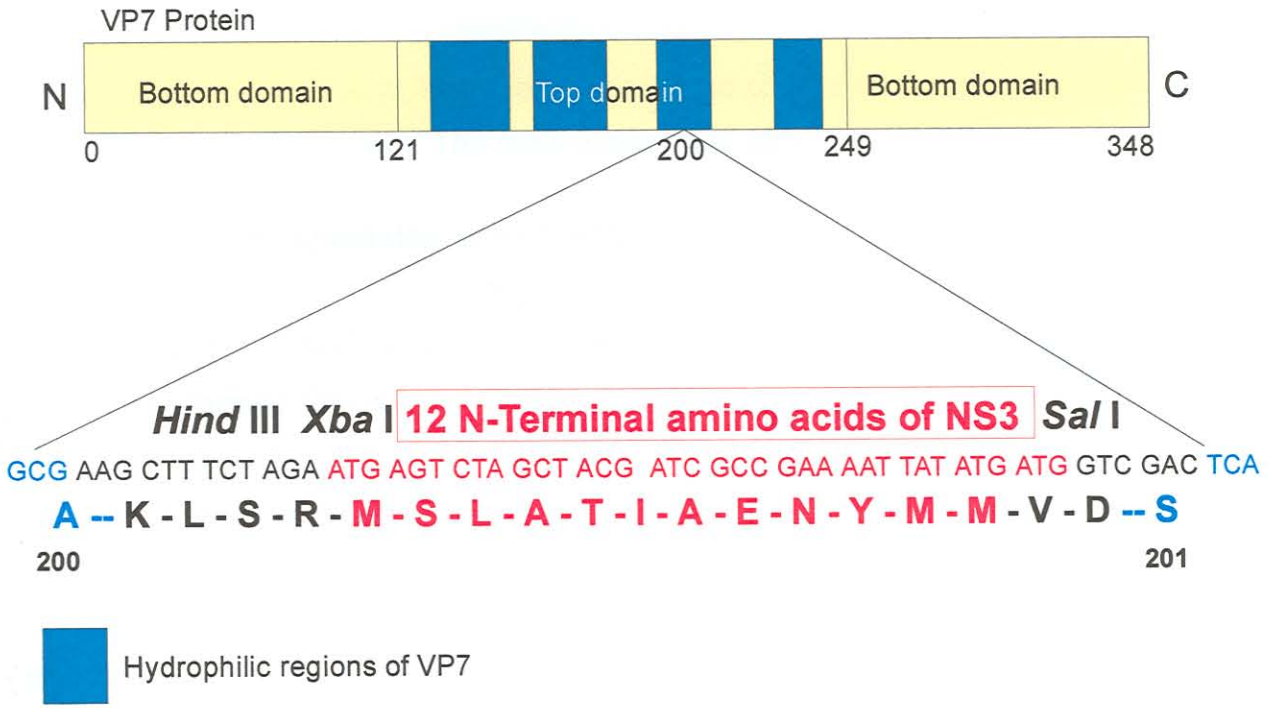

Figure 3.1 Schematic representation of the recombinant VP7-NS3 protein. A 36 bp region of the AHSV-3 NS3 gene (red) was cloned into the XbaI/SalI sites (black) of the VP7mt200 vector (yellow and blue). This would result in the expression of the first 12 amino acids of NS3 (red) as an insert at position 200 in a hydrophilic or surface region (blue) in the top domain of AHSV-9 VP7.

the recombinant plasmids verified the presence and correct sequence of the NS3 insert in VP7-NS3 (results not shown). The recombinant was termed pFBVP7-NS3.

3.3.2 Baculovirus expression of VP7-NS3

The pFBVP7-NS3 plasmid identified above was used to prepare a recombinant baculovirus, termed BACVP7-NS3, that would express the VP7-NS3 chimera in insect cells. Recombinant baculoviruses expressing the wild-type AHSV-9 VP7 protein (BAC-s9VP7) and the mutated version, VP7mt200 (BAC-VP7mt200), were also prepared for use as controls in all subsequent experiments. Plaque purified and amplified baculovirus stocks were used to infect *Sf9* cells and protein expression confirmed by analysis under a light microscope. Chuma and co-workers (1992) demonstrated that VP7 forms distinct disc-shaped crystals that are visible under a light microscope, when expressed as a baculovirus recombinant. Between one and three distinct morphological structures were visible in BAC-s9VP7, BAC-VP7mt200 and BACVP7-NS3-infected *Sf9* cells 2 days post infection. No such structures were visible in mock or wild-type infected cells. Crude cell lysates were prepared 72 h.p.i. and protein expression analysed by SDS-PAGE. The results are shown in Fig 3.3 (A). The predicted molecular weight of VP7-NS3 is approximately 42 kDa based on its amino acid sequence. A unique band corresponding to this expected size was detected in lane f, which represents BACVP7-NS3 infected *Sf9* cells (Fig 3.3A). The protein was larger than VP7mt200 (39 kDa, Fig 3.3, lane e) and VP7 (38 kDa, Fig 3.3A, lane d) as expected. The viral origin of the VP7 and modified VP7 proteins was confirmed by a Western blot with anti-AHSV-9 serum (not shown).

The presence of the NS3-specific insert in VP7-NS3 was confirmed by Western blots with anti-β-gal-NS3 and anti-NS3 sera. Neither the VP7 nor the VP7mt200 proteins reacted with these sera, while the VP7-NS3 chimeric protein reacted with the sera directed against either prokaryotic or eukaryotic expressed NS3. Fig 3.3(B) shows the results obtained with the anti-β-gal-NS3 serum. No immune reaction was observed in BAC-VP7 (Fig 3.3, lane d) or BAC-VP7mt200 (Fig 3.3, lane e) infected cells. A distinct protein band of 42 kDa, representing the VP7-NS3 chimera, was, however, observed in

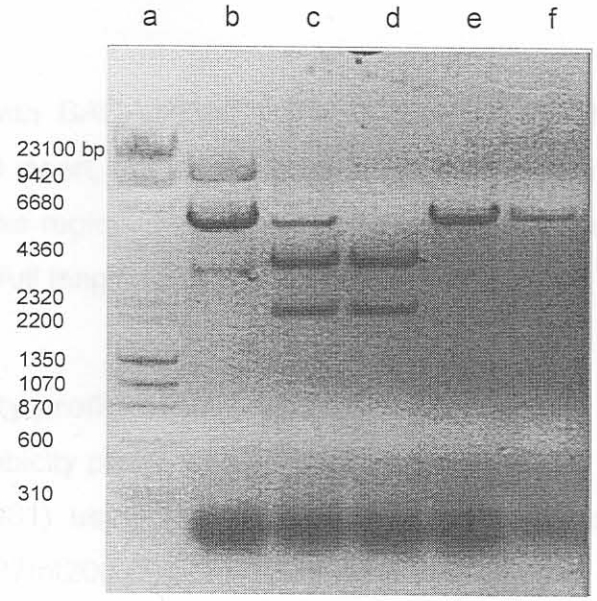

Figure 3.2 Agarose gel electrophoretic analysis of *Pvu*I digestion of possible pFBVP7-NS3 recombinants (lanes c – f). *Pvu*I linearised pFBmt200 was included as a control (lane b). Molecular weight markers (lane a) were *Hae*III-digested ΦX174 and *Hin*dIII-digested λ DNA.

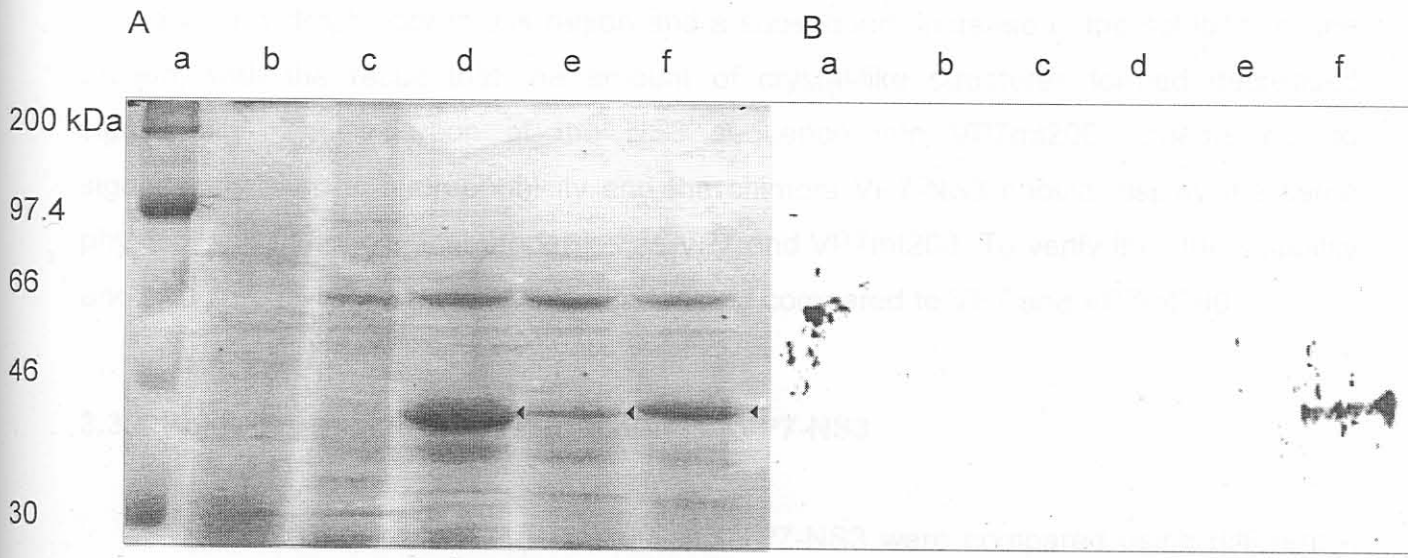

Figure 3.3 SDS-PAGE analysis (A) and Western blot (B) of recombinant baculovirus expressed VP7-NS3. *Sf*9 cells were mock-infected (b) or infected with wild type (c), VP7 (d), VP7mt200 (e) and VP7-NS3 (f) using recombinant baculoviruses. Cultures were harvested 72 h.p.i, separated by SDS-PAGE and stained with Coomassie brilliant blue (A) or blotted and reacted with anti-β-gal-NS3 serum (B). Rainbow protein markers were molecular weight markers (a). Arrows in A indicate the position of AHSV-9 VP7 (d), VP7mt200 (e), and VP7-NS3 (f).

Sf9 cells infected with BAC-VP7-NS3 (Fig 3.3B, lane f). This not only confirmed the presence of the NS3 insert, but also indicated that the polyclonal anti-NS3 sera contained antibodies against this region. This region of NS3 appears, therefore, to be immunogenic when present in the full length NS3 protein.

3.3.3 Hydrophobicity profile of VP7-NS3

The hydrophobicity profile of VP7-NS3 was determined according to the method of Hopp & Woods (1981) using the ANTHEPROT package, and compared to those of AHSV-9 VP7 and VP7mt200 (Fig 3.4). Excluding the region of insertion, the profiles of the VP7 proteins were identical. The profile of the inserted NS3 region in VP7-NS3 corresponded to the profile of this region in AHSV-3 NS3 (Van Staden, 1993), with a net increase in hydrophobicity at this site. Maree (2000) showed that the insertion of six amino acids (KLSRVD) between residue 177 and 178 of VP7 (VP7mt177) caused a large increase in hydrophilicity in this region and a subsequent increase in the solubility of the protein, with the result that the amount of crystal-like structures formed decreased significantly. The insertion of the NS3 sequence into VP7mt200 appears not to significantly alter its hydrophobicity and the chimera VP7-NS3 should display the same physical and morphological properties as VP7 and VP7mt200. To verify this, the solubility and structure of VP7-NS3 was investigated and compared to VP7 and VP7mt200.

3.3.4 Solubility analysis and purification of VP7-NS3

The solubility of VP7, VP7mt200 and VP7-NS3 were compared using differential centrifugation and sedimentation analysis. Low speed centrifugation was used to separate cytoplasmic *Sf9* cell extracts containing these proteins into particulate and soluble fractions as outlined in 3.2.4. SDS-PAGE analysis revealed that, like VP7 and VP7mt200, VP7-NS3 was present predominantly in the particulate form (not shown). The particulate fractions were subsequently fractionated further by one-step sucrose gradient (40 – 75%) centrifugation and analysed by SDS-PAGE. Fig 3.5 illustrates the results obtained with the VP7-NS3 protein. Approximately 70% of the VP7-NS3 protein was present in the 5 bottom

(A) Hydrophobicity profile of VP7

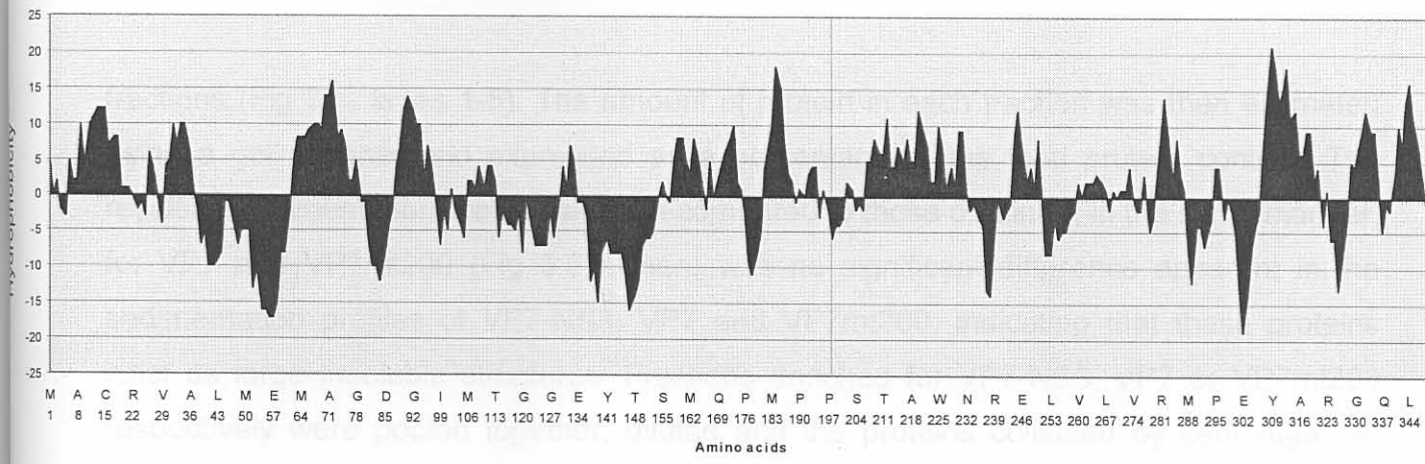

(B) Hydrophobicity profile of VP7-200

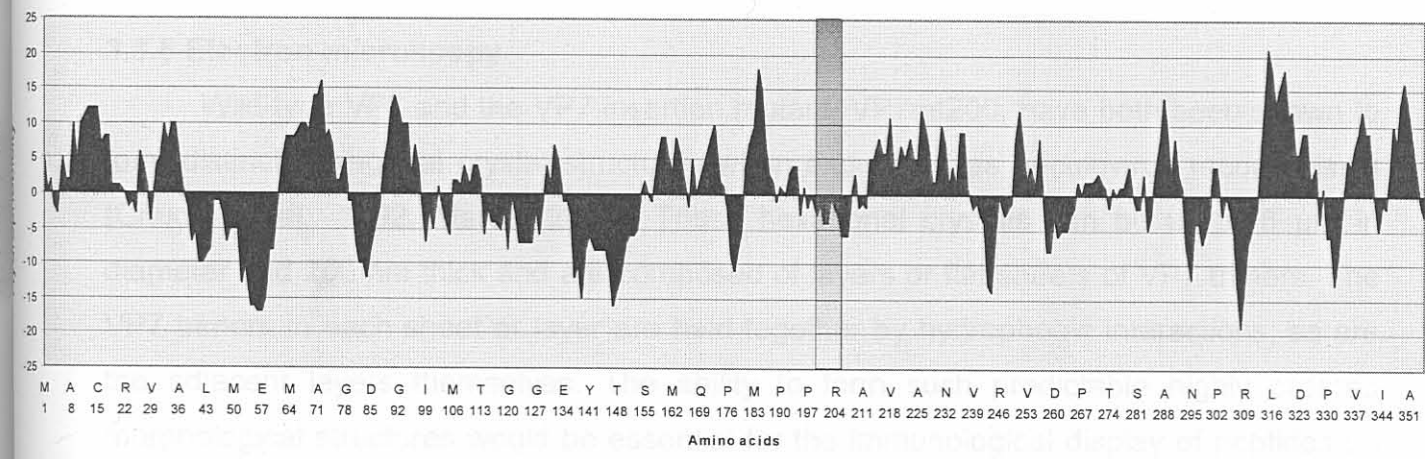

(C) Hydrophobicity profile of VP7-NS3

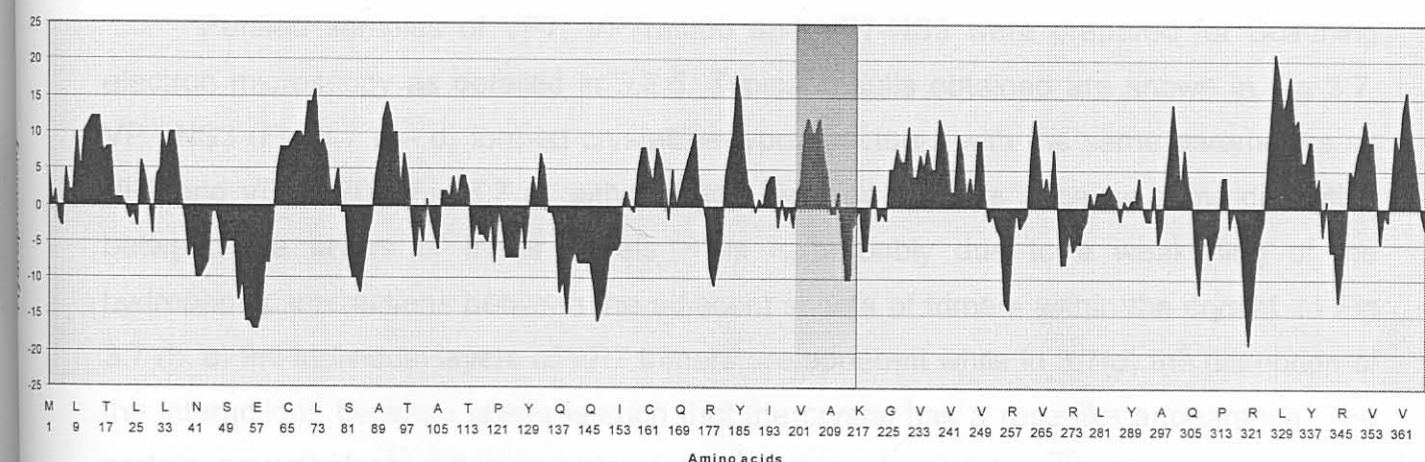

Figure 3.4 Hydrophobicity profiles of AHSV-9 VP7 (A), VP7mt200 (B) and VP7-NS3 (C), displaying regions with a net hydrophobicity (positive value) or hydrophilicity (negative value). Shaded regions represent the sites of insertion.

fractions (Fig 3.5, lanes 1-5). The amount of protein in each fraction was then estimated using a gel scanner and expressed as a percentage of the total protein content. The resulting sedimentation profile was then compared to those obtained, in the same manner, for VP7 and VP7mt200 (Fig 3.6). There was no significant difference apparent in the sedimentation profiles of VP7-NS3, VP7 and VP7mt200, indicating that these proteins exist as large insoluble structures. Fractions enriched for VP7-NS3, VP7 or VP7mt200 respectively were pooled together, diluted and the proteins collected by centrifugation. Proteins purified in this way were analysed by SDS-PAGE (not shown) and used for electron microscopical analysis and antiserum production.

3.3.5 Electron microscopy

Wild-type VP7 and the VP7 insertion mutant, VP7mt200, have both been shown to form distinct hexagonal crystal structures when expressed as baculovirus recombinants (Chuma *et al.,* 1992, Maree, 2000). These hexagonal crystals can be up to 6 µm in diameter and 200 nm thick and are composed of layers or flat sheets of VP7 trimers. The VP7 trimers in each sheet or layer are held together by hydrophobic interactions, as are the adjacent layers themselves. The ability to form such predictable highly ordered morphological structures would be essential for the immunological display of peptides on the surface of this protein. The ability of the VP7-NS3 chimera to form these typical structures was, therefore, investigated here.

Purified samples of VP7, VP7mt200 and VP7-NS3 were prepared for Scanning electron microscopy as detailed in 3.2.5. Typical results obtained are shown in Fig 3.7. VP7-NS3 (Fig 3.7 b – d) formed crystalline-type structures with the same parameters as VP7 and VP7mt200 (Fig 3.7 a), although the insertion appears to cause some disruption between the layers of trimer sheets. This is probably due to a weakening of the hydrophobic interactions between the adjacent sheets of trimers within the crystal. In Fig 3.7 (b, c) the individual layers of VP7 trimers are apparent while in 3.7(d) the disruption of the interactions between layers is such that the crystal has a rose-like appearance. The protein nevertheless still assembles into an ordered crystal structure, a feature that appears to be important in the immune response against AHSV VP7. This is based on the

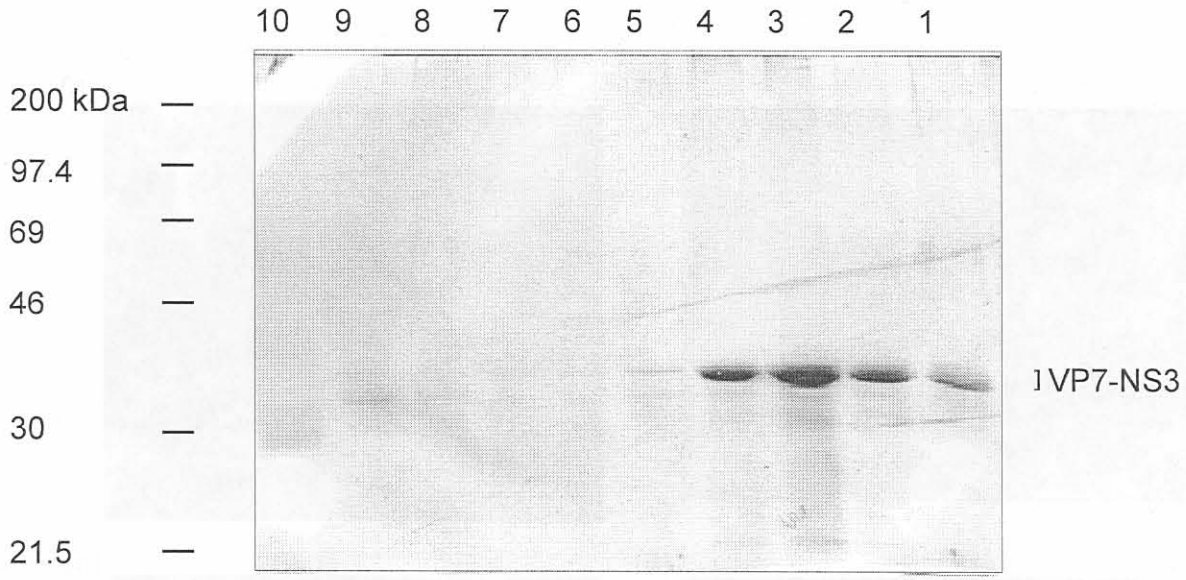

Figure 3.5 SDS-PAGE analysis of subcellular sucrose gradient fractionation of particulate fractions from *Sf*9 cells infected with a baculovirus recombinant expressing VP7-NS3. Fractions were collected from the bottom (1) to the top (10) of the gradient, analysed by SDS-PAGE and Coomassie blue staining. The molecular weight of the Rainbow size markers are indicated. The position of VP7-NS3 is indicated.

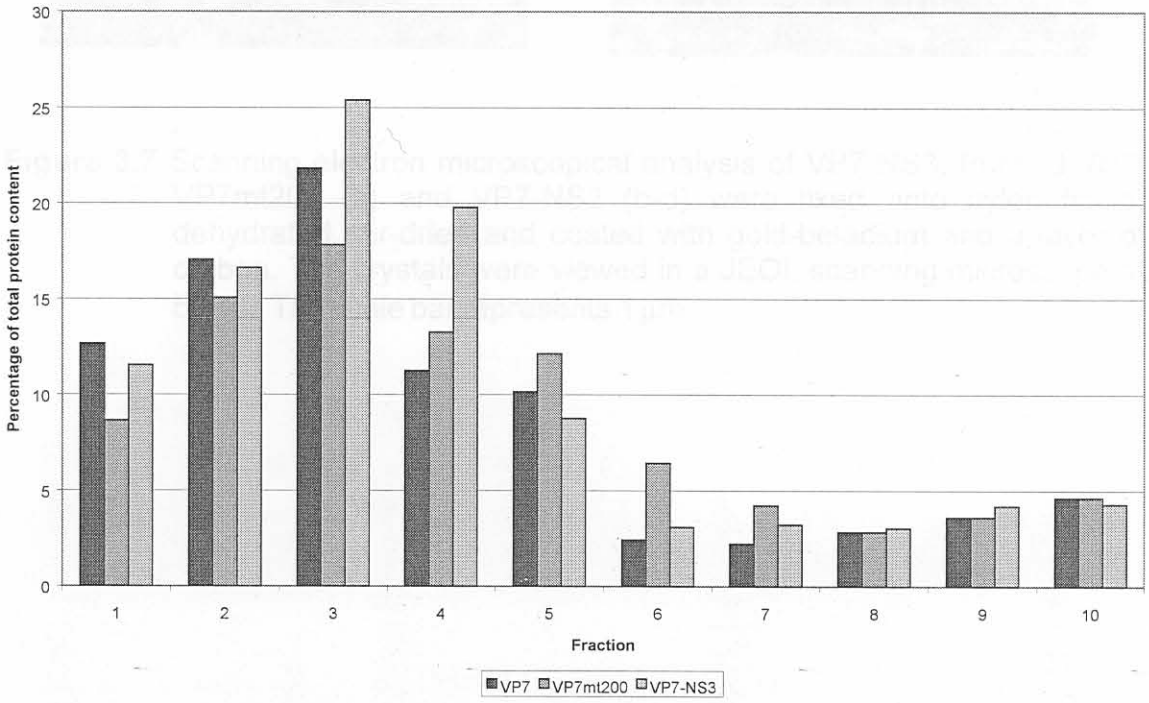

Figure 3.6 Comparison of sedimentation profiles of AHSV-9 VP7, VP7mt200 and VP7-NS3.

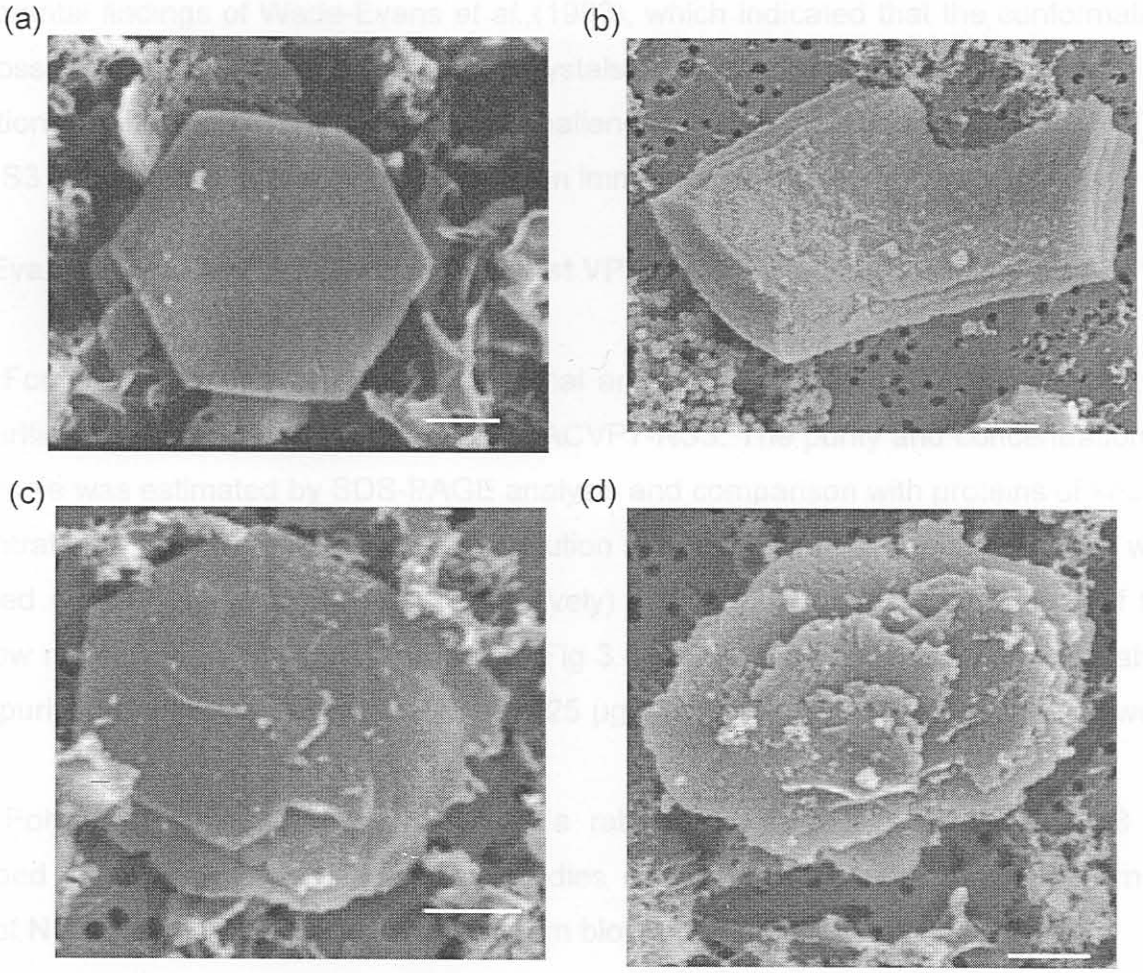

Figure 3.7 Scanning electron microscopical analysis of VP7-NS3. Purified VP7, VP7mt200 (a) and VP7-NS3 (b-d) were fixed onto nylon filters, dehydrated, air-dried and coated with gold-beladium and a layer of carbon. The crystals were viewed in a JEOL scanning microscope at 5.0 kV. The scale bar represents 1 μm.

experimental findings of Wade-Evans *et al.*,(1998), which indicated that the conformation and possibly the assembly of VP7 into crystals was important in the mechanism of protection against heterologous serotype challenge in mice immunised with VP7. The VP7-NS3 crystals should therefore still elicit an immune response.

3.3.6 Evaluation of antiserum raised against VP7-NS3

For the purpose of producing polyclonal antibodies against VP7-NS3, the protein was purified from insect cells infected with BACVP7-NS3. The purity and concentration of the sample was estimated by SDS-PAGE analysis and comparison with proteins of known concentration (Fig. 3.8). A 1x, 5x and 10x dilution series of the VP7-NS3 preparation was prepared (Fig 3.8, lanes b, d and f respectively) and compared to 1 µg of each of the Rainbow molecular weight marker proteins (Fig 3.8, lanes a, c and e). The concentration of the purified protein was estimated to be 0.25 µg/µl and no contaminating proteins were visible.

Polyclonal antiserum was raised in a rabbit against the purified VP7-NS3 as described in 3.2.6. The presence of antibodies directed against the N-terminal amino acids of NS3 was then evaluated by a Western blot and immunoprecipitation.

In a Western blot analysis with the anti-SfVP7NS3 antiserum (Fig 3.9) a single non-specific band was detected in mock (a), wild-type (b), BacVP7-NS3 (c), Bac-NS3 (d) and Bac-NS3A (e) infected cells. Several non-specific bands were present in all the lanes (excluding mock) that were not detected when the pre-inoculation serum was tested (not shown). These bands probably represent contaminating proteins co-purified with VP7-NS3. A single unique protein of the correct size (42 K) was detected in VP7-NS3 infected cells (Fig 3.9, lane c) and presumed to be VP7-NS3. The lane containing purified VP7-NS3 (Fig 3.9 lane f) contained a single band at the same position as this unique band, thereby confirming that it was VP7-NS3. No unique band corresponding to NS3 (24 K) was visible in the Bac-NS3 infected cells (Fig 3.9, lane d). The Western blot was repeated with similar results, and it was concluded that the antiserum did not contain antibodies directed against the linearised form of the N-terminal of NS3, only against VP7 epitopes.

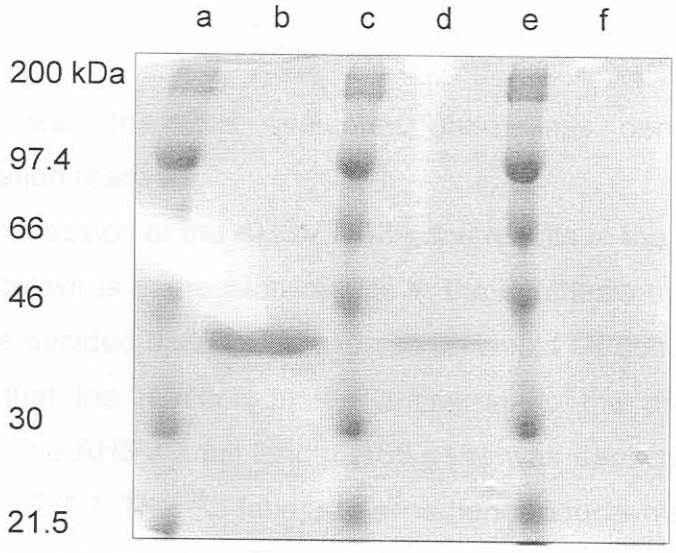

Figure 3.8 SDS-PAGE estimation of concentration and purity of the VP7-NS3 preparation for immunisation. A dilution series of purified VP7-NS3 (b,d,f) was compared to 1 µg of each of the Rainbow molecular weight marker proteins (a,c,e) by SDS-PAGE and Coomassie Blue staining.

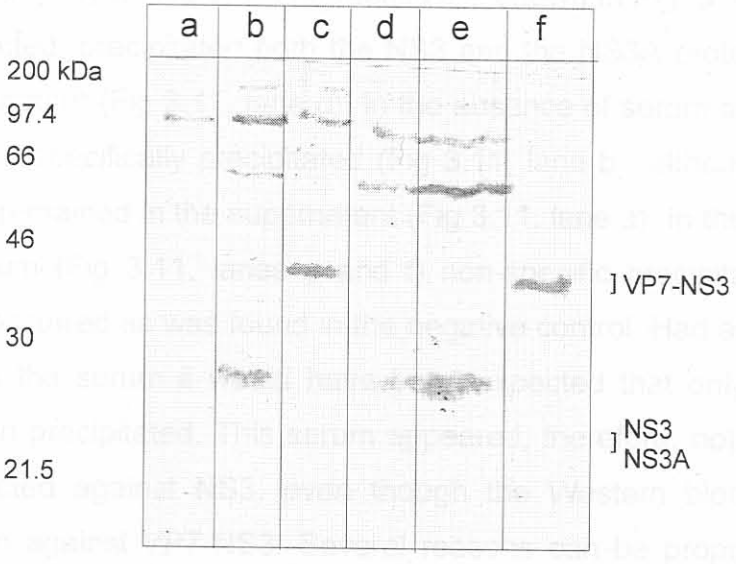

Figure 3.9 Western blot analysis of rabbit anti-SfVP7-NS3. *Sf*9 cells were mock infected (a) or infected with wild-type baculovirus (b), BACVP7-NS3 (c), BAC-NS3 (d), and BAC-NS3A (e). Purified VP7-NS3 was included as a control (f). Proteins were separated by 15% SDS-PAGE and transferred to nitrocellulose membranes for reaction with the anti-Sf-VP7-NS3 serum. The position of the VP7-NS3 protein (c,f) and the expected position of NS3 (d) are indicated. The molecular weights of the rainbow markers are indicated on the left.

The antiserum was therefore evaluated under less denaturing conditions in an immunoprecipitation reaction.

In vitro expression of the AHSV NS3 gene results in the synthesis of both NS3 and NS3A while baculovirus expression results in the synthesis of NS3 only (Van Staden *et al.*, 1995). It was decided that *in vitro* expression would be used for the production of NS3 and NS3A so that the reaction of the antiserum to the proteins could be analysed simultaneously. The AHSV-3 full length NS3 gene was transcribed and translated *in vitro* as described in 3.2.7.2. The ^{35}S-labeled translation products were analysed by 15% SDS-PAGE and autoradiography (Fig. 3.10). As expected, two unique proteins of approximately 24 K and 23 K were synthesised, presumed to be NS3 and NS3A (Fig 3.10 lanes b,c,d). A translation reaction without the NS3 mRNA was performed as a negative control (Fig 3.10 lane a) and neither of these two proteins was detected in this lane.

The NS3 and NS3A proteins were precipitated in the presence of rabbit anti-SfVP7-NS3 and anti-β-gal-NS3 (positive control). As a negative control a precipitation reaction was set up without any antiserum. The results are shown in Fig. 3.11. The anti-β-gal-NS3 serum, as expected, precipitated both the NS3 and the NS3A proteins (Fig 3.11, lane d) out of the supernatant (Fig 3.11, lane c). In the absence of serum a small amount of both proteins was non-specifically precipitated (Fig 3.11, lane b), although the majority of the NS3 and NS3A remained in the supernatant (Fig 3.11, lane a). In the presence of the anti-SfVP7-NS3 serum (Fig 3.11, lanes e and f) non-specific precipitation of the NS3 and NS3A proteins occurred as was found in the negative control. Had antibodies against NS3 been present in the serum it would have been expected that only NS3 and not NS3A would have been precipitated. This serum appeared, therefore, not to contain antibodies specifically directed against NS3, even though the Western blot clearly indicated an immune reaction against VP7-NS3. Several reasons can be proposed to explain these findings and will be discussed in the following section.

One possible reason could be that the NS3 sequence was not, in fact, exposed on the surface of the VP7 crystal. In an attempt to investigate this the purified VP7-NS3 crystals were labeled with the anti-β-gal-NS3 serum, that gave a positive reaction in the Western blot (3.3.2), and then reacted with a secondary antibody labeled with gold particles (3.2.8). Purified VP7mt200 crystals were labeled in the same manner as a

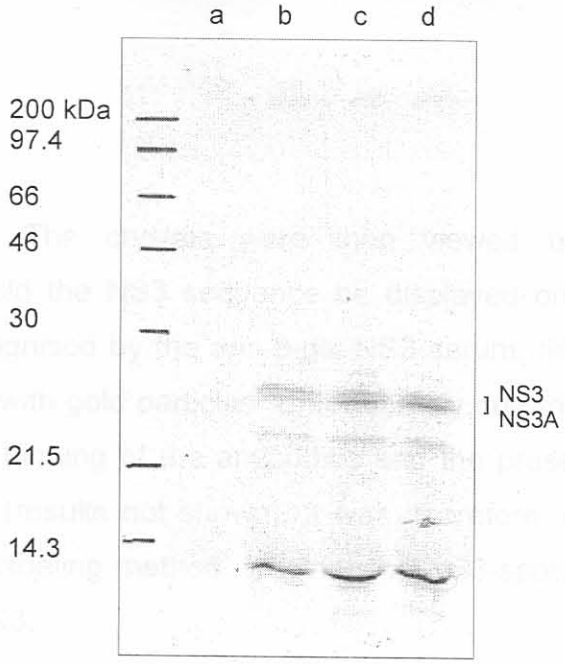

Figure 3.10 Analysis of *in vitro* translation of mRNA from *in vitro* transcribed pBS-NS3. Varying amounts of mRNA were used as templates and the ^{35}S labeled translation products (b,c,d) analysed by 15% SDS-PAGE and autoradiography. The positions of NS3 and NS3A are indicated. As a negative control RNA was excluded from the reaction (a). Rainbow molecular weight markers are indicated.

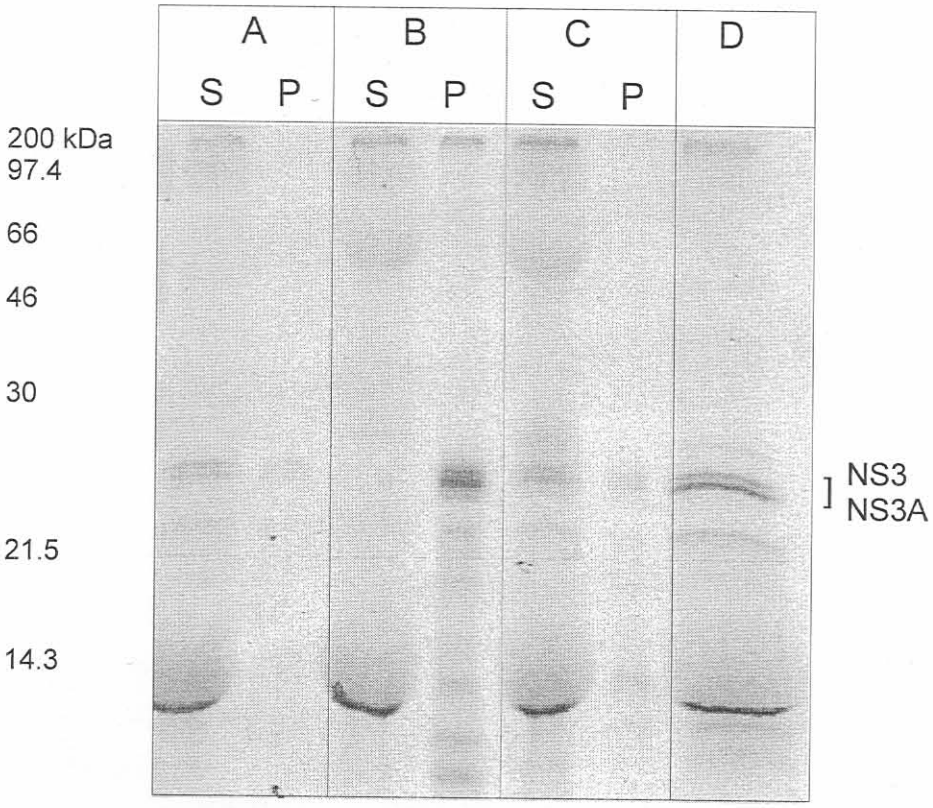

Figure 3.11 Immunoprecipitation analysis of *in vitro* translated AHSV-3 NS3 and NS3A. ^{35}S-labeled translation products were precipitated in the absence of serum (A) and in the presence of anti-β-gal-NS3 (B) or anti-SfVP7-NS3 (C). Unprecipitated proteins in the supernatant (S) and precipitated proteins in the pellet (P) after centrifugation were analysed by 15% SDS-PAGE and autoradiography. *In vitro* translated NS3 and NS3A were included as a control (D) and the positions of NS3 and NS3A are indicated. Rainbow molecular weight markers are indicated.

negative control. The crystals were then viewed under a transmission electron microscope. Should the NS3 sequence be displayed on the surface of VP7-NS3, in a conformation recognised by the anti-β-gal-NS3 serum, then the crystal would have been uniformly labeled with gold particles. Unfortunately due to the extreme electron density of the VP7 crystals, binding of the antibodies and the presence of the gold particles could not be visualised (results not shown). It was, therefore, not possible to ascertain, using this immunogold labeling method, whether the NS3-specific insert was displayed on the surface of VP7-NS3.

3.4 DISCUSSION

Proteins encoded from the same ORF from in-frame start codons, like NS3 and NS3A of AHSV, may be functionally distinct as a result of, for example, a domain in the N-terminal region of the full length protein. Alternatively the absence of the N-terminal extension in the smaller protein(/s) may result in the exposure of a functional domain. These functional domains could, in both cases, control the localisation, or even the activity or specificity of the protein. The S and L surface antigens of Hepatitis B virus, for example, have been shown to be functionally distinct (Oess & Hildt, 2000, see section 1.6.2b), while the P1-P5 proteins of Rabies virus have been shown to be differentially localised (Chenik *et al.,* 1995, see section 1.6.2c).

Comparison of the localisation of the NS3 and NS3A proteins of AHSV would require not only a system capable of monitoring the synthesis and transport of these proteins through the cell, but also a means of differentiating between these almost identical proteins. Antibodies that are directed against the N-terminal of NS3 would provide a means of detecting NS3 in AHSV infected cells. Using these antibodies, in techniques such as immunogold labelling and electron microscopy of infected cells, the ultrastructural localisation of NS3 and NS3/A could be compared. This could potentially also facilitate the identification of cell or virus components that are associated with NS3 and/or NS3A. Alternatively AHSV-infected cells could be fractionated and the presence of NS3 and/or NS3A investigated in each fraction. This would then allow possible insight into a distinct role for these two related proteins in the viral life cycle. Antibodies directed against the N-terminal of NS3 may furthermore be used to experimentally analyse the orientation of the NS3 protein in the cell membrane. The orientation of the influenza virus M2 protein was determined in this way (Lamb *et al.,* 1985). The topology of the NS3 protein has not yet been experimentally elucidated.

Polyclonal antibodies directed against the 12 N-terminal amino acids of NS3 could be prepared against a synthetic peptide representing this region. Peptides are usually synthesized using the solid-phase techniques pioneered by Merrifield in 1963 (Harlow & Lane, 1988). Because of their size, peptides may not be immunogenic on their own. To elicit an antibody response directly, they must contain all of the features of an immunogen,

notably they must have an epitope for B-cell binding and a site for class II-T-cell receptor binding. Some peptides, even surprisingly small ones, contain both these sites usually as a single sequence that can serve both these functions (Harlow & Lane 1988). Unfortunately, there are no methods, short of immunisation, to test this. Most peptides are therefore coupled to carrier proteins prior to immunization. Typical carrier proteins include keyhole limpet hemacyanin (KLH) and bovine serum albumin (BSA). The carrier protein provides good sites for class II-T-cell receptor binding and the peptide itself can be seen as an epitope. Using this approach high-titered antibodies are commonly prepared that characteristically bind well to denatured proteins, but may or may not recognise the native protein (Harlow & Lane, 1988). Alternatively the synthetic peptide could be coupled to a synthetic class II-T-cell receptor (Harlow & Lane, 1988) or to a promiscuous T-cell epitope (Frangione-Beebe *et al.,* 2000). The central problems to this type of strategy are the fact that the native protein is often not recognised by the antisera produced and that the synthesis of peptides is costly.

An alternative would be to clone the DNA sequence encoding the peptide into the surface region of a structural protein that has a predictable high-order particulate structure and that is immunogenic. This type of strategy has become quite common in, for example, particulate vaccine strategies. In fact the VP7 protein of AHSV is currently being engineered for this purpose as it has the characteristics of an antigen display vector (Maree 2000). The protein is immunogenic and spontaneously assembles into a high-order structure. VP7 crystals purified from BHK cells infected with AHSV-9 were shown to be highly immunogenic, eliciting a strong immune response and effective as a subunit vaccine in a mouse model (Wade-Evans *et al.,* 1997, Wade-Evans *et al.,* 1998). Passive transfer of antibodies from immunised mice failed to protect syngeneic recipients from AHSV challenge, indicating that an antibody response is unlikely to represent the primary mechanism involved. It is possible that immunisation with VP7 induces an initial protective T-cell response. Furthermore, the conformation and possibly the assembly of VP7 into crystals appear to be important in the mechanism of protection against heterologous serotype challenge (Wade-Evans *et al.,* 1998). VP7 of BTV, furthermore, contains immunodominant, serotype cross-reactive T-cell epitopes (Wade-Evans *et al.,* 1998). An extension mutant of BTV VP7 containing 48 amino acids of Hepatitis B virus preS2 region

at the N-terminus was found to be highly immunogenic, although the results indicated that the suitability of the N-terminus of BTV VP7 for the insertion of foreign epitopes was relatively restricted due to instability (Belyaev & Roy, 1992; Le Blois & Roy, 1993).

Regions on the AHSV VP7 top or exposed domain have been identified and targeted for the insertion of unique restriction enzyme sites for the cloning and display of foreign epitopes. The insertion of these cloning sites between residues 200 and 201 were shown not to alter the ability of the protein to assemble into hexagonal crystals (Maree, 2000). This insertion mutant, VP7mt200, should be an ideal vector for antigen display. It was therefore decided to use this vector, VP7mt200, for the immunological display of the NS3 N-terminal region as this would simultaneously allow for the production of antibodies against NS3 and for the testing of this protein as an antigen display vector, as this has not previously been done.

Insertion of the NS3 sequence into VP7mt200 was achieved by the synthesis of oligonucleotides representing the N-terminus of NS3 and cloning of this into the *Xba*I and *Sal*I sites at position 200 of pFB-7mt200. The hydrophobicity profile of the amino acid sequence of VP7 remained unaltered by the insertion of the NS3 sequence. Expression of the VP7-NS3 chimera as a baculovirus recombinant resulted in a unique protein of the correct size (± 42 K). This protein reacted positively in an immunoblot with anti-NS3 and anti-β-gal-NS3 sera, indicating that the chimera did contain the NS3 sequence. This furthermore indicated that the N-terminal region of NS3 was immunogenic and should give some immune reaction in VP7-NS3. The solubility and sedimentation profile of VP7-NS3 were compared to the native VP7 protein and the VP7mt200 protein, and found not to differ significantly, remaining highly hydrophobic and insoluble. The VP7-NS3 protein was purified and viewed under a scanning electron microscope.

AHSV VP7 and VP7mt200 aggregate into flat, hexagonal crystals (Roy *et al.,* 1991; Chuma *et al.,* 1992; Burroughs *et al.,* 1994; Maree, 2000). These crystals are composed of layers or flat sheets of VP7 trimers. In each layer of the crystal the trimers are arranged as hexagonal rings, similar to the rings of VP7 trimers found on the surface of AHSV core particles (Burroughs *et al.,* 1994; Basak *et al.,* 1996; Grimes *et al.,* 1998; Stuart *et al.,* 1998). These layers are believed to be held together by hydrophobic interactions, similar to the interactions between VP7 and the underlying VP3 molecules in the core particles.

The VP7-NS3 chimera produced here appears to still form the sheets of trimers although the hydrophobic interactions between these sheets appears to be disrupted, so that the crystals no longer appear flat and the individual layers of trimers are apparent. In extreme cases the crystals have a rose-like appearance. The VP7-NS3 protein, nevertheless, still forms a highly ordered structure and should still be suitable for antigen display.

Monospecific polyclonal antibodies were raised against purified VP7-NS3 crystals. The antiserum produced recognised VP7-NS3 although no specific reaction with denatured or non-denatured AHSV-3 NS3 was detected. Antibodies directed against the NS3 N-terminal may be present in the serum but at a negligibly low titre. This may be due to immunodominance, where the antibody response against one compound, in this case the VP7 epitopes, dominates the response when the immunogenicity of that compound is higher (Harlow & Lane, 1988). The NS3 sequence, which has a net hydrophobic charge, may have folded inwards in such a way that it was not exposed on the surface of the crystal and therefore not accessible to the environment. Alternatively the peptide could not have been exposed on the surface of the crystal simply due to its small size. This could be tested by immunogold labelling of VP7-NS3 crystals using the anti-β-gal-NS3 serum that reacted with this protein in a Western blot. This was attempted, but the extreme electron density of the crystals prevented any clear indication of antibody binding. This could also be tested by immunofluorescent labelling of the crystals in infected cells and viewing with a fluorescent microscope.

A model of the three-dimensional structure of an AHSV VP7 trimer is shown in Fig 3.12 (Maree, 2000), sites that have been targeted for insertion are indicated (VP7mt144, blue, VP7mt177 green and VP7mt200 red). From this Figure it can be seen that position 200 is less exposed on the surface and although insertions at this site do not alter the hydrophobicity, solubility or crystal structure of the protein, the alternative sites (144, 177) may represent better targets for the display of such a small peptide. Conversely tandem repeats of the NS3 sequence could be cloned into the VP7mt200 vector, with a greater probability of being exposed on the surface of the resulting crystals.

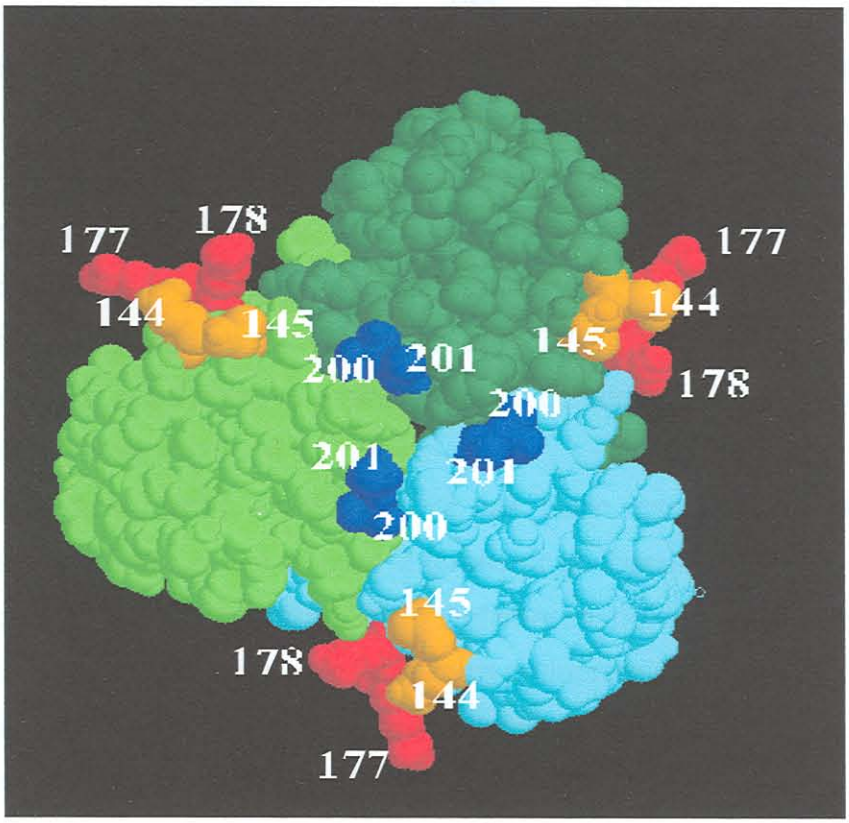

Figure 3.12 Model of the VP7 trimer 3-D structure indicating mutational insertions that have been made at hydrophilic regions exposed on the surface of the protein. The backbone of the VP7 protein is indicated in green and the insertion sites 144-145, 177-178 and 200-201 are indicated in orange, red and navy blue respectively (Maree, 2000).

The insertion of six amino acids at position 177-178 of VP7 (recombinant VP7mt177) caused a significant increase in the solubility of the VP7 protein with the result that only a fraction of the protein formed morphological structures. The structures formed by VP7mt177 were not the distinct hexagonal crystals observed with wild type VP7, but small ball-like structures which only later, when examined with a transmission electron microscope, were shown to possess an ordered crystalline lattice (Maree, 2000). This insertion site is more exposed on the surface of the VP7 crystal (Fig 3.12) and may be a more suitable vector for the display of a small peptide considering it has now been shown to posses a highly ordered structure.

A 105 amino acid region of AHSV VP2 has been inserted into VP7mt200 and VP7mt177. These chimeric proteins were expressed as baculovirus recombinants and found to have an increased solubility. These chimeras no longer formed the typical hexagonal crystals but did however appear to form multiprotein structures (Maree, 2000). The immunogenicity of these chimeras has not been investigated.

The use of AHSV VP7 as an antigen display vector definitely still merits further investigation. The use of viral particulate structures for antigen or epitope display has been successful in a number of cases. Heal and coworkers (1999), for example, modified the coat protein of the RNA bacteriophage MS2 for the display of antigens as a novel vaccine strategy. The coat protein of MS2 self-assembles into capsids that elicit both humoral and cellular immune responses. The N-terminus of this protein contains a beta-hairpin loop that forms the most radially exposed feature of the mature capsid. This site was targeted and modified to enable insertion of DNA at the central part of the beta-hairpin loop for the display of foreign peptides on the surface of RNA-free bacteriophage capsids. A putative protective epitope, T1, from the immunodominant liver stage antigen-1 (LSA-1) of the malaria parasite *Plasmodium falciparum* was subsequently cloned into this site. The recombinant construct was expressed in *E. coli* and the immunogenicity of the resulting chimeric capsids was found to correspond well to naturally acquired resistance to liver stage malaria (Heal *et al.,* 1999).

A similar type of approach was also taken with the development of an antigen presentation system based on the plum pox potyvirus (PPV). The amino-terminal part of PPV capsid protein was chosen as the site for the expression of foreign antigenic

peptides. Different forms of an antigenic peptide (single or tandem repeats) from the VP2 capsid protein of canine parvovirus (CPV) were expressed at the chosen site. Mice and rabbits immunised with purified chimeric virions developed CPV-specific neutralising antibodies (Fernandez-Fernandez *et al.,* 1998). Other examples of particulate vector systems for the presentation of immunogenic epitopes include recombinant BTV core-like particles (Mikhailov *et al.,* 1996), BTV NS1 tubules (Mikhailov *et al.,* 1996) and hepatitis B virus core protein (Chambers *et al.,* 1996).

To summarize, the AHSV core protein VP7 was used as an antigen presentation vector for the display of the N-terminal region of NS3. The chimeric protein assembled as a highly-ordered crystal structure and was used for the production of polyclonal serum. Although no antibodies against AHSV-3 NS3 were obtained in this study, the VP7 vector is still in its developmental stages and the use of alternative sites on VP7 are proposed for the display of such a small peptide.

CHAPTER 4

CONCLUDING REMARKS

A common feature of the smallest dsRNA genome segment of all known orbiviruses is that they encode two related proteins, NS3 and NS3A, from two in-frame overlapping ORFs. Why this feature has been conserved is not yet clear and one of the objectives of this investigation was to analyse and compare the NS3 and NS3A proteins of AHSV. This study forms part of a larger project to understand the role of NS3/A in the life cycle, virulence and pathogenesis of AHSV.

The AHSV segment 10 products may be related to a family of viral proteins that cause membrane permeabilisation, termed viroporins. This is based on the fact that NS3 and NS3A cause membrane damage and eventual cell death when expressed as baculovirus recombinants in insect cells (Van Staden *et al.,* 1995; Van Niekerk *et al.,* 2001a). The NS3 and NS3A proteins also display many of the characteristic structural features common to viroporins. The cytotoxicity of these proteins has been shown to be dependant on their membrane association (Van Niekerk *et al.,* 2001a), but little else is known about the cytotoxic properties of NS3 and NS3A. Several aspects of the functioning of these proteins, therefore, remain to be investigated including whether the proteins cause membrane permeabilisation in mammalian cells and if they are able to exert their effect extracellularly. The effect of NS3 on mammalian cells following extracellular addition of the protein was investigated here.

As the NS3 protein has not yet been purified in a biologically active form, it was decided to use crude extracts from Bac-NS3-infected *Sf9* cells for initial experiments in determining the effect of exogenous NS3 on the membranes of Vero cells. Extracellular NS3 was found to cause an increase in the uptake of the membrane impermeable translation inhibitor, Hygromycin B in Vero cells. Thus the cytotoxic properties of NS3 appear not to be limited to causing membrane damage in insect cells alone. This property of NS3 needs to be investigated as this furthers the idea that NS3 is a viroporin and is involved in the pathogenesis of AHSV. Future

research could investigate the molecular mechanism of membrane damage caused by NS3 and also determine the correlation, if any, between the virulence of a strain of AHSV and the membrane damaging properties of the NS3 protein of that strain. The extracellular cytotoxic effect of NS3 should, furthermore, be compared to that of NS3A.

Three possible molecular mechanisms of toxin-membrane interaction and subsequent increased membrane permeability can be postulated. These are: receptor-mediated, transmembrane ionic channel and/or pore formation and nonspecific membrane pertubation.

The enterotoxic behaviour of rotavirus NSP4, for example, is mediated by its interaction with a putative plasma membrane receptor triggering a phospholipase C-mediated increase in intracellular Ca^{2+} (Dong *et al.,* 1997; Morris *et al.,* 1999). HIV-1 gp120 increases the permeability of rat brain endothelium by a receptor-mediated mechanism involving substance P (Annunziata *et al.,* 1998).

HIV-1 Vpr added extracellularly to intact cells forms ion channels that cause a large inward cation current, depolarization of the plasmalemma and eventual cell death (Piller *et al.,* 1998). This extracellular toxic effect of Vpr is caused by a region of the protein containing the sequence HFRIGCRHSRIG (Macreadie *et al.,* 1996). An amphipathic region (designated lentivirus lytic peptide, LLP-1) of HIV-1 transmembrane protein was also found to be toxic to both prokaryotic and eukaryotic cells when added exogenously. The LLP-1 peptide causes membrane pertubation by forming pores of defined size in cytoplasmic membranes (Miller *et al.*1993). Other examples of pore forming cytolytic proteins include M2 of influenza A, NB of influenza B, Vpu of HIV-1 (Sansome *et al.,* 1998), the synthetic amphipathic peptide GALA (Parente 1990), polypeptide venoms such as melittin, and polypeptide antibiotics such as magainins (Segrest *et al.,* 1990). A common structural feature in many pore forming cytotoxic proteins is the presence of an amphipathic helix motif.

Membrane pertubation may also be nonspecific, occurring via a detergent-like action such as was found with the cytolytic endotoxin Cyt A (Butko *et al.*1996).

The mechanism by which extracellular NS3 causes membrane permeabilisation could be investigated by determining whether the protein is toxic to both prokaryotic and eukaryotic cells. Membrane damage is unlikely to be via a receptor-mediated mechanism in prokaryotic cell membranes. Alternatively, it may be that the effects of the protein are not limited simply to direct membrane damage alone but also occur through interactions with membrane proteins and receptors. Although extracellular rotavirus NSP4 causes an increase in Ca^{2+} via a receptor-mediated mechanism (Tian *et al.,* 1994), the protein has also been shown to have direct membrane destabilising activity that does not require receptors (Tian *et al.,* 1996). The requirement for receptors could also be investigated by treating eukaryotic cells with protease prior to exogenous addition of the NS3 protein.

To determine which regions of the protein are involved and important in membrane destabilisation a variety of truncated mutants of the NS3 protein could be made and investigated. Synthetic peptides could then be produced, representing this region(/s), and the dynamics and conditions of cell lysis determined. The change in permeability of cell membranes to a variety of compounds of various molecular weights should also be investigated. If a transmembrane pore is formed by NS3 then there is expected to be a size or molecular weight dependance on the leakage or uptake of compounds, while size should not be a factor if the protein acts in a detergent-like fashion.

The role that this aspect of NS3 plays in viral virulence and pathogenicity of AHSV also needs to investigated. Studies of AHSV virulence characteristics have been carried out using a mouse model system and genome segment reassortments between virulent and avirulent strains. Exchange of genome segment 10, and therefore variations in the protein sequence of NS3, were shown to influence the virulence characteristics of the progeny virus strain (O'Hara *et al.,* 1998). This furthermore implicates NS3 in the pathogenicity and virulence of AHSV (O'Hara *et al.,* 1998). The toxic effect of the NS3 protein of virulent and avirulent strains of AHSV should be compared to one another and related to the virulence of the strain.

The specificity of the NS3 extracellular cytotoxic effect can be investigated by using a variety of eukaryotic cells such as equine lung cells and endothelial cells in

membrane permeability assays. Laegried and co-workers (1992) suggest that difference in ability of virulence variants of AHSV to cause acute disease may be related to their ability to infect and damage endothelial cells.

The toxicity of NS3 to mammalian cells exogenously should also be compared to the effect of the protein when expressed endogenously. For this reason the NS3, NS3A and NS3-mutant proteins should be expressed as recombinants in a mammalian expression system. Browne *et al.,* (2000) postulate that the membrane-destabilising and enterotoxic properties of NSP4 may be mediated by different regions of the protein.

Macreadie *et al.,* (1996) propose that the cytotoxic HIV-1 Vpr could be responsible for the death of uninfected bystander cells surrounding HIV-1-infected cells. Cell death in uninfected bystander cells has also been observed during AHSV infection, the role that NS3 may play in this should be investigated. It would also be interesting to determine whether AHSV-infected cells secrete NS3 or a functional peptide thereof. Rotavirus-infected cells have been shown to secrete a functional NSP4 enterotoxin peptide (Zhang *et al.,* 2000).

Another aspect of the functioning of NS3 and NS3A that was addressed in this study was the effect of co-expression of NS3 and NS3A on the cytotoxicity of the proteins to insect cells. This was necessary as AHSV infection of Vero cells results in the synthesis of NS3 and NS3A in equimolar amounts (Van Staden *et al.,* 1995), while expression of S10 in insect cells results in the synthesis of NS3 alone. NS3 and NS3A were therefore co-expressed here in insect cells to mimic the expression patterns seen in AHSV infected cells. This was achieved through the co-infection of insect cells with recombinant baculoviruses expressing NS3 and NS3A. The cytotoxic effect of co-expression of the NS3 and NS3A proteins was similar to the effect of individual expression of either protein. The NS3 protein is therefore representative of NS3 and NS3A together in terms of its cytotoxic effect and no interactions between these proteins occurs that affects this aspect of their functioning.

One of the objectives of this study was to purify large quantities of NS3 and NS3A, expressed in an eukaryotic system for comparative and functional studies.

The NS3 and NS3A proteins were expressed as histidine tag fusion products in insect cells using the baculovirus expression system. The HTc-NS3 protein was found, however, to be only partly soluble and did not bind to charged Nickel resin. This may be due to the folding of the tag in such a way that it is not exposed to the environment. HTc-NS3 and wild type NS3 were furthermore found to differ significantly in solubility, this insolubility of HTc-NS3 may be due to incorrect folding due to the presence of the histidine tag.

The N-terminal NS3 sequences of AHSV, Palyam virus, BRD virus, BTV and EHDV were compared and found to differ significantly in both length and amino acid identity. The presence of the second methionine, representing the N-terminal amino acid of NS3A, was however conserved throughout, indicating a selective conservation of the second start codon in the S10 gene of orbiviruses. Sequence and pattern searches of this region in NS3 of AHSV-3, using protein profile databases, did not reveal potential motifs or domains that may represent a functional domain. The N-terminal region of NS3 of the different serotypes of AHSV furthermore displays little conservation. The presence of a functional domain in this region appears to be unlikely.

The final aim of this study was to produce polyclonal antibodies that would specifically recognise the short N-terminal region of NS3 that is absent in the NS3A protein, for use in distinguishing between these proteins in AHSV infected cells. The AHSV core protein VP7 was used as a vector for immunological display of this small peptide. This would allow for both the production of serum against the N-terminal of NS3 and for an investigation into the suitability of the VP7 protein as an antigen display vector. The chimera, VP7-NS3, was found to still be able to assemble as highly ordered crystal structures and was used for polyclonal antiserum production. The resulting serum contained antibodies directed against VP7, but not NS3, epitopes.

Future research may target different sites on VP7 for the display of such a small peptide or tandem repeats of the peptide could be displayed. Once available this serum could be used in localisation studies in AHSV infected cells and may aid in determining whether both proteins are necessary and involved in virus

morphogenesis. Antiserum directed against the N-terminal amino acids of NS3 may also be used to experimentally determine the orientation of the NS3 protein in the cell membrane.

The orientation of the influenza virus M2 protein was determined in this way (Lamb *et al.*, 1985). Oligopeptides representing the N-terminal residues 2–10 and C-terminal residues 69-79 of M2 were synthesised and coupled to keyhole limpet hemocyanin (Lamb *et al.*, 1985). Rabbit antisera were then prepared against these peptides and used for immunofluorescent-staining of cells infected with the Influenza virus. Only the antibodies directed against the N-terminus were shown to bind to the M2 protein on the cell surface indicating that this region is located in the extracellular space whereas the carboxy terminus is cytoplasmic. M2 is, thus, a type I integral membrane protein (Lamb *et al.*, 1985). The membrane topology of AHSV NS3 has not yet been experimentally elucidated.

Other aspects of NS3 that remain to be investigated include the oligomerisation state of the protein. As discussed in chapter 1, the presence of different polypeptide monomers, like NS3 and NS3A could increase the range of potential complexes formed. As NS3 and NS3A are involved in virus morphogenesis the interaction between these proteins and the viral capsid proteins needs to be examined. Rotavirus NSP4 has been shown to bind VP6 and VP4 on SSP and facilitate translocation of viral particles across the ER membrane (Au *et al.*, 1989; Meyer *et al.*, 1989; Mattion *et al.*, 1994).

The recent development of a reovirus reverse genetics system may be applicable to all dsRNA viruses, including orbiviruses (Roner & Joklik 2001). This system allows for the introduction of mutations into the dsRNA genome and may in the future be a powerful system for studies on the role of S10 in AHSV virulence.

An understanding of the molecular mechanisms of the functioning of NS3 and the role that the membrane damaging properties of this protein plays in the pathogenesis of AHSV, may potentially lead to the development of new therapies for this devastating disease.

CONGRESS PARTICIPATION AND PUBLICATIONS

Parts of the results in this thesis are being published:

Maree, FF., J.E. Riley, Q. Meyer, T.L. Meiring, V. van Staden & H. Huismans. Effects of site directed insertion mutagenesis on the solubility and particulate structure formation of major core protein VP7 of African horsesickness virus. (Publication pending).

Parts of the results in this thesis have been presented at scientific meetings:

A comparison of Nonstructural protein NS3 sequence variation amongst isolates of African horsesickness, bluetongue and equine encephalosis viruses in Southern Africa
Huismans, H., M. Van Niekerk, TL. Meiring, M. Freeman, K. Lombardi, V. Van Staden, AA. Van Dijk, and A. Guthrie.
Seventh International Symposium on Double-Stranded RNA viruses, Palm Beach, Aruba, December, 2000.

A novel method for the immunological display of the N-terminal amino acids of nonstructural protein NS3 of African Horsesickness virus by insertion into major structural protein VP7.
Huismans, H. TL. Meiring, FF Maree and V. Van Staden
Seventh International symposium on Double-stranded RNA viruses, Palm Beach, Aruba, December, 2000.

A novel method for the immunological display of the N-terminal amino acids of nonstructural protein NS3 of African horsesickness virus by insertion into major structural protein VP7.
Meiring,TL., FF Maree, V. Van Staden and H. Huismans.
South African Genetics Society XVII Th congress, Pretoria, June, 2000.

REFERENCES:

ABI Prism Comparative PCR sequencing guide, Perkin Elmer 1995.

ABI Prism DNA Sequencing, Chemistry guide, Perkin Elmer 1995.

Annunziata, P., C. Cioni, S. Toneatto and E. Paccagnini. 1998. HIV-1 gp120 increases the permeability of rat brain endothelium cultures by a mechanism involving substance P. *AIDS* **12**, 2377-2385.

Au, K., W. Chan, J.W. Burns and M.K. Estes. 1989. Receptor activity of rotavirus nonstructural glycoprotein NS28. *J. Virol.* **63**, 4553-4562.

Au, K., N.M. Mattion and M.K. Estes. 1993. A subviral particle binding domain on the rotavirus nonstructural glycoprotein NS28. *Virology* **194**, 665-673.

Ausubel, F.M., R. Brent, R.E. Kingston, D.D. Moore, J.G. Seidman, J.A. Smith and K. Struhl. 1988. *Current protocols in molecular biology*. John Wiley and sons, New York.

BAC-TO-BAC baculovirus expression system manual, Life technologies GIBCO BRL.

Ball, J.M., P. Tian, C.Q.-Y Zeng, A.P. Morris and M.K. Estes. 1996. Age-dependant diarrhea induced by a rotaviral nonstructural glycoprotein. *Science* **272**, 101-104.

Bansal, O.M., A. Stokes, A. Bansal, D. Bishop and P. Roy. 1998. Membrane organisation of bluetongue virus nonstructural glycoprotein NS3. *J. Virol.* **72**, 3362-3369.

Barco, A and L. Carrasco. 1998. Identification of regions of poliovirus 2BC protein that are involved in cytotoxicity. *J. Virol.* **72**, 3560-3570.

Basak, A.K., P. Gouet, J. Grimes, P. Roy and D. Stuart.1996. Crystal structure of the top domain of African horsesickness virus VP7: comparisons with bluetongue virus VP7. *J Virol* **70**, 3797-3806.

Bassel-Duby, R., A. Jayasuriya, D. Chatterjee, N. Soneberg, J.V. Maizel and B.N. Fields. 1985. Sequence of reovirus haemaglutinin predicts a coiled-coil structure. *Nature* **315**, 421-423.

Belsham, G.J. 1992. Dual initiation sites of protein synthesis on foot-and-mouth disease virus RNA are selected following internal entry and scanning of ribosomes *in vivo*. *EMBO J.* **11**, 1105-1110.

Belyaev, A.S. and P. Roy. 1992. Presentation of hepatitis B virus preS2 epitoped on bluetongue virus core-like particles. *Virology* **190**, 840-844.

Benedetto, A., G.B. Rossi, C. Amici, F. Belardelli, L. Cioe, G. Carruba and L. Carrasco. 1980. Inhibition of animal virus production by means of translation inhibitors unable to penetrate normal cells. *Virology* **106**, 123-132.

Bentley, L., J. Fehrsen, F. Jordaan, H.Huismans and D.H. Du Plessis. 2000. Identification of antigenic regions on VP2 of African horsesickness virus serotype 3 by using phage-display epitope libraries. *J. Gen. Virol.* **81**, 993-1000.

Birnboim, H.C. and J. Doly. 1979. A rapid alkaline extraction procedure for screening recombinant plasmid DNA. *Nucleic Acids Res.* **7**, 1513-1523.

Borden, E.C., R.E. Shorpe and F.A. Murphy. 1971. Physicochemical and morphological relationships of some arthropod-borne viruses to bluetongue virus – a new taxonomic group. Physicochemical and serological studies. *J. Gen. Virol.* **13**, 261-271.

Bremer, C.W. 1976. A gel electrophoretic study of the protein and nucleic acid components of African horsesickness virus. *Onderstepoort J. vet. Res.* **43**, 193-200.

Browne, E.P., A.R. Bellamy and J.A. Taylor. 2000. Membrane–destabilising activity of rotavirus NSP4 is mediated by a membrane-proximal amphipathic domain. *J. Gen. Virol.* **81**, 1955-1959.

Burrage, T.G., T. Trevejo, M. Stone-Marschat and W.W. Laegried. 1993. Neutralising epitopes of African horsesickness virus serotype 4 are located on VP2. *Virology* **196**, 799-803.

Burrage, T.G. and W.W. Laegried. 1994. African horsesickness: pathogenesis and immunity. *Comp. Immun. Microbiol. Infect. Dis.* **17**, 275-285.

Burroughs, J.N., R.S. O'Hara, C.J. Smale, C. Hamblin, A. Walton, R. Armstrong and P.P.C. Mertens. 1994. Purification and properties of virus particles, infectious subviral particles, cores and VP7 crystals of African horsesickness virus serotype 9. *J. Gen. Virol.* **75**, 1849-1857.

Butko, P., F. Huang, M. Pusztai-Carey and W.K. Surewicz. 1996. Membrane permeabilisation induced by cytolytic δ-endotoxin CytA from *Bacillus thuringiensis* var. *israelensis. Biochemistry* **35**, 11355-11360.

Cao, X., I.E. Bergmann, R. Fullkrug and E. Beck. 1995. Functional analysis of the two alternative translation initiation sites of foot-and-mouth disease virus. *J. Virol.* **69**, 560-563.

Carrasco, L. 1994. Modification of membrane permeability by animal viruses. *Adv. Vir. Res.* **45**, 61-112.

Carrasco, L., M.J. Otero and J.L. Castrillo. 1989. Modification of membrane permeabilty by animal viruses. *Pharmac. Ther.* **40**, 171-212.

Chambers, M.A., G. Dougan, J. Newman, F. Brown, J. Crowther, A.P. Mould, M.J. Humphries, M.J. Francis, B. Clarke, A.L. Brown and D. Rowlands. 1996. Chimeric hepatitis B virus core particles as probes for studying peptide-integrin interactions. *J. Virol.* **70**, 4045-4052.

Chan, W.K., K.S. Au, and M.K. Estes. 1988. Topography of the simian rotavirus nonstructural glycoprotein (NS28) in the endoplasmic reticulum membrane. *Virology* **164**, 435-442.

Chang, Y., C. Liao, C. Tsao, M. Chen, C. Liu, L. Chen and Y. Lin. 1999. Membrane permeabilisation by small hydrophobic nonstructural proteins of Japanese encephalitis virus. *J Virol* **73**, 6257-6264.

Chenik, M. K. Chebli and D. Blondel. 1995. Translation initiation at alternate in-frame AUG codons in the rabies virus phosphoprotein mRNA is mediated by a ribosomal leaky scanning mechanism. *J Virol.* **69**, 707-712.

Chuma, T., H. Le Blois, J.M. Sánchez-Vizcaíno, M. Diaz-Laviada and P. Roy. 1992. Expression of the major core antigen VP7 of African horsesickness virus by a recombinant baculovirus and its use as a group-specific diagnostic reagent. *J. Gen. Virol.* **73**, 925-931.

Chung, C.T. and R.H. Miller. 1988. A rapid and convenient method for the preparation and storage of competent cells. *N.A.R.* **16**, 3580.

Coetzer, J.A.W. and B.J. Erasmus. 1994. African horsesickness virus. In *Infectious diseases of Livestock with Special Reference to South Africa.* eds J.A.W Coetzer, G.R. Thomas, R.C. Tustin. Oxford University Press. pp 460-475.

Crowe, J., B.S. Masone and J. Ribbe. 1995. One-step purification of recombinant proteins with the 6xHis tag and Ni-NTA resin. *Mol. Biotechnol.* **4**, 247-258.

Dabrowski, C and J.C. Alwine. 1988. Translational control of synthesis of simian virus 40 late proteins .from polycistronic 19S late mRNA. *J. Virol.* **62**, 3182-3192.

De Sá, R., Zellner, M. and M.J. Grubman. 1994. Phylogenetic analysis of segment 10 from African horsesickness virus and cognate proteins from other orbiviruses. *Vir. Res.* **33**, 157-165.

Devaney, M.A., J. Kendall and M.J. Grubman. 1988. Characterisation of a nonstructural protein of two orbiviruses. *Virus Res.* **11**, 151-164.

Doms, R.W., R.A. Lamb, J.K. Rose and A. Helenius. 1993. Folding and assembly of viral membrane proteins. *Virology* **193**, 545-562.

Dong, Y., C.Q.-Y. Zeng, J.M. Ball, M.K. Estes and A.P. Morris. 1997. The rotavirus enterotoxin NSP4 mobilizes intracellular calcium in human intestinal cells by stimulating phospholipase C-mediated inositol 1,4,5-triphosphate production. *Proc. Natl. Acad. Sci. USA* **94**, 3960-3965.

Du Toit, R.M. 1944. The transmission of blue-tongue and horse-sickness by *Culicoides. Onderstepoort J.* **19**, 7-16.

Erasmus, B.J. 1972. The pathogenesis of African horsesickness. *Proc. 3rd Int. Conf. Equine. Infectious diseases*, Paris, pp 1-11.

Estes, M.K., G. Kang, C.Q. Zeng, S.E. Crawford and M. Ciarlet. 2001. Pathogenesis of rotavirus gastroenteritis. *Novartis Found. Symp.* **238**, 82-96.

Felgner, P.L, T.R. Gadek, M. Holm, R. Roman, H.W. Chan, M. Wenz, J.P. Northrop, G.M. Ringold and M. Danielsen. 1987. Lipofection: a highly efficient, lipid mediated DNA-transfection procedure. *Proc. Natl. Acad. Sci USA* **84**, 7413-7417.

Fernandez-Fernandez, M.R., J.L. Martinez-Torrecuadrada, J.I. Casal and J.A. Garcia. 1998. Development of an antigen presentation system based on plum pox potyvirus. *FEBS Lett.* **427**, 229-235.

Frangione-Beebe, M., B. Albrecht, N. Dakappagari, R.T. Rose, C.L. Brooks, S.P. Schwendeman, M.D. Lairmore and P.T. Kaumaya. 2000. Enhanced immunogenecity of a conformational epitope of human T-lymphotropic virus type 1 using a novel chimeric peptide. *Vaccine* **19**, 1068-1081.

French, T.J., S. Inumaru and P. Roy. 1989. Expression of two related nonstructural proteins of bluetongue virus (BTV) type 10 in insect cells by a recombinant baculovirus; production of polyclonal ascitic fluid and characterization of the gene product in BTV-infected BHK cells. *J. Virol.* **63**, 3270-3278.

French, T.J and P. Roy. 1990. Synthesis of bluetongue virus (BTV) corelike particles by a recombinant baculovirus expressing the two major structural core proteins. *J. Virol.* **64**, 1530-1536.

Gale, M., S.-L. Tan and M.G. Katze. 2000. Translational control of viral gene expression in eukaryotes. *Micro. Mol. Biol. Rev.* **64**, 239-280.

Gallina, A., A. De Koning, F. Rossi, R. Calogero, R. Manservigo and G. Milanesi. 1992. Translational modulation in Hepatitis B virus preS-S open reading frame expression. *J. Gen. Virol.* **73**, 139-148.

Garoff, H. 1985. Using recombinant DNA techniques to study protein targeting in eukaryotic cells. *Ann. Rev. Cell. Biol.* **1**, 403-450.

Geourjon, C., G. Deleage and B. Roux. 1991. Antheprot: an interactive graphics software for analyzing protein structures from sequences. *J. Mol. Graph.* **9**., 188-190.

Good, P.J., R.C. Welch, A. Barkan, M.B. Somasekhar and J.E. Mertz. 1988. Both VP2 and VP3 are synthesised from each of the alternatively spliced late 19S RNA species of Simian virus 40. *J. Virol.* **62**, 944-953.

Gonzalez, M.E. and L. Carrasco. 1998. The human immunodeficiency virus type 1 Vpu protein enhances membrane permeability. *Biochem.* **29**, 13710-13719.

Gorman, B.M. and J. Taylor. 1985. Orbiviruses. In: *Virology*. eds B.M. Fields. Raven press, New York. pp 907-925.

Grimes, J.M., A.K. Basak, P. Roy and D. Stuart. 1995. The crystal structure of bluetongue virus VP7. *Nature* **373**, 167-170.

Grubman, M.J., and S.A. Lewis. 1992. Identification and characterisation of the structural and nonstructural proteins of African horsesickness virus and determination of the genome coding assignments. *Virology* **186**, 444-451.

Haarr, L., H.S. Marsden, C.M. Preston, J.R. Smiley, W.C. Summers and W.P. Summers. 1985. Utilization of internal AUG codons for initiation of protein synthesis directed by mRNAs from normal and mutant genes encoding Herpes simplex virus-specified thymidine kinase. *J. Virol.* **56**, 512-519.

Harlow, E. and D. Lane. 1988. *Antibodies: A laboratory manual*. Cold Spring Harbour Laboratory, USA, 726 pp.

Hassan, S.H., C. Wirblich, M. Forzan and P. Roy. 2001. Expression and functional characterisation of bluetongue virus VP5 protein: role in cellular permeabilisation. *J. Virol.* **75**, 8356-8367.

Heal. K.G., H.R. Hill, P.G. Stockley, M.R. Hollingdale and A.W.Taylor-Robinson. 1999. Expression and immunogenecity of a liver stage malaria epitope presented as a foreign peptide on the surface of RNA-free MS2 bacteriophage capsids. *Vaccine*. **18**, 251-258.

Hedge, R.S. and V.R. Lingappa. 1997. Membrane protein biogenesis: Regulated complexicity at the endoplasmic reticulum. *Cell* **91**, 575-582.

Heermann, K.H., U. Goldman, W. Schwartz, T. Seyffarth, H. Baumgarten and W.H. Gerlich. 1984. Large surface proteins of hepatitis B virus containing the pre-S sequence. *J. Virol.* **52**, 396-402.

Hewat, E.A., T.F. Booth, P.T. Loudon and P. Roy. 1992. Three-dimensional reconstruction of baculovirus expressed bluetongue virus core-like particles by cryo-electron microscopy. *Virology* **189**, 10-20.

Hjelmeland, LM. 1990. Solubilisation of native membrane proteins in *Methods in Enzymology*. Academic Press Inc. New York.

Hopp, T.P. and K.R. Woods. 1981. Prediction of protein determinants from amino acid sequences. *Proc. Natl. Acad. Sci USA* **78,** 3824-3828.

Hochuli, E., H. Döbeli, A. Schaber. 1987. New metal chelate adsorbent selective for proteins and peptides containing neighbouring histidine residues. *J. Chromatography* **411**, 177-184.

Holton, R.H. and G.A. Gentry. 1996. The Epstein-Barr virus genome encodes deoxythymidine kinase activity in a nested internal open reading frame. *Intervirol.* **39**, 270-274.

Horton, P. and K. Nakai. 1996. A probabilistic classification system for predicting the cellular localisation sites of proteins. *Proc. Int. Conf. Intell. Syst. Mol. Biol.* 4, 109-115.

Horton, P. and K. Nakai. 1997. Better predition of protein cellular localisation sites with the k nearest neighors classifier. *Proc. Int. Conf. Intell. Syst. Mol. Biol.* **5**, 147-152.

Howell, P.G. 1962. The isolation and identification of further antigenic types of African horsesickness virus. *Onderstepoort J. vet. Res.* **29**, 139-149.

Huismans, H. 1979. Protein synthesis in bluetongue virus-infected cells. *Virology* **92**, 385-396.

Huismans, H. and H.J. Els. 1979. Characterisation of the tubules associated with the replication of three different orbiviruses. *Virology* **92**, 397-406.

Hwang, G., Y. Yang, J. Chiou and J.K. Li. 1992. Sequence conservation among the cognate nonstructural NS3/3A protein genes of six bluetongue viruses. *Virus Res.* **23**, 151-161.

Hyatt, A.D., A.R. Gould, B. Coupar and B.T. Eaton. 1991. Localisation of the non-structural protein NS3 in bluetongue virus-infected cells. *J. Virol.* **72**, 2263-2267.

Hyatt, A.D., Y. Zhao and P. Roy. 1993. Release of bluetongue virus-like particles from insect cells is mediated by BTV nonstructural protein NS3/NS3A. *Virology* **193**, 592-603.

Jecht, M., C. Probst and V. Gauss-Müller. 1998. Membrane permeability induced by hepatitis A virus proteins 2B and 2BC and proteolytic processing of HAV 2BC. *Virology* **252**, 218-227.

Jensen, M.J., I.W. Cheney, L.H. Thompson, J.O. Mecham, W.C. Wilson, M. Yamakawa, P. Roy and B.M. Gorman. 1994. The smallest genome segment of the orbivirus, epizootic hemorrhagic disease, is expressed in virus-infected cells as two proteins and the expression differs from that of the cognate gene of bluetongue virus. *Virus Res.* **32**, 353-364.

Jensen, M.J and W.C. Wilson. 1995. A model for the topology of the NS3 protein as predicted from the sequence of segment 10 of epizootic haemorrhagic disease virus serotype 1. *Arch. Virol.* **140**, 799-805.

Johnston, J.C. and D.M. Rochon. 1996. Both codon context and leader length contribute to efficient expression of two overlapping open reading frames of cucumber necrosis virus bifunctional subgenomic mRNA. *Virol*ogy **221**, 232-239.

Kirkwood, C.D., B.S. Coulson and R.F. Bishop. 1996 G3P2 rotaviruses causing diarrhoeal disease in neonates differ in VP4, VP7 and NSP4 sequence from G3P2 strains causing asymptomatic neonatal infection. *Arch. Virol.* **141**, 1661-1676.

Kirkwood, C.D and E.A. Palombo. 1997. Genetic characterization of the rotavirus nonstructural protein, NSP4. *Virology* **236**, 258-265.

Kozak, M. 1987. At least six nucleotides preceding the AUG initiator codon enhance translation in mammalian cells. *J. Mol. Biol.* **196**, 947-950.

Kozak, M. 1991. An analysis of vertebrate mRNA sequences: Intimations of translational control. *J. Cell. Biol.* **115**, 887-903.

Kozak, M. 1995. Adherence to the first AUG rule when a second AUG codon follows closely upon the first. *Proc. Natl. Acad. Sci. USA* **92**, 2662-2666.

Kozak, M. 1999. Initiation of translation in prokaryotes and eukaryotes. *Gene* **234**, 187-208.

Kuo, M.D., C. Chin, S.L. Hsu, J.Y. Shiao, T.M. Wang and J.H. Lin. 1996. Characterisation of the NTPase activity of Japanese encephalitis virus NS3 protein. *J. Gen. Virol.* **77**, 2077-2084.

Laegried, W.W., T.G. Burrage, M. Stone-Marschat and A. Skowneck. 1992a. Electron microscopical evidence for endothelial infection by African horsesickness virus. *Vet. pathol.* **29**, 554-556.

Laegried, W.W., M. Stone-Marschat, A. Skowneck and T. Burrage. 1992b. Infection of endothelial cells by African horsesickness virus. In: *Bluetongue, African horsesickness, and related orbiviruses.* Eds. T.E Watson and B.I. Osburn. CRC Press Boca Raton, FL. pp. 807-814.

Laegried, W.W., A. Skowneck, M. Stone-Marshcat and T. Burrage. 1993. Characterisation of virulence variants of African horsesickness virus. *Virology* **195**, 836-839.

Lamb, R.A., S.L. Zebedee and C.D. richardson.1985. Influenza virus M2 protein is an integral membrane protein expressed on the infected cell-surface. *Cell* **40**, 627-633.

Lasnik, M.A., V.G. Porekar and A. Stalc. 2001. Human granulocyte colony stimulating factor (hG-CSF) expressed by methylotrophic yeast pichia pastoris. *Pflugers Arch.* **442**, R184-186.

Laviada, M.D., M. Arias and J.M. Sanchez-Vizcaino. 1993. Characterisation of African horsesickness virus serotype 4-induced polypeptides in Vero cells and their reactivity in Western immunoblotting. *J. Gen. Virol.* **74**, 81-87.

Le Blois, H. and P. Roy. 1993. A single point mutation in the VP7 major core protein of bluetongue virus prevents the formation of core-like particles. *J. Virol.* **67**, 353-359.

Lecat, S., P. Verkade, C. Theile, K. Fiedler, K. Simons and F. Lafont. 2000. Different properties of two isoforms of annexin XIII in MDCK cells. *J. Cell Sci.* **113**, 2607-2618.

Lewin, B. 1994. *Genes V.* Oxford University Press, Oxford. pp 1272.

Lewis, S.A. and M.J. Grubman. 1991. VP2 is the major exposed protein on orbiviruses. *Arch. Virol.* **121**, 233-236.

Lin, Y., Y-X Liu, T. Cislo, B.L. Mason and M.W. Yu. 1991. Expression and characterization of the pre-S1 peptide of Hepatitis B virus surface antigen in *Escherichia coli. J. Med. Virol.* **33**, 181-187.

Loddenkotter, B., B. Kammerer, K. Fischer and U. Flugge. 1993. Expression of the functional mature chloroplast triose phosphate translocator in yeast internal membranes and purification of the histidine-tagged protein by a single metal-affinity chromatography step. *Proc. Natl. Acad. Sci. U.S.A.* **15**, 2155-2159.

López de Quinto, S. and E. Martinez-Salas. 1999. Involvement of the Aphthovirus RNA region located between the two functional AUGs in start codon selection. *Virology* **255**, 324-336.

Lubroth, J. 1988. African horsesickness and the epizootic in Spain 1987. *Equine Pract.* **10**, 26-33.

Luckow, V.A., S.C Lee, G.F Barry and P.O. Olins. 1993. Efficient generation of infectious recombinant baculoviruses by site-specific transposon mediated insertion of foreign genes into a baculovirus genome propagated in *Escherichia coli. J Virol* **67**, 4566-4579.

Maass, D.R. and P.H. Atkinson. 1990. Rotavirus proteins VP7, NS28, and VP4 form oligomeric structures. *J. Virol.* **64**, 2632-2641.

Macreadie, I.G., C.K. Arunagirl, D.R. Hewish, J.F. White and A.A Azad. 1996. Extracellular addition of a domain of HIV-1 Vpr containing the amino acid sequence motif H(S/F)RIG causes cell membrane permeabilization and death. *Mol. Micro.* **19**, 1185-1192.

Maree, F.F. 2000. Multimeric protein structures of African horsesickness virus and their use as antigen delivery systems. PhD thesis. Faculty of Biological and Agricultural Sciences, University of Pretoria.

Maree, F.F. and H. Huismans. 1997. Characterization of tubular structures composed of nonstructural protein NS1 of African horsesickness virus expressed in insect cells. *J. Gen. Virol.* **78**, 1077-1081.

Maree, S, S. Durbach, F.F. Maree, F. Vreede and H. Huismans. 1998. Expression of the major core structural proteins VP3 and VP7 of African horsesickness virus, and production of core-like particles. *Arch. Virol. Suppl.* **14**, 203-209.

Martin, L.A., A.J. Meyer, R.S. O'Hara, H. Fu, P.S. Mellor, N.J. Knowles and P.P. Mertens. 1998. Phylogenetic analysis of African horsesickness virus segment 10: sequence variation, virulence characteristics and cell exit. *Arch. Virol. Suppl.* **14**, 281-293.

Martínez-Torrecuadrada, J.L., J.P.M. Langeveld, R.H. Meloen and J.I. Casal. 2001. Definition of neutralizing sites on African horse sickness virus serotype 4 VP2 at the level of peptides. *J. Gen. Virol.* **82**, 2415-2424.

Mattion, N.M., J. Cohen and M.K. Estes. 1994. Rotavirus proteins. In: *Viral infection in the Gastrointestinal Tract.* Eds. A. Kapikian. New York, Marcel Dekker. pp. 169-249.

McGeoch, D.J. 1985. On the predictive recognition of signal peptide sequences. *Virus Res.* 3, 271-286.

McIntosh, B.M. 1958. Immunological types of horsesickness virus and their significance in immunisation. Onderstepoort *J. vet. Res.* **27**, 465-538.

Mecham, J.O. and V.C. Dean. 1988. Protein coding assignment of epizootic haemorrhagic disease virus. *J. Gen Virol.* **69**, 1255-1262.

Medina, M., E. Domingo, J.K. Brangwyn and G.J. Belsham. 1993. The two species of the Foot-and-mouth disease virus leader protein, expressed individually, exhibit the same activities. *Virology* **194**, 355-359.

Mellor, P.S. 1993. African horse sickness: transmission and epidemiology. *Vet Res.* **24**, 199-212.

Meyer, J.C., C.C. Bergmann and A.R. Bellamy. 1989. Interaction of rotavirus cores with the nonstructural glycoprotein NS28. *Virology* **171**, 98-107.

Mertens, P.P.C., F. Brown and D.V. Sangar. 1984. Assignment of the genome segments of bluetongue virus type 1 to the proteins which they encode. *Virology* **135**, 207-217.

Minai, L. A. Fish, M. Darash-Yahana, L. Vershovsky and R. Nechushtai. 2001. The assembly of the PsaD subunit into the membranal photosystem I complex occurs via an exchange mechanism. B*iochemistry.* **30**, 12754-12760.

Mikhailov, M., K. Monastyrskaya, T. Bakker and P. Roy. 1996. A new form of particulate single and multiple immunogen delivery system based on recombinant bluetongue virus-derived tubules. *Virology* **217**, 323-331.

Miller, M.A., M.W. Cloyd, J. Liebmann, C.R. Rinaldo, K.R. Islam, S.Z.S. Wang, T.A. Mietzner and R.C. Montelaro. 1993. Alterations in cell membrane permeability by the lentivirus lytic peptide (LLP-1) of HIV-1 transmembrane protein. *Virology* **196**, 89-100.

Miller, M.A. and R.C. Montelaro. 1992. Amphipathic helical segments of HIV-1 transmembrane (TM) proteins and their potential role in viral cytopathicity. In "*Advances in Membrane Fluidity*". R.C. Aloia, Ed. A.R. Liss, New York. Vol 6, pp351-364.

Miller, M.A., R.F. Gary, J.M. Jaynes and R.C. Montelaro. 1991. A structural comparison between lentivirus transmembrane proteins and natural cytolytic peptides. *AIDS Res. Hum. Retroviruses* **7**, 511-519.

Moore, D.L. and V.H. Lee. 1972. Antigenic relationship between the virus of epizootic haemorrhagic disease of deer and bluetongue virus. *Arch. Gesamte. Virusforsch.* **37**, 282-284.

Morris, A.P., J.K. Scott, J.M. Ball, C.Q. Zeng, W.K. O'Neal and M.K. Estes. 1999. NSP4 elicits age-dependant diarrhes and Ca^{2+} mediated I^- influx into intestinal crypts of CF mice. *Am. J. Physiol.* **277**, 431-444.

Moss, S.R., L.D. Jones and P.A. Nuttall. 1992. Comparison of the nonstructural protein, NS3, of tick-borne and insect-borne orbiviruses. *Virology* **187**, 841-844.

Murti, K.G., R.G. Webster and I.M. Jones. 1988. Localisation of RNA polymerases on influenza viral ribonucleoproteins by immunogold labeling. *Virology* **164**, 562-566.

Newton, K., J.C. Meyer, A.R. Bellamy and J.A. Taylor. 1997. Rotavirus nonstructural glycoprotein NSP4 alters plasma membrane permeability in mammalian cells. *J. Virol.* **71**, 9458-9465.

Nunez, E., X. Wei, C. Delgado, I. Rodriguez-Crespo, B. yelamos, J. Gomez-Gutierrez, D.L. Peterson and F. Gavilanes. 2001. Cloning, expression and purification of histidine-tagged preS domains of hepatitis B virus. *Protein Expr. Purif.* **21**, 183-191.

Oess, S. and E. Hildt. 2000. Novel cell permeable motif derived from the preS2-domain of hepatitis-B virus surface antigens. *Gene Ther.* **7**, 750-758.

O'Brein, J.A., J.A. Taylor and A.R. Bellamy. 2000. Probing the structure of rotavirus NSP4: a short sequence at the extreme C terminus mediates binding to the inner capsid particle. *J. Virol.* **74**, 5388-5394.

Oellerman, R.A., H.J. Els and B.J. Erasmus. 1970. Characterisation of African horsesickness virus. *Archiv. gesammte Virusforsch.* **29**, 163-174.

O'Hara, R.S., A.J. Meyer, L. Pullen, L-A Martin and P.P.C. Mertens. 1998. Development of a mouse model system and identification of individual genome segments of African horsesickness virus serotypes 3 and 8 involved in determination of virulence. In: African horse sickness. P.S. Mellor, P.P.C. Mertens, M. Baylis, C. Hamblin (eds). Springer, Wien New York, pp 259-279.

O'Reilly, D.R., L.K. Miller and V.A. Luckow. 1992. Baculovirus expression vectors: A laboratory manual. W.H. Freeman and Company, New York.

Parente, R.A., S. Nir and F.C. Szoka, Jr. 1990. Mechanism of leakage of phospholipid vesicle contents induced by the peptide GALA. *Biochem.* **29**, 8720-8728.

Parks, T.D., K.K. Leuther, E.D. Howard, S.A. Johnston and W.G. Dougherty. 1994. Release of proteins and peptides from fusion proteins using a recombinant plant virus proteinase. *Anal. Biochem.* **216**, 413-417.

Petrie, B.L., D.Y. Graham and M.K. Estes. 1983. Effects of tunicamycin on rotavirus morphogenesis and infectivity. *J. Virol.* **46**, 270-274.

Petty, I.T.D. and A.O. Jackson. 1990. Two forms of the Major Barley Stripe Mosaic virus nonstructural protein are synthesised in vivo from alternative initiation codons. *Virology* **177**, 829-832.

Piccone, M.E., E. Rieder, P.W. Mason and M.J. Grubman. 1995. The Foot-and-mouth leader proteinase gene is not required for viral replication. *J. Virol.* **69**, 5376-5382.

Piller, S.C., G.D Edwart, A. Premkumar, G.B Cox and P.W. Gage. 1996. Vpr protein of human immunodeficiency virus type 1 forms cation-selective channels in planar lipid bilayers. *Proc Natl Acad Sci USA* **93**, 111-115.

Piller, S.C., P. Jans, P.W. Gage and D.J. Jans. 1998. Extracellular HIV-1 virus protein R causes a large inward current and cell death in cultured hippocampal neurons: Implications for AIDS pathology. *Proc. Natl. Acad. Sci. USA* **95**, 4595-4600.

Pinto, L.H., L.J. Holsinger and R.A Lamb. 1992 Influenza virus M2 protein has ion channel activity. *Cell* **69**, 517-528.

Poisson, F., A. Severac, C. Hourioux, A. Goudeau and R. Roingeard. 1997. Both pre-S1 and S domains of Hepatitis B virus envelope proteins interact with the core particle. *Virology* **228**, 115-120.

Portner, A and K.G. Murti. 1986. Localisation of P, NP and M proteins on sendai virus nucleocapsid using immunogold labeling. *Virology* **150**, 469-478.

Prasad, B.V. S. Yamaguchi and P. Roy. 1992. Three-dimensional structure of single-shelled bluetongue virus. *J. Virol* **66**, 2135-2142.

Prober, J.M., G.L. Trainor, R.J. Dam, F.W. Hobbs, C.W. Robertson, R.J. Zagursky, A.J. Cocuzza, M.A. Jensen and K. Baumeister. 1987. A system for rapid DNA sequencing with fluorescent chain-terminating Dideoxynucleotides. *Science* **238**, 336-341.

Roner, M.R., and W.K. Joklik. 2001. Reovirus reverse genetics: Incorporation of the CAT gene into the reovirus genome. *PNAS* **98**, 8036-8041.

Roy, P. 1991. *Towards the control of emerging bluetongue disease*. Oxford Virology Publications, London, 71pp.

Roy, P., T. Hirasawa, M. Fernandez, V.M. Blinov and J.J. Sanchez-Vixcain Rodrique. 1991. The complete sequence of the group-specific antigen, VP7, of African horsesickness disease virus serotype 4 reveals a close relationship to bluetongue virus. *J. Gen. Virol.* **72**, 1237-1241.

Roy, P., P.P.C. Mertens and I. Casal. 1994. African Horsesickness virus structure. *Comp. Immun. Microbiol. Infect. Dis.* **17**, 243-273.

Roy, P. 1996. Orbivirus structure and assembly. *Virology* **216**, 1-11.

Ruiz, M.C., J. Cohen and F. Michelangeli. 2000. Role of Ca^{2+} in the replication and pathogenesis of rotavirus and other viral infections. *Cell calcium* **28**, 137-149.

Rumlova, M., J. Benedikova, R. Cubinkova, I. Pichova and T. Ruml. 2001. Comparison of classical and affinity purification techniques of Mason-Pfizer monkey virus capsid protein: the alteration of the product by an affinity tag. *Protein Expr. Purif. 23*, 75-83.

Sailleau, C., C. Hamblin, J.T. Paweska and S. Zientara. 2000. Identification and differentiation of the nine African horse sickness virus serotypes by RT-PCR amplification of the serotype-specific genome segment 2. *J. Gen Virol.* **81**, 831-837.

Sambrook, J., E.F. Fritsch and T. Maniatis. 1989. *Molecular cloning, a laboratory manual.* Second edition. Cold Spring Harbor Laboratory Press.

Sanderson, C.M., J.E. Parkinson, M. Hollinshead and G.I. Smith. 1996. Over expression of the vaccinia virus A38L integral membrane protein promotes Ca2+ influx into infected cells. *J Virol* **70**, 905-914.

Sangar, D., S.E. Newton, D.J. Rowlands and B.E. Clarke. 1987. All foot-and-mouth disease virus serotypes initiate protein synthesis at two separate AUGs. *Nucleic Acids Res.* **15**, 3305-3315.

Sanger, F., S. Nicklen and A.R. Coulson. 1977. DNA sequencing with chain-terminating inhibitors. *Proc. Natl. Acad. Sci. USA* **74**, 5463-5467.

Sansom, M.S.P., L.R. Forrest and R. Bull. 1998. Viral ion channels: molecular modelling and simulation. *BioEssays* **20**, 992-1000.

Santantonio, T., M. Jung, R. Schneider, D. Fernholz, M. Milella, L. Monno, G. Pastore, G.R. Pape and H. Will. 1992. Hepatitis B virus genomes that cannot synthesize pre-S2 proteins occur frequently and as dominant virus populations in chronic carriers in Italy. *Virology* **188**, 948-952.

Sanz, M.A., L. Perez, and L. Carrasco. 1994. Semliki Forest virus 6K protein permeability after inducible expression in *Escherichia coli* cells. *J. Biol. Chem.* **269**, 12106-12110.

Schlegel, R. and M. Wade. 1985. Biologically active peptides of the vesicular stomatitis virus glycoprotein. *J. Virol.* **53**, 319-323.

Schmidt, M., N. tuominen, T. Johansson, S.A. Weiss, K. Keinanen and C. Oker-Blom. 1998. Baculovirus-mediated large-scale expression and purification of a polyhistidine-tagged rubella virus capsid protein. *Protein Expr. Purif.* **12**, 323-330.

Sedman, S.A. and J.E. Mertz. 1988. Mechanisms of synthesis of virion proteins from the functionally bigenic late mRNAs of simian virus 40. *J. Virol.* **62**, 954-961.

Segrest, J.P., H. De Loof, J.G. Dohlman, C.G. Brouillette and G.M. Anantharamaiah. 1990. Amphiphathic helix motif: classes and properties. *Proteins* **8**, 103-117.

Sheu, S.Y. and S. Lo. 1992. Preferential ribosomal scanning is involved in the differential synthesis of Hepatitis B virus surface antigens from subgenomic transcripts. *Virology* **188**, 353-357.

Skowneck, A.J., L. LaFranco, M.A. Stone-Marschat, T.G. Burrage, A.H. Rebar and W. W. Burrage. 1995. Clinical pathology and Hemostatic abnormalities in experimental African horsesickness. *Vet. Pathol.* **32**, 112-121.

Small, I., H. Wintz, K. Akashi and H. Mireau. 1998. Two birds with one stone: genes that encode products targeted to two or more compartments. *Plant Mol. Biol.* **38**, 265-277.

Smit, C.C. 1999. Identification of critical functional domains of nonstructural protein NS3 of African horsesickness virus. MSc Thesis, Faculty of Biological and Agricultural Sciences, University of Pretoria.

Souicet, G., B. Menand, J. Ovesnat, A. Cosset, A. Dietrich and H. Wintz. 1999. Characterization of two bifunctional *Arabdopsis thaliana* genes coding for mitochondrial and cytosolic forms of valyl-tRNA synthetase and threonyl-tRNA synthetase by alternative use of two in-frame AUGs. *Eur. J. Biochem.* **266**, 848-854.

Stoltz, M.A., C.F. van der Merwe, J. Coetzee and H. Huismans. 1996. Subcellular localisation of the nonstructural protein NS3 of African horsesickness virus. *Onderstepoort J. vet. Res.* **63**, 57-61.

Stuart, D.I., P. Gouet, J. Grimes, R. Malby, J. Diprose, S. Zientara, J.N. Burroughs and P.P. Mertens. 1998. Structural studies of orbivirus particles. *Arch Virol Suppl* **14**, 235-250.

Summers, J., P.M. Smith, M. Huang and M. Yu. 1991. Morphogenetic and regulatory effects of mutations in the envelope protein of an avian hepadnavirus. *J. Virol.* **65**, 1310-1317.

Suzuki, N., M. Harada and T. Kusano. 1991. Molecular analysis of rice dwarf phytoreovirus segment S11 corresponding to wound tumour phytoreovirus segment S12. *J. Gen. Virol.* **72**, 2233-2237.

Suzuki, T., T. Yoshida and S. Tuboi. 1992. Evidence that rat liver mitochondrial and cytosolic fumarases are synthesised from one species of mRNA by alternative translational initiation at two in-phase AUG codons. *Eur. J. Biochem.* **207**, 767-772.

Swaggerty, C.L., A.A. Frolov, M.J. McArthur, V.W. Cox, S. Tong R.W. Compans and J.M. Ball. 2000. The envelope glycoprtotein of Simian immunodeficiency virus cotains an enterotoxin domain. *Virology* **277**, 250-261.

Tan, B-H, E. Nason, N. Staeuber, W. Jiang, K. Monastryrskaya and P. Roy. 2001. RGD tripeptide of bluetongue virus VP7 protein is responsible for core attachment to Culicoides cells. *J. Virol.* **75**, 3937-3947.

Taylor, J.A., J.C. Meyer, M.A. Legge, J.A. O'Brein, J.E. Street, V.J. Lord, C.C. Bergmann and A.R. Bellamy. 1992. Transient expression and mutational analysis of the rotavirus intracellular receptor: the C-terminal methionine residue is essential for ligand binding. *J. Virol.* **66**, 3566-3572.

Taylor, J.A., J.C. O'Brein, V.J. Lord, J.C. Meyer and A.R. Bellamy. 1993. The RER-localised rotavirus intracellular receptor: a truncated purified soluble form is multivalent and binds virus particles. *Virology* **194**, 807-814.

Taylor, J.A., J.A. O'Brein and M. Yeager. 1996. The cytoplasmic tail of NSP4, the endoplasmic reticulum-localised non-structural glycoprotein of rotavirus, contains distinct virus binding and coiled coil domains. *EMBO J.* **15**, 4469-4476.

Theiler, A. 1921. African horsesickness. Science Bulletin no. 19, Department of Agriculture. S.A. Pretoria.

Theron, J., J.M. Uitenweerde, H. Huismans and L.H. Nel. 1994. Comparison of the expression and phosphorylation of the non-structural protein NS2 of three different orbiviruses: evidence for the involvement of an ubiquitous cellular kinase. *J. Gen. Virol.* **75**, 3401-3411.

Tian, P., Y. Hu, W.P. Schilling, D.A. Lindsay, J. Eiden and M.K. Estes. 1994. The nonstructural glycoprotein of rotavirus affects intracellular calcium levels. *J. Virol.* **68**, 251-257.

Tian, P., J.M. Ball, C.Q.-Y. Zeng and M.K. Estes. 1996. The rotavirus nonstructural glycoprotein NSP4 possesses membrane destabilization activity. *J. Virol.* **70**, 6973-6981.

Tian, P., M.K. Estes, Y. Hu, J.M. Ball, C.Q.-Y. Zeng and W.P. Schilling. 1996a. The rotavirus nonstructural glycoprotein NSP4 mobilizes Ca^{2+} from the endoplasmic reticulum. *J. Virol.* **69**, 5763-5772.

Turnbull, P.J., S.B. Cormack and H. Huismans. 1996. Characterization of the gene encoding core protein VP6 of two African horsesickness virus serotypes. *J. Gen. Virol.* **77**, 1421-1423.

Ueda,K., T. Tsurimoto and K. Matsubara. 1991. Three envelope protein of Hepatitis B virus: Large S, Middle S and Major S proteins needed for the formation of Dane particles. *J. Virol.* **65**, 3521-3529.

Uitenweerde, J.M., J. Theron, M.A. Stoltz and H. Huismans. 1995. The multimeric nonstructural NS2 proteins of bluetongue virus, African horsesickness virus and epizootic haemorrhagic disease virus differ in their single-stranded RNA binding ability. *Virology* **209**, 624-632.

Urakawa, T and P. Roy. 1988. Bluetongue virus tubules made in insect cells by recombinant baculoviruses: expression of the NS1 gene of bluetongue virus serotype 10. *J. Virol.* **62**, 3919-3927.

Urbano U. and G.F. Urbano. 1994. The Reoviridae family. *Comp. Immun. Microbiol. Infect. Dis.* **17**, 151-161.

Van Dijk, A.A. and H. Huismans. 1988. In vitro transcription and translation of bluetongue virus mRNA. *J. Gen. Virol.* **69**, 573-581.

Van Niekerk, M., C.C. Smit, W.C. Fick, V. van Staden and H. Huismans. 2001a. Membrane association of African horsesickness virus nonstructural protein NS3 determines its cytotoxicity. *Virology* **279**, 499-508.

Van Niekerk, M., V. van Staden, A.A. van Dijk and H. Huismans. 2001b. Variation of African horsesickness virus nonstructural protein NS3 in southern Africa. *J. Gen. Virol.* 82, 149-158.

Van Staden, V. 1993. Characterization and expression of the gene that encodes nonstructural protein NS3 of African horsesickness virus. PhD Thesis, Faculty of Science, University of Pretoria 162pp.

Van Staden, V. and H. Huismans. 1991. A comparison of the genes which encode nonstructural protein NS3 of different orbiviruses. *J. Gen. Virol.* **72**, 1073-1090.

Van Staden, V., C.C. Smit, M.A. Stoltz, F.F. Maree and H. Huismans. 1998. Characterization of two African horsesickness virus nonstructural proteins, NS1 and NS3. *Arch. Virol.* **14**, 251-258.

Van Staden, V., M.A. Stoltz and H. Huismans. 1995. Expression of nonstructural protein NS3 of African horsesickness virus (AHSV): evidence for a cytotoxic effect of NS3 in insect cells, and characterisation of the gene products in AHSV-infected VERO cells. *Arch. Virol.* **140**, 289-306.

Venter, G.J., S.D. Graham and C. Hamblin. 2000. African horse sickness epidemiology: vector competence of South African Culicoides species for virus serotypes 3, 5 and 8. *Med. Vet. Entomol.* **12**, 245-250.

Verwoerd, D.W., H. Huismans and B.J. Erasmus. 1979. Orbiviruses. In: *Comprehensive Virology*, Vol. 14, H. Fraekel-Conrat and R.R. Wagner (Eds.), pp. 285-345. Plenum Press, New York.s

Vreede, F.T. and H. Huismans. 1994. The cloning, characterization and expression of the gene that encodes the major neutralisation-specific antigen of African horsesickness virus serotype 3. *J. Gen. Virol.*

Wade-Evans, A.M., L. Pullen, C. Hamblin, R.S. O'Hara, J.N. Burroughs and P.P.C. Mertens. 1997. African horsesickness virus VP7 sub-unit vaccine protects mice against a lethal, heterologous serotype challenge. *J. Gen. Virol.* **78**, 1611-1616.

Wade-Evans, A.M., L. Pullen, C. Hamblin, R.S. O'Hara, J.N. Burroughs and P.P.C. Mertens. 1998. VP7 from African horse sickness virus serotype 9 protects mice against a lethal, heterologous serotype challenge. *Arch. Virol.* **14**, 211-219.

Walter, P. and V.R. Lingappa. 1986. Mechanism of protein translocation across the endoplasmic reticulum membrane. *Annu. Rev. Cell. Biol* **2**, 499-516.

Westra, D.F., G.W. Welling, D.G. Koedijk, A.J. Scheffer, T.H. The and S. Welling-Wester. 2001. Immobilised metal-ion affinity chromatography purification of histidine-tagged recombinant proteins: a wash step with a low concentration of EDTA. *J. Chromatogr. Biomed. Sci. Appl.* **25**, 129-136.

Xia, X. and G. Serrero. 1999. Multiple forms of p55PIK, a regulatory subunit of phosphoinositide 3-kinase, are generated by alternative initiation of translation. *Biochem J.* **341**, 831-837.

Yamakawa, M., M. Kubo and S. Furuuchi. 1999. Molecular analysis of the genome of Chuzan virus, a member of the Palyam serogroup viruses, and its phylogenetic relationship to other orbiviruses. *J. Gen. Virol.* **80**, 937-941.

Zhang, M., C.Q. Zeng, A.P. Morris and M.K. Estes. 2000. A functional NSP4 enterotoxin peptide secreted from rotavirus-infected cells. *J Virol* **74**, 11663-11670.

Zhao, Y., C. Thomas, C. Bremer and P. Roy. 1994. Deletion and mutational analysis of bluetongue virus NS2 protein indicates that the amino- but not the carboxy-terminal of the protein is critical for RNA-protein interactions. *J. Virol.* **68**, 2179-2185.